Quantifying uncertainties in Landslide Runout Modelling

Tuba Zahra

January, 2010

Quantifying uncertainties in Landslide Runout Modelling

by

Tuba Zahra

Thesis submitted to the International Institute for Geo-information Science and Earth Observation in partial fulfilment of the requirements for the degree of Master of Science in Geo-information Science and Earth Observation, Specialisation: Geohazards

THESIS ASSESSMENT BOARD

Prof. Dr.Victor Jetten, ITC (Chairman)
Drs. Michiel Damen, ITC
Mr. I.C. Das, IIRS
Dr. P. K. Champatiray, IIRS

Dr. S. Sarkar
CBRI, IIT-Roorkee
External Expert

SUPERVISORS

ITC
Dr.Cees-van Westen
Associate Professor
Department of Earth Systems Analysis

IIRS
Prof.R.C.Lakhera
Scientist SG
In-charge, Geosciences Division
Mr. I.C.Das
Scientist SE
Geosciences Division

ADVISORS

Byron Quan Luan
PhD Scholar, ITC

Sekhar Lukose Kuriakose
PhD Scholar, ITC

INTERNATIONAL INSTITUTE FOR GEO-INFORMATION SCIENCE AND EARTH OBSERVATION
ENSCHEDE, THE NETHERLANDS, AND
INDIAN INSTITUTE OF REMOTE SENSING (IIRS-NRSC)
DEHRADUN, INDIA

Disclaimer

This document describes work undertaken as part of a programme of study at the International Institute for Geo-information Science and Earth Observation. All views and opinions expressed therein remain the sole responsibility of the author, and do not necessarily represent those of the institute

Tuba Zahra

To my Mother for inspiring me to dream
To my Father for instilling the strength to look beyond
To my sister and brother for believing in me
To my friends for their presence and care.

Abstract

The most essential part of landslide hazard assessment revolves around the prediction of the failure and the post failure movement or the runout of landslides. This approach requires the accurate prediction of the intensity or magnitude of the landslide with special reference to the runout behaviour. The runout behaviour maybe characterised by the quantitative spatially distributed runout parameters like, runout distance, runout width, depth of the moving mass & deposited material, velocity, pressure, volume of the material, scouring processes involved and saturation.

In order to get a detailed understanding of the dynamic characteristics of debris flow often numerical methods are applied. A continuum method numerical solution includes conservation equations of mass, momentum, energy and describes the dynamic motion of debris along with the rheological models that determine material behaviour of the landslides (Dai et al. 2002). Attempts to streamline and create a framework for an acceptable method of uncertainty quantification for landslide runout modelling are largely lacking. In this research, an attempt is made to quantify the spatial uncertainty (including extent, depth and volume) that emerges from numerically modelling landslide runout.

This research uses a numerical model called MassMov2D, which is a two dimensional numerical model of mass movement runout over complex topography to model the debris flow kinematics based on the depth-averaged form of the equation of motion for a fluid continuum applying the Voellmy rheology. The model has been implemented using the raster based environmental modelling language PCRaster.

The observed areal extent, volume and deposit depth were used to back analyse the event and estimate the values for the leading rheological parameters, turbulence coefficient and basal frictional angle. An attempt was made to calibrate the model for souring rate, though a difficult process, to estimate the influence on runout deposit depth and volume. The results for calibration were used to back analyse the event and to adjust the parameters for the observed values of area, depth and volume. A sensitivity analyses of the model revealed that the acceptable range of parameters for which the uncertainty analysis was conducted was in the range of 100-1000 m.sec-2 for turbulence coefficient, a basal frictional angle of 9- 34 degrees and a synthetic range was chosen for the scouring rate. It was observed that the variability in the deposit depth was found to be nearer to the observed value of 6.4m with turbulence coefficient values between 200-300 m.sec-2, basal frictional angle values between 24-26 degrees and scouring rate values between 0.0053-0.0095m.sec. The Monte Carlo technique was used to derive random parameter values within these range. Owing to the time taken for each simulation the random number simulation was limited to 100 scenarios. Probabilities for runout reaching each pixel were calculated and also for reaching particular deposit depths (0-2m, 2-4m, 4-6m and above 6m). Maps were generated showing the probabilities of runout in each of the deposit depths. Accurate predictions were found for 62% of the area whereas an area of 23% was considered to be moderately uncertain because there were occurrences of runout observed in this area though they were very low falling in the probability interval of 0.2-0.8.

Acknowledgements

I was looking forward for the moment to write this part of my thesis with a very relaxed mind, coffee in hand and snuggled to keep myself warm from the cold winters in Dehradun and with a sense of déjà vu of having completed my thesis. The moment is not quite as I had imagined. But all's well that ends well….I am still enjoying though.

First and foremost I would like to thank my IIRS supervisor Prof. R.C. Lakhera who retired during the last phase of my project work for all his support from the beginning to the end in all possible ways. I would also like to thank my co-supervisor Mr. I.C.Das for actually initiating me to choose a topic related to uncertainty and go ahead with it. I would also like to thank my ITC supervisor Dr. Cees van Westen for his continuous support and advice at all crucial moments of my project work. Though a 'distant student' he never failed to respond to any of my mails tagged 'URGENT' and encouraged me to successfully complete my thesis.

Special thanks goes to my advisors Byron Quan Luna and Sekhar Lukose Kuriakose, who are most responsible for helping me complete the writing of this dissertation from the proposal stage till date. They were always there to listen and to give advice. The small words of encouragement were at the time when I needed them the most and stressed with work. They guided me to pen down the research proposal, had confidence in me when I doubted myself and brought out the good ideas. They were always there to talk and clarify my doubts, to proof read my papers and chapters, and to ask me good questions to help me think about my problems. (Most importantly I developed an affinity to fly my small flying machine!)

They showed me the different ways to approach a research problem and also the need to be persistent to accomplish my goals. Without their encouragement and constant guidance, I could not have finished my dissertation.

I would extend my thanks to Mr. V. Hari Prasad, ex-programme co-ordinator without whom the NUFFIC funding would have been a distant dream. I would also like to thank both my IIRS librarian Mr. Sardar and ITC librarian Ms. Marga Koelen who provided me with sufficient literature to understand the topic better. Thank you to Ms. Carla Gerritson as well for fulfilling all my needs of journal articles which I could not avail from the library directly.

I would like to offer my thanks to my fellow batchmates Jagannath Nayak for his sense of humour even when deadlines had to be met; Bantehsonglang Blahwar (the man with the longest name) for his attitude that said 'Do it Man! No Worries!!,'and Veena Chowdhary, for being my coffee mate at wee hours in the morning (not to forget the vending machine that conquered over sleep and kept me awake till late).

I would like to extend my thanks to a friend turned Scientist, Prasun K.Gupta for being the best of friends, a guide and a philosopher who was there at every beck and call. He supported me in all possible ways so that I could successfully complete my dissertation in time. Would bear my frantic mood swings when I was stressed with work and most importantly make me smile when I was in tears of not being able to make it in time. He has been a gem of a person throughout my project phase.

Last, but not the least, I thank my family: my parents for giving me life in the first place, for educating me with aspects from both arts and science, for unconditional support and encouragement to pursue my interests, even when interests went beyond boundaries of language, field and geography. My sister for listening to my complaints and frustrations and yet believing in me. My brother for his consistent caring calls even when I (confess) ignored them at times.

And to God, who made all things possible.

Table of contents

List of figures

List of tables

List of equations

1. Introduction

Landscapes as dynamic earth systems contain not only objects but also stores of energy and matter, maintained by processes of growth, decay, flow and transformations (Thomas 2001). The release of this energy and matter has had many forms and landslides or mass movements are among them. According to the USGS (2004), the generic term '*landslide*' describes processes like rock fall, topple, slide, spread and flow emphasising the downward and the outward movement of materials. Landslides, which are also termed as mass movements are one of the most important hill slope processes and frequently occurring disastrous events.

As such determining the spatial and temporal probability of occurrence of landslides has been of major research interest amongst earth scientists' example (Aleotti 2004; Choubey and Litoria 1990; van Westen et al. 2008)). The most essential part of landslide hazard assessment revolves around the character of the failure and the post failure movement or the runout of landslides. This approach requires the accurate prediction of the intensity or magnitude of the landslide with special reference to the runout behaviour. Intensity of the landslide (IL) being determined as a function of the landslide volume (VL) and the expected velocity (SL) of the runout, that is IL = f (VL, SL) (Hungr 1997). Intensity or magnitude helps in the quantitative analyses of hazard in an area. Physical parameters like velocity, volume, thickness of the materials displaced and the energy and impact forces that together determine the destructive potential of landslides are in turn a measure of intensity (van Asch et al. unpublished). The quantification and qualitative expression of intensity requires spatial distribution of the materials. This refers to answer queries like how far and how fast a landslide could travel once mobilized (Dai et al. 2002) and also the thickness and the velocity of the flow affecting the runout area in consideration.

1.1. Runout of Landslides

A landslide system is theoretically divided into three components: an initiation zone, transport and deposition zone (Figure 1.1).

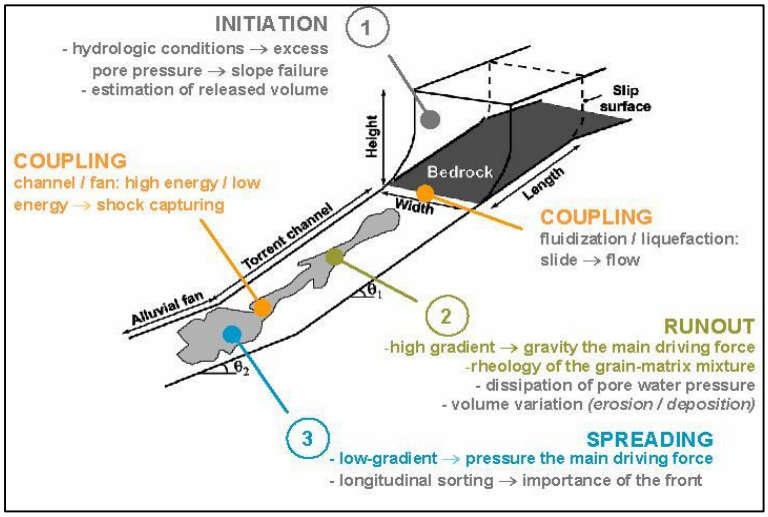

Figure 1.1: Components of Debris flow (Begueria 2009)

Accurate prediction of the runout of landslide debris requires the study of the runout behaviour. The runout behaviour maybe characterised by the quantitative spatially distributed runout parameters like,

Table 1.1: Parameters for Landslide Runout

Parameters	Description
Runout distance	Also referred to as the travel distance that commences from the point of origin of an event. More specifically the transportation zone in which events may initiate in a gully or open slope and maybe of two types; confined and unconfined slide or flow. This distance is influenced by properties of the material and the attributes of the path of movement (Fannin and Bowman 2008).
Runout width	Determines the amount of deposits that would be entrained from the runout zone into the zone of deposition. It may also be called the damage width corridor (Dai et al. 2002) or the area lying in the distal path of the landslide path that is prone to landslide damage.
Depth of the moving mass & deposited material	The former influences the force which determines the severity with which the landslide may move along the runout distance. Resulting accumulation of the debris material may lead to collapse of structures in its corridor (Dai et al. 2002). While the deposited material affects the area of distribution. A thin mantle of deposits is less damaging than thicker deposit depths. The latter has a tendency of spreading and distributing over larger areas, that in turn, being saturated may create havoc.
Velocity	Indicates the intensity of the landslide event when estimated with the volume of the deposits which may lead to potential damage (Hungr 1997). The velocity profile is helpful to evaluate the shear behaviour of different materials. Now this velocity is the maximum velocity of the front head leading to a runout. The maximum (mean cross-sectional) velocity referring to the variation of the mean velocity along the flow wave of the material (Rickenmann 1999) is an important parameter determining the intensity of the material affecting the runout area. The impact velocity is determined by the determination of the velocity at the front of the runout fan.
Pressure	This parameter is influenced by the volume of the material which initiates the initial velocity of the movement of material. Pressure is assumed to be parallel along the runout path increasing linearly with depth (Hungr 1995) and dependent on the type of material. Pressure of the increasing volume of deposits due to entrainment and deposition includes the lateral pressure of confinement determined by the Rankine's active and passive coefficients k_a and k_p. A landslide comprising of dry granular material with friction consists of a range of active 0.2 and passive 5.0 whereas coefficient k at rest equals 1. Such a landslide material does not spread or contracts like the fluid materials (Hungr 1995).
Volume of the material	Is influenced by the entrainment and deposition along the path. In order to design mitigation measures the prediction of volume of the moving mass of material is of considerable importance (Revellino et al.2008; Hungr et al. 2003). Moreover volume of the material drives the material forward due to pressure of the material affecting normal stress.
Scouring processes	Entrainment of additional materials on the runout travel path thereby influencing the volume of the material which influences the other parameters as well.

Saturation	This parameter plays an important role in entrainment and deposition of material. It may so happen that while travelling along the runout path the materials maybe moving over confined channels. This leads to saturation of the materials which flows with greater velocity and added energy and is a cause of large scale damage. Also rock avalanches may seldom move along confined channels and take the shape of debris flows.

All the above parameters are influenced by the slope characteristics, modes of movement, mechanism of failure and the flow path. All these parameters together influence and vary according to the different types of mass movements. These maybe classified in brief as follows depending on the classification of Varnes (1978) and Cruden and Varnes (1996) with further recommendations made by Hutchinson (1988), Hungr et al. (2001);

Type of movement			Type of material		
			Bedrock	Engineering soils	
F				Predominantly fine	Predominantly coarse
Falls			Rockfall	Earth fall	Debris fall
Topples			Rock topple	Earth topple	Debris topple
Slides	Rotational		Rock slump	Earth slump	Debris slump
	Translational	Few units	Rock block slide	Earth block slide	Debris block slide
		Many units	Rock slide	Earth slide	Debris slide
Lateral spreads			Rock spread	Earth spread	Debris spread
Flows			Rock flow	Earth flow	Debris flow
			Rock avalanche		Debris avalanche
			(Deep creep)	(Soil creep)	
Complex and compound			Combination in time and/or space of two or more principal types of movement		

Figure 1.2: Types of Mass Movements (Landslide Report, No 247)

Figure 1.2 provides the different types of mass movements which lead to runout of respective types. According to Casagrande ((1976) in Hungr et al. (2005) flow slides are accompanied by saturation zones at the rupture surface leading to catastrophic acceleration. Hungr et al. (2005) further classified these flows into dry granular flows that are characteristically slow and clay flow slides that are extremely rapid. He also emphasized that in case of rotational or compound slides that maybe rapid or slow and can be transformed into earthflows. Moreover, shallow slides on steep slopes being rapid may override materials downslope and form debris avalanche which in confined stream channels may take the form of debris flow. Similarly a rock slide in steep slope may become fragmented and flow-like known as rock avalanches. Hence it can be inferred that characteristics of runout may change. What may appear to be a rock slide and may be classified as a rockslide according to Varnes may technically transform into a debris slide due to the disruption of the displaced mass into fragments (Mc Saveney and Davis in Sassa et al. 2007). Thus whatever maybe the type of movement the role of the above parameters (Table 1.1) is crucial in determining the complexity of runout of the displaced material that may change due to changes in the dynamic behaviour of the landslides.

There has been an increasing concern to study the complexity and the dynamic changes of the above processes. The development of models has been used inevitably in order to generate hazard and risk maps. Computer models capable of spatial dynamic modelling (Karssenberg 2002) do not only reduce the time and effort but also are able to reproduce the real world phenomena with consistency which can be put to effective use by the decision making bodies.

1.2. Landslide Runout Models

In order to study landslide risk, delimitation of the endangered area is a fundamental necessity. The hazard area entails the source zone, the runout path and deposition fan (Chen and Lee 2004). Hence any modelling for landslide prevention should enable the prediction and identification of the runout distance and the zone of sedimentation.

Three different approaches, namely, Empirical approach, Physical scale modelling and Dynamic modelling (Figure 1.3) have been identified by Chen and Lee (2004) in order to model the kinematic parameters and hazard zones.

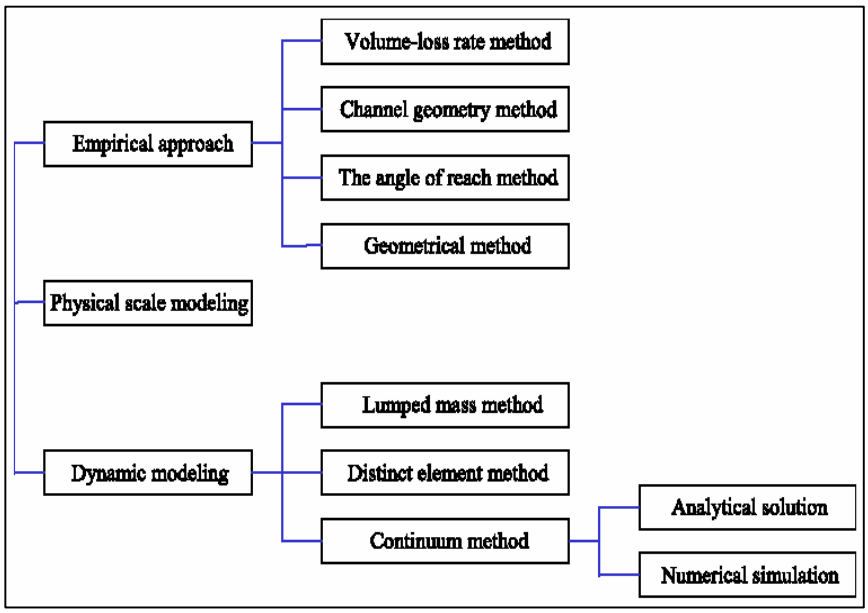

Figure 1.3: Three Modelling Approaches [After (Chen and Lee, 2004)]

Hungr and Mc Dougall (2004) suggest empirical and analytical methods for the runout prediction. Empirical method involves the use of measurement of landslide data like surface displacement etc (Hungr et al. 2005).Though this method does not involve the use of the rheological approach nor the kinematics of the material movement essential for the prediction of runout (Chen and Lee 2004) it is a simple tool for the analysis of travel distance. In case of the physically based models, parameters are derived from field measurements and have high data and storage requirements (Brunsden 1999). These models have been used for both large, deep, complex landslides (Brunsden 1999) as well as the shallow landslides (Carrara et al. 2008), though they have been based on hydrological models.

In order to get a detailed and better understanding of the quantitative estimations of the dynamic characteristics of debris flow often numerical methods are applied. A continuum method numerical solution includes conservation equations of mass, momentum, energy and describes the dynamic motion of debris along with the rheological models that determine material behaviour of the landslides (Dai et al. 2002); the estimation of appropriate rheological model being the most difficult part. This is because

changes in the dynamic behaviour of the landslide may occur throughout the events and the model is affected by inevitable uncertainties (Arattano et al. 2006).

1.3. Dynamic Models in Landslide Runout

Owing to the increasing concerns of uncertainty in the GIS environment measures of uncertainties either in the model parameters or model results are becoming available to the users. But availability of a wide plethora of models (details can be found in the Literature Review) makes choice difficult. A simple runout model can be carried out in a two dimensional framework and MassMov2D (briefed below and details are found in Chapter 2) was selected which is a dynamic model that enables the study of individual causative parameters in detail. But the best advantage of the model is cost effectiveness as it is an open source model with ease of availability.

1.4. MassMov2D Model Description

The MassMov2D is a numerical model of mass movement runout over complex topography and is two dimensional in nature. It is a model of mud and debris flow kinematics based on the depth-averaged form of the equation of motion for a fluid continuum, and controlled by rheology (Begueria 2009). The model has been implemented using the raster based environmental modelling language PCRaster. The performance of this model has been tested against debris-flow characteristics as revealed in various studies (Begueria et al. 2009; Kuriakose et al. 2009c). Begueria et al. (2009) in his study analysed that MassMov2D was able to predict the extension of the deposits, the lateral flow expansion and the run-up with a low frictional angle as also the entrainment of the deposits along the runout channel.

The model is available on request and works in the PCRaster software in an open source domain. The PCRaster provides the model a GIS environment making it possible for the user to modify it in order to experiment various modelling concepts due to the availability of the code in an easy to use language. This package provides tools that help in the editing of the input maps, visualization of the output using animations and time series. The model is flexible enough to work with a variety of initial and boundary conditions so as to provide simulations for situations ranging from dispersion in alluvial fans to overflow in the channels. Moreover the model is able to implement a number of rheologies to determine the flow characteristics.

A further detail of the underlying equations of the model is elaborated in the Literature Review (Chapter 2). The purpose of the model in this study is to serve as a generic framework to determine the uncertainty in landslide runout assessment. So before we delve into the topic further it is important to understand the concept of uncertainty, its types, the various sources of uncertainty and its applicability in the present context. This will not only provide a clear understanding of what uncertainty is but also provide a brief review of the type of uncertainty that this study will quantify and help in forward prediction of runout.

1.5. Uncertainty

Uncertainty can be defined as "*a general concept that reflects our lack of sureness about something or someone, ranging from just short of complete sureness to an almost complete lack of conviction about an outcome*" (NRC 2000). In recognising the uncertainty we are able to recognise the lack of knowledge of the system (knowledge uncertainty) and thereby restrict ourselves to the inherent variability (natural variability) which lead to the decision uncertainty.

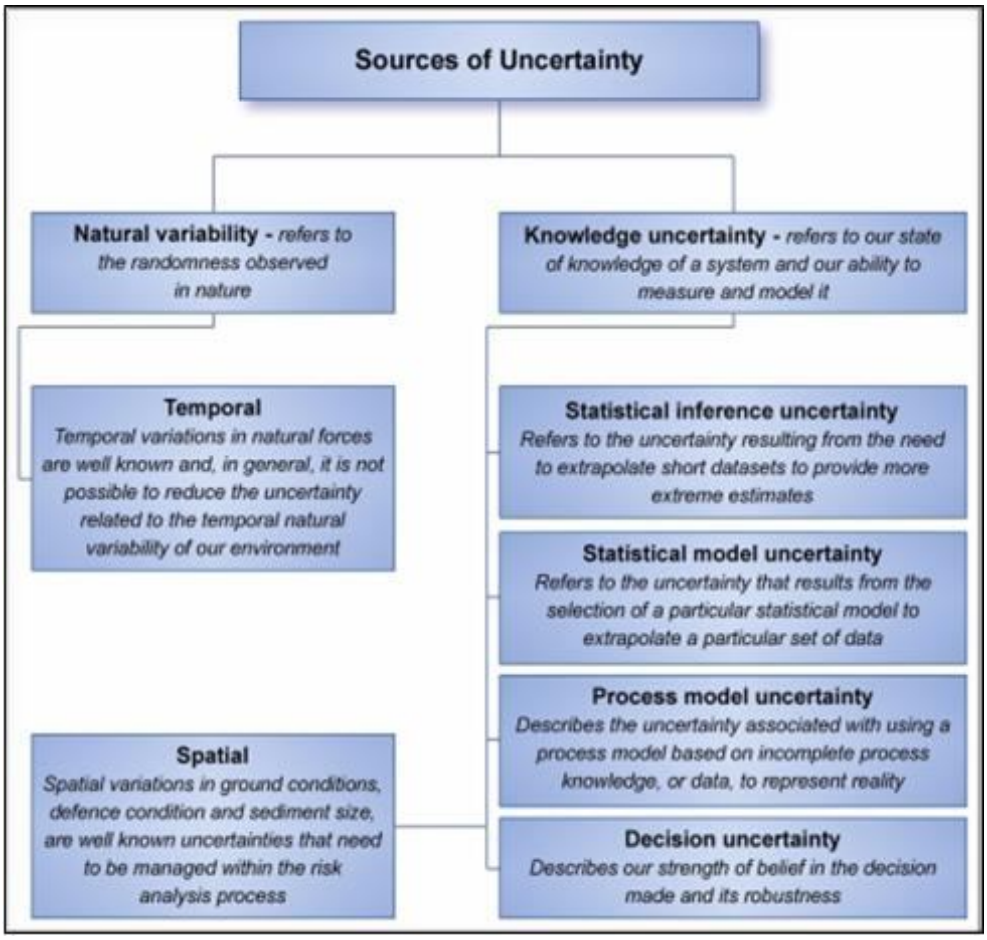

Figure 1.4: Sources of Uncertainty Highlighting the Types of Uncertainty
(Delft University of Technology, Accessed 31.05.09)

In the Figure (1.4) above the sources of uncertainty has been differentiated into Natural variability and Knowledge uncertainty. The former referring to the randomness observed in nature signifying both temporal and spatial randomness in this respect. Whereas knowledge uncertainty includes the following;

- Statistical Inference uncertainty deals with befitting of the datasets to the sample rather than to the entire population and is also referred to as the parameter uncertainty.
- Statistical Model uncertainty deals with the uncertainty evolved by extrapolation of data by a particular model due to varying results from different models.
- Process model uncertainty is derived from the incomplete knowledge of the processes involved in the modelling.
- Decision uncertainty results from the selection or choice of a particular action. Thus some or all of the uncertainty described above are inherent in some from or the other; both qualitative and quantitative, and investigation of these uncertainties requires emphasis.

When assessing hazards the uncertainty expressed in qualitative terms gives a false precision since the uncertainties in the analyses are not quantified. Moreover for the estimation of risk it is required to know the uncertainty in the hazard. Thus quantitative uncertainty estimation is a better option applying both numerical and analytical methods (Hammonds et al. 1994).

Uncertainty begins from the very process of "*geographical abstraction, data acquisition and geo-processing to the use of the data*" (Zhang and Goodchild 2002). Uncertainty lies in the parameters that are required as inputs in the model. It can be stated that uncertainties may arise also from the methods used meaning "*uncertainties from measuring, uncertainties from sampling, uncertainty from*

reference data that may be incompletely described and uncertainties from expert judgement" (IPCC Report 2006). Thus uncertainty is a cumulative effect of the a) measurement errors, b) methodological errors and c) natural variability.

It can be stated here that uncertainty is an important part of decision making and is of two main types namely, aleatory and epistemic (Swiler and Giunta 2007). Aleatory uncertainty can be defined as an inherent variation associated with the physical system or the environment, also referred to as variability, irreducible uncertainty, stochastic uncertainty or random uncertainty. Epistemic uncertainty on the other hand, is due to a lack of knowledge of quantities or processes of the system or the environment, referred to as subjective, reducible and model form uncertainty (Oberkampf 2005). Aleatory uncertainty is variable over space and time, or populations of individuals or objects. This variability is characterised as random or stochastic and probabilistic models are used for its expression. Epistemic uncertainty consists of model or structural uncertainty and parameter uncertainty. The former is considered as the appropriateness of the model structure while the latter arises in the process of employing a specific value to the quantity ranges concerned. Thus epistemic uncertainty results from the inability to measure variables at all points in space and time (Merz and Thieken 2005).

Uncertainties in models range from the exact to the inexact. It is inherent in the mathematics, the computational representations and computational aspects of the models which lead to generate uncertainty in the GIS results (Hwang et al. 1998). Emphasising the uncertainty in models Hwang et al (1998) formalised uncertainty as follows:

$$\left| O_d - O_r \right| = \varepsilon \quad \textbf{Eq 1}$$

Where, O_d is the set of desired output; O_r is the set of actual output; ε is the set of homomorphism values, where homomorphism refers to the same basic structure in which the elements and operations may appear to be entirely different where the results of one system often apply to the other system. Thus ε must decrease to increase homomorphism or to reduce uncertainty which requires improvement of the model. Though the models maybe improved there lies an inherent uncertainty which needs to be identified, described in order to formalize it in a GIS environment so that information for the propagation of uncertainty can be availed.

Attempts to streamline and create a framework for an acceptable method of uncertainty quantification for landslide runout modelling are largely lacking. Generation of the inherent uncertainties in the numerical models and of the input parameters would make landslide hazard assessment more quantitative. In this research, an attempt is made to quantify the spatial uncertainty (extent and depth) that emerges from numerically modelling landslide runout. The study is expected to create a framework for determining uncertainty in the determination of the parameter derived through back analysis and the uncertainty in the prediction of depth and velocity. Uncertainty assessment of landslide hazard models are closely linked to the sensitivity of the model results to the input parameters, a statistical method for the propagation of uncertainty.

1.6. Sensitivity

A sensitivity analysis is the result of the effects of changes brought about in the input values (Henrion and Small 1992). It can be stated as "*the study of how uncertainty in model predictions is determined by uncertainty in model inputs*" (Lilburne and Tarantola 2009). If uncertainty concerns with the quantification of the magnitude of the uncertainty in the prediction as a result of input uncertainties, sensitivity analysis computes the source of uncertainty in the model (Saltelli et al. 2004). It is the

quantification of the rate of change of the model output as a result of minor variations in the uncertain inputs.

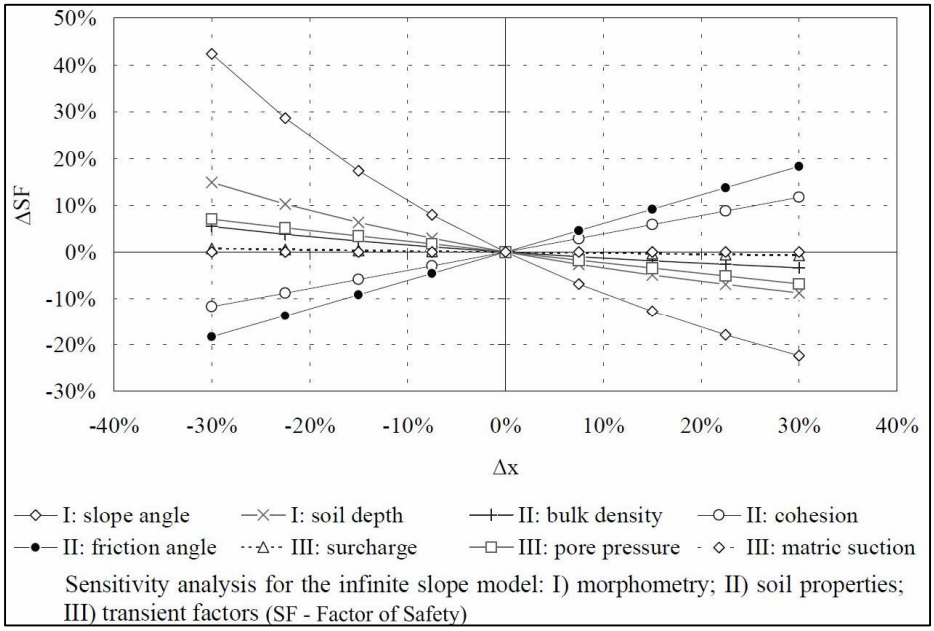

Figure 1.5: An example of model sensitivity to input parameters and the resultant uncertainty (Adopted from (van Beek, 2002))

The present study tries to evaluate the uncertainty in the parameter of the model by conducting a sensitivity analyses with respect to the rheological parameters. Calibrating the model and back analyzing the values for the sensitive parameters would help in the determination of the intrinsic parameter uncertainty. In this case the parameters for which the uncertainty will be judged through sensitivity analyses are the basal frictional angle μ (Mu), the turbulence coefficient (ξ, Si the turbulent factor in Voellmy Rheology) and the scour rate (the rate at which the materials are entrained from the landslide path). An attempt has been made to determine the variability of each of these parameters using the Z-Score method (Hussin, 2004). This will help visualise the variability of not only each of the parameter but the ranges of parameter values used for the calibration procedure. The second moment of the mean is used as the standardizing values and the curve derived is transformed into a standardized distribution curve or the Z distribution. This helps in the determination of the amount of variability of each of the ranges of values used for the above parameters while calibrating the model.

1.7. Aims and Objectives

The aim of the study is to quantitatively analyse the uncertainties in physically-based landslide run out modelling. To understand the amount of uncertainty derived as a result of various factors. This includes the parameter uncertainty as well as the uncertainty in the model output in an attempt to determine the uncertainty in the range of parameters as well as the prediction of the deposit depth and velocity for the case study scenario using the MassMov2D numerical simulation model. The specific objectives of the present study have been stated below:

- **To analyse the applicability of MassMov2D in landslide runout estimation**

- **To analyse the sensitivity of the model to various input parameters**
- To use the Z score method to conduct the sensitivity analysis and subsequently determine the variability of the possible range of parameters
- To identify the most uncertain parameter(s)
- **To analyse the overall uncertainty in the model output (depth and area)**
- To quantify the uncertainty in the prediction of the deposit depth
- To demarcate the area for which there is uncertainty in the prediction of varying deposit depths

1.8. Research Questions

- ✓ What are the different parameters used in physically based landslide runout models?
- ✓ What is the natural (synthetic) variability of each of these parameters?
- ✓ What are the different types of rheologies used in landslide runout models?
- ✓ Which is the simplest rheology applicable for modelling landslide runout?
- ✓ Which are the parameters to which MassMov2D is the most sensitive?
- ✓ Which parameters are to be used for the model calibration and why?
- ✓ How to express the overall uncertainty of model predictions?

1.9. Study Area

The choice of the study area was based on the availability of the dataset for the current study.

1.9.1. Location of the study area

The study area is a shallow landslide that occurred in Peringalam, a asmall village located in the upper catchment basin of the of the Meenachil river in Kerala and falls administratively in the Kottayam district. This region has experienced various types of landslides of which the local 'Urol Pottal' or debris flow is most frequent (Kuriakose et al. 2009a). This area was chosen for dynamically modelling due to the availability of data from previous research comprising in various parts of the region (Kuriakose et al. 2009a, Kuriakose et al. 2009b).

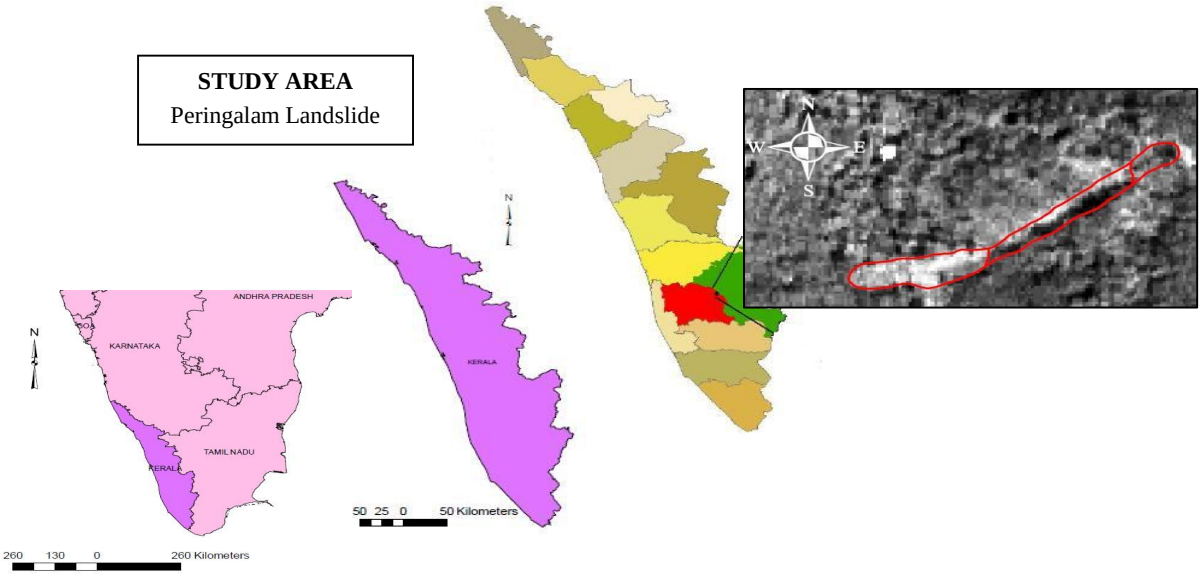

Figure 1.6: Location Map (Modified after(van Westen et al. 2009, Under Review))

1.9.2. The Physiographic Setting

The study area lies in the Central part of the Western Ghats. Since the region lies in the state of Kerala a brief review of the physiographic setting of Kerala is also relevant.

The state of Kerala lies between 80 17’ 30”N to 12027’40”N and 74051’57”E to 77024’47”E with an areal extent of 38,863 km3 flanked by the Arabian Sea on the west and the Western Ghats towards the east, along a north-south stretching coastline of 560 kms, varying in width of 35 to 124 kms (Kuriakose 2006). Around 47% of the state of Kerala lies in the Western Ghats and is one of the most densely populated (819 people/m2) states of India (Census 2001). A detailed description of the physio-climatic setting of the region can be found in Kuriakose et al. (2008)

1.9.3. The Meenachil catchment, Peringalam

The study area is surrounded on its eastern and north eastern parts by escarpments. The area forms part of the highland region of Kerala (Thampi et al. 1998) and falls within the Western Ghats scarpland (Kuriakose et al. 2009a). The region is bounded on the East by the Perimedu plateau margin with all the requisites of slope failure or mass movements. The Meenachil river originates form this plateau edge with all its tributaries flowing along the plateau edge. Peringalam is a small village in the upper catchmment of the Meenachil river. Research in the region revealed that continuous rain spell lasting for 9 hours and with 147mm rainfall is sufficient to cause landslides (Kuriakose et al. 2009a). Most of the debris flows in the region occur in slopes > 20 degrees and above 300m a.s.l (Thampi et al. 1998).

Figure 1.7: Debris Flow at Kaipalli, Meenachil Catchment, (Hamsa,CGIST, University of Kerala

The area is composed of hard crystalline rocks with quartzite, charnokite, biotite gneiss, pink/grey granite and dolerite as the cropping material. Chornokite occupies 93 % of the area (Vijith and Madhu, 2007). These rocks weather very slowly, forming layers of shallow frictional sandy soils interbedded with thin saprolite and lithomargic clay (Kuriakose et al. 2009a). The soil inherently lacks significant cohesion (Chandrakaran et al., in Kuriakose et al. 2009a). An attempt to physically model shallow landslide initiation in the region reveals that the stability of the slope is highly sensitive to soil depth (Kuriakose 2006).

1.9.4. The Peringalam Landslide

The Peringalam landslide occurred in the a hollow upstream of a first order non perennial stream (c.f Figure 1.6 for the location) on 14/10/04 at 5.00 pm (Figure 2.3) causing considerable damage to cultivable land and blocking a road that connects the village of Peringalam to the nearest major town, Poonjar. A similar event had occurred in the same first order stream in 1994 (Kuriakose et al. 2009c). The landslide originated at an altitude of 500 m a.m.sl and had a total runout distance of 290.5 m. The landslide was thoroughly investigated in the year 2007 for deriving post event (post hereafter) and pre event (pre hereafter) DEMs of the landslide affected area. A precision GPS survey (using Leica SR20) was conducted all along the landslide resulting in over 15000 points both on the landslide and spanning

few meters around it. Using this data a 1 m resolution post DEM was derived by interpolating it with simple IDW. The resultant DEM had a coefficient of determination of 0.8 with respect to independent data points that were not used for interpolation. Further, by excluding the landslide body and linearly interpolating between the GPS points that falls on the sides of the landslide body and a 20 m interval contour map (converted to 1 m interval points), a pre DEM was generated. This interpolated pre DEM had an accuracy of 0.6 (coefficient of determination estimated with independent data points not used for interpolation). By subtracting the post DEM from the pre DEM an estimate of the initial volume, final deposition volume and scoured volume was estimated. Table 1.2 provides the details of the Peringalam landslide.

Table 1.2: Characteristics of Peringalam Landslides

Initial Volume (m^3)	**Deposit Volume (m^3)**	**Angle of Internal Friction (°)**	**Average Soil Cohesion (InitiationZone) (kPa)**	**Area of Landslide Body (m^2)**	**Average Slope (°)**
437	1533	~ 35 (Standard Deviation 7.1)	3.16 (Standard Deviation 0.7)	Initiation Zone: 784 Runout Zone: 2336 Deposition Zone: 2680	Initiation Zone: 142.63° Transport Zone: 109.76° Deposition /Runout Zone: 114.01°
The Peringalam debris flow modelled in the study using MassMov2D is a confined debris flow consisting of an observed volume of 437 m3, at an elevation of above 500 m elevation, which flows over a runout distance of 290.59 m approximately as measured by demarcating the landslide part over the Cartosat I image (date of pass, November 18, 2007). For the purpose of modelling the entire landslide area within a boundary was taken for the simulation. An analysis of uncertainty was carried out in the deposition zone termed in the present study as the region where the post event runout of material occurred.					

1.10. Structure of the Thesis

The thesis is structured so as to provide an overview of the work done. The ***first chapter*** of the thesis provides a brief overview of the concept of landslide runout, the significant parameters affecting landslide runout depending upon the type of mass movements, the concept of landslide modelling with emphasis on dynamic modelling and a brief introduction of the MassMov2D model used in the study. It also lays emphasis on the concept of uncertainty and sensitivity providing a glimpse in to the location and the type of landslide to be modelled.

The ***second chapter*** is a detailed account of the dynamic models in landslide runout modelling and the various modelling approaches. It also explains the governing equations on which the model is dependent, the rheological models and their significance in runout modelling. It is here that the detail of MassMov2D is also provided. The chapter also lays emphasis on the state of the art research carried on in this field and the approaches used to move ahead in the current study.

The ***fourth chapter*** is devoted to the methodology used in the current study and the materials required for the parameterization of the model and derivation of the observed values for back analysis. It is here that the reliability of the input parameters of the model is also available. In the ***fifth chapter***, ***sixth*** and the ***seventh*** chapters contain the results and discussions of the present study. The ***final chapter*** provides the Conclusion and Recommendations of this study.

2. Literature Review

2.1. Landslide phenomena

Landslides result in disasters with impacts on society that are irreparable (Sassa in Sassa, Fukuoka et al. (2007)). A typical landslide consists of the source zone, runout path and the deposition fans (Chen and Lee 2004). A typical landslide long profile can be distinguished as the zone of depletion and the zone of accumulation.

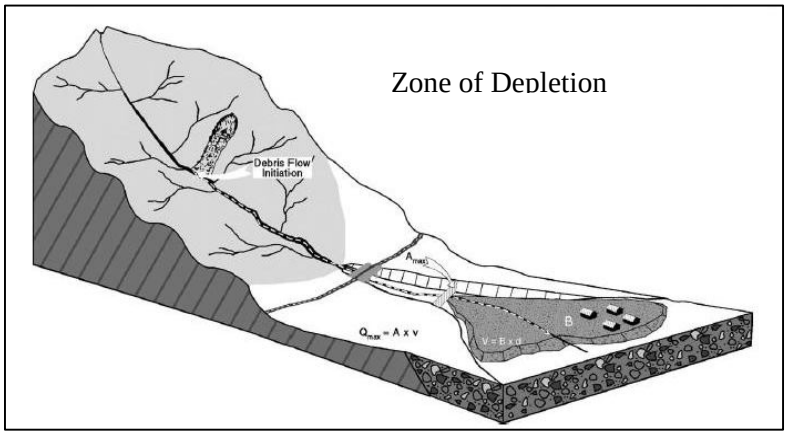

Figure 2.1: Conceptual framework of landslide phenomena (Modified after Jakob 2005)

In the case of the former the elevation is said to decrease where as in the case of the latter the ground elevation is said to increase. Both these changes can be determined from the differences of the topographic maps or the digital elevation models of the pre and post event scenario. As stated in the Landslide Special Report 247, the volume increase determines the zone of accumulation which is considered to be larger than the zone of depletion because the ground dilates profoundly. This area serves as the potentially disastrous zone and can be further classified into long and short runout landslides depending upon the runout length. Now the length of the runout or the travel path of a landslide is dependent upon the volume of the material displaced (Legros 2002). Moreover other factors like velocity, the rate of shear, slope and material property also play important role in the determination of the characteristics of runout of the displaced material. There may also be occurrences where the rock slide is converted into a debris flow or a rock avalanche this may change the character of the flow which determines the type of runout. Geertsema et al. (2006) have provided a detailed classification of the various landslide phenomena in a diagrammatic representation, in Figure 2.2. The diagram illustrates the runout of landslides in rocks in soils and in earth flows most of which take catastrophic forms. It also emphasizes the fact that the runout of landslides is dependent upon the type of the material displaced. Distinction has been made in the diagram between slides in rocks and those in soils and the latter part of the diagram provides a detail of a complex slide that may begin as a rock slide and may end in earth flow, debris flow or debris avalanches.

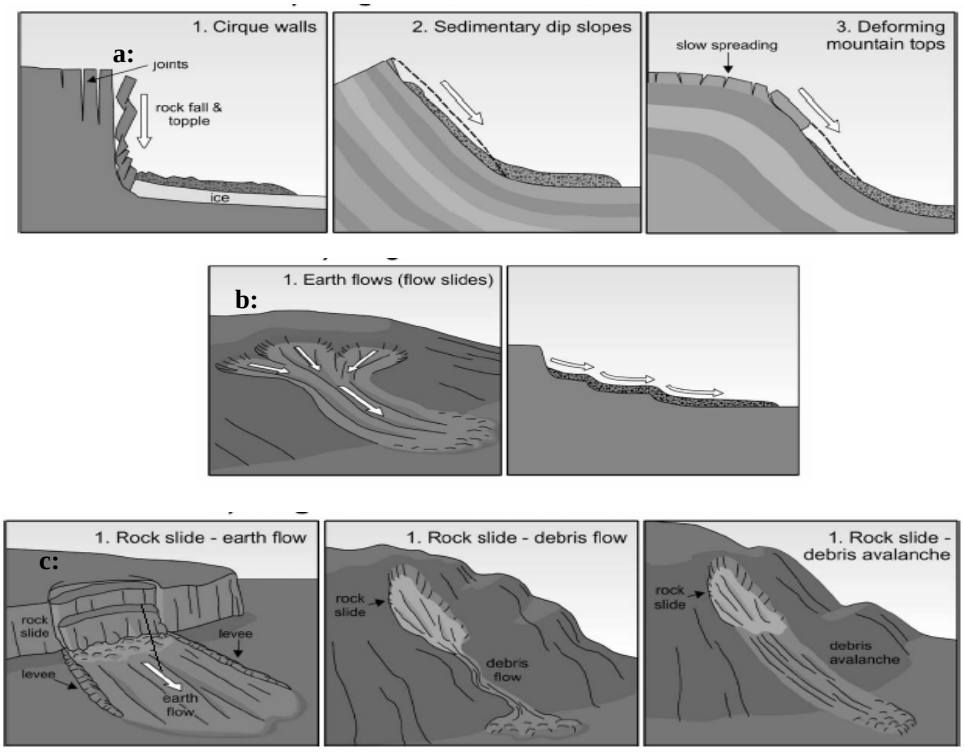

Figure 2.2: Long landslide runout, a: In Rocks, b: In Soils, c: In Rocks and Soils

Similarly short landslides though not diagrammatically represented here have severe effects that lead to immense loss of lives and damage. A series of smaller rock slides, collapses, and/or rockfalls for example have shorter runout but when infrastructure is located close to the toe of the slope this may result have a large destructive potential (Willenberg et al. 2009). Thus a range of behaviour of different types of landslide runout enables the necessity to determine the processes that act on the unstable rock or debris volume so that the post failure runout (that include travel distance, velocity, deposit depth) can be quantified with respect to the area under risk (Hungr et al. 2005). What needs to be emphasised is not the initiation of the landslides but the post failure runout hazard. It is this segment of the landslide where human life is most vulnerable and the impact of which cannot be set right.

2.2. Landslide Risk and Hazard

Risk can be defined, in the words of Varnes (1984), as the '*expected number of lives lost, persons injured, damage to property and disruption of economic activity due to a particular damaging phenomenon for a given area and reference period*.' It is quantified as the product of hazard and the vulnerability, cost or amount of the elements at risk explained by the following,

$$Risk = \sum \left(H \sum (VA) \right) \quad \text{Eq 2}$$

Where, H= the probability of occurrence of a phenomena and can be both spatial with respect to a location and temporal with respect to time.

V = Physical vulnerability of a particular type of element at risk (0 to 1) for a specific hazard and for a specific element at risk, A= Amount or cost of the elements at risk example number of buildings etc.

The formula though looks simple involves the calculation of not only the elements at risk for each of the locations of landslides but also the determination of hazard. Thus landslide risk assessment and management requires a decision framework which can be portrayed as follows (Dai et al. 2002):

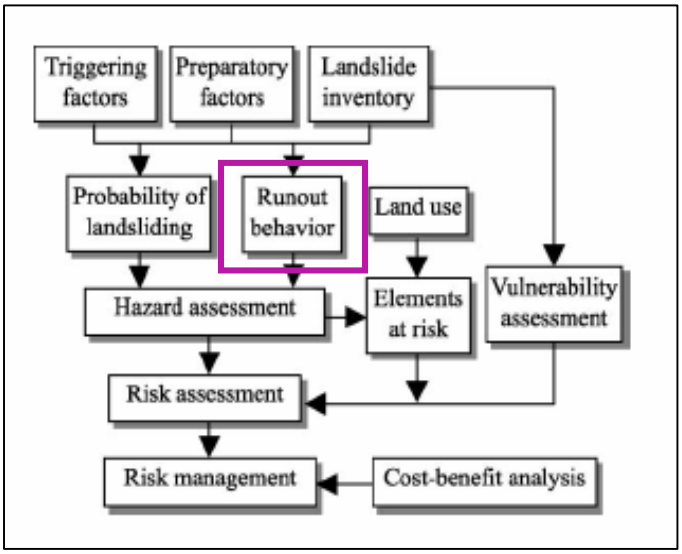

Figure 2.3: Framework for landslide risk assessment and management (Dai et al. 2002)

In this light *hazard* assessment has gained considerable significance and according to the physical scientists maybe defined as the probability of a reasonably stable condition to change abruptly (Scheidegger 1994) or as defined by Varnes, as "*the probability of occurrence of a potentially damaging phenomenon within a given area and in a given period of time*". Hence hazard is a function of the spatial probability related to static environmental factors such as slope, strength of materials, slope, etc and the temporal probability linked to static factors like slope and hydraulic conductivity indirectly and directly to the dynamic factors like rainfall and drainage (van Westen et al. 2005). Guzetti et al. (1999) have stated that the definition incorporates the concepts of *magnitude, geographical location and time recurrence*. It was stated that *magnitude* signifies the dimension or intensity of the phenomena, the *geographical location* implied the identification of the location of the event and the third referred to the temporal frequency of the event.

But *landslide hazard*, the term does not specifically signify the landslide deposit or the movement neither of material downslope nor to the movement of an existing landslide mass. The inherent inadequacy of the term due to the vistas of landslide phenomena which are both complex and variable make the acceptance of a single definition of landslide hazard unsuitable. This is because each type of slope failure and related phenomena requires to be dealt separately. Moreover for landslide risk assessment purposes an accurate prediction of the dynamic behaviour of potential landslides is a basic factor in order to define the limits and extension of damageable areas (Revellino et al. 2008).

Thus *Landslides* defined as the *movement of mass*, debris or earth down slope (Cruden 1991) incorporates within the field of landslide science the dynamics of landslides. Now the study of dynamics includes the science of fluids that is air, water and gases. Of late, the study of landslide as a dynamic science has become the core study of landslide science as a new discipline in landslides (Fukuoka et al. 2007).

2.3. Methods of Predicting the Hazard Area and the Kinematic parameters

Owing to the increasing concerns of quantifying risk in landslide studies the generation of quantitative risk zonation maps has gained considerable significance (Van Westen et al. 2005). Moreover, natural phenomena like landslides being difficult to predict due to the complex nature of interactions (both inter and intra) between the various factors (Karam 2005) leads to various difficulties

related to generation of landslide inventory maps that include information on the date, type and the volume of the landslide, the spatial and temporal probability, the assessment of landslide vulnerability and also the runout of landslides (van Westen et al. 2005). Soeters and van Westen (1996); van Westen et al. (1997); and van Westen et al. (2005) are of the consensus that the probability of land sliding can be assessed by inventory, heuristic, statistical and deterministic approaches. Hurlimann et al. (2006), provide a four step method of multidisciplinary hazard assessment as illustrated in Figure 2.4.

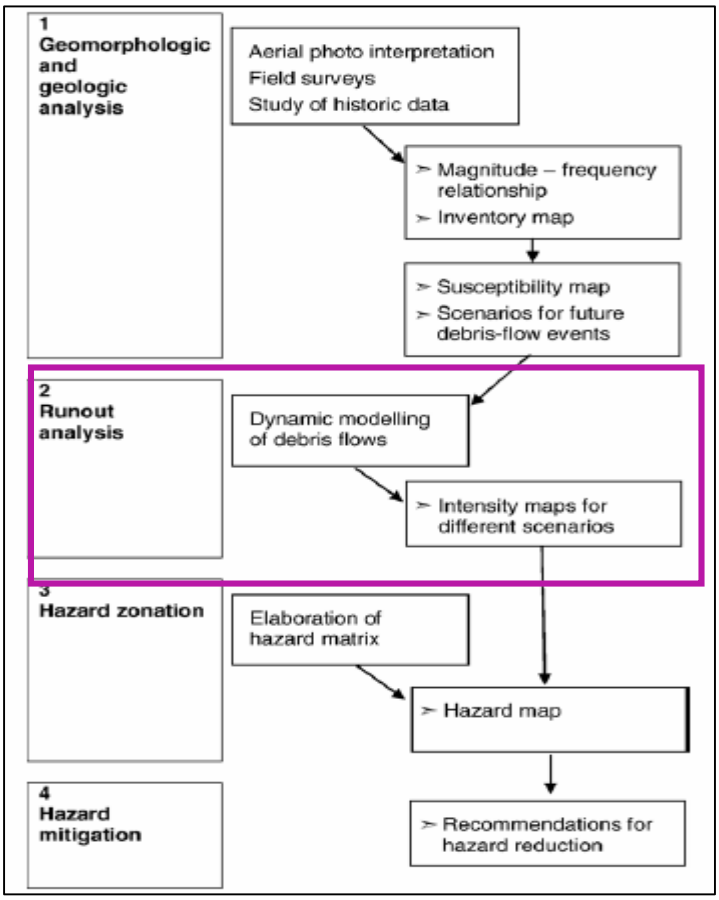

Figure 2.4: Four Step Multidisciplinary for Hazard Assessment (Hurlimann et al. 2006)

It can be emphasized that the analyses of the characteristics of the runout area have gained considerable significance in the quantitative hazard assessment. In the view of estimating hazard intensities used as inputs in risk studies accurate prediction of the runout distances, velocities and flow rheology provides insight for the design of protective measures (Armento et al. 2008). Revellino et al. (2008), identified a three step approach for hazard assessment, firstly to identify the geomorphologic factors controlling landslides, secondly, determination of the parameters defining landslide intensity (Section 1.1) and thirdly to predict the landslide runout distance. Dynamic codes are hence essential for the determination of hazards under different scenarios. Before we delve further into the discussion the following provides a glimpse of the concept of modeling, as well as approaches and types of modeling.

2.4. Modeling Runout of Landslides: Methods and Approaches

Modelling landslide dates back to the conceptual model which required the identification and mapping of a set of geologic-geomorphologic factors that were related to slope stability (Carrara 1993). It involved the contribution of these parameters to landslide and hazard zonation. Models can be defined as the representation of the real world scenario. They maybe considered as a logical sequence of possible events which are based on small scale processes that are known and for which there exists no hypothesis as such (van Loon 2004). Models can be precisely defined as "*a simplified representation of an object of investigation for purposes of description, explanation, forecasting or planning"* (Frotheringham and Wegener 2000). Models can be broadly classified as spatial model which is a two dimensional investigation of space and attribute and a space-time model where the time dimension adds a tri-space to it. Bromhead ((1986) in Frotheringham 2000) has broadly classified landslide models as follows:

- Slope stability model
- Rheological model

- Hydrological landslide model

Considering landslide phenomena as not only a simple two dimensional feature but rather a three dimensional one with a complex temporal context, Brunsden (1999) is of the opinion that they are dynamic systems linked to space and time and are sensitive to inherited and current controls. He further went on to distinguish models as Slope stability models which he further distinguishes as models of plane slip surfaces and method of slices. Further mention was also made of the advanced computer models for refined analyses of internal stress state of the slope, residual strength models and models of slope failures.

Dynamic models were classified based on equations of motion. Modelling landslides during motion the numerical models of rock slopes to explore the site specific behaviour and fundamental mechanisms were determined and based on different methods such as the continuum methods, finite element method, etc.

Landslide models can be grouped in various ways (c.f Section 1.2, Fig. 1.2). They maybe identified as empirical approach, physical scale modelling and dynamic modelling (Chen and Lee 2004) or can simply be classified as empirical, analytical and numerical models (Dai et al. 2002).

The latter has been used most effectively in runout analyses (Dai et al. 2002). Dynamic models have the merits of predicting the single causative factor and being related to deterministic or physically based models have some correlations between the inputs and the output. Moreover they are used for the study of landslides in different dimensions be it 1D, 2D or 3D. The can also be applied at various scales.

2.5. Dynamic Models

Dai et al. (2002) have discussed in detail the runout behaviour of landslide materials that consists of the three approaches for the determination of the runout distance they being classified as the Empirical methods, the Analytical methods and the Numerical methods.

The empirical methods include most specifically the mass-change methods and the angle of reach methods. In case of the former the mass and volume of the moving material is considered to increase or decrease due to deposition or loss of materials and the landslide halts when the volume diminishes considerably. The influence of the factors of slope gradient, vegetation types and the channel morphology on the changes in volume was studied by a multivariate regression analysis. The rate of change of volume was derived from the average of the volume and the runout length. Another method that can be discussed in this context is the angle of reach method where angle of reach is defined as the angle formed by the line connecting the crest of the zone of initiation to the distal margins of the zone of deposition of a landslide.

Applying this method Corominas (1996), in a detailed study of the influence of the factors on the angle of reach reveals that there exists a linear relationship between the decreasing angle of reach and the volume of the mass. It was conferred by him that the earthflows have the highest mobility and that rock falls have lowest mobility. Mention must be made of the UBCD Model (Fannin and Bowman 2008) an empirical model developed primarily in order to understand factors influencing the travel distance. The initial failure volume of the event together with the changes in the magnitude of the landslide as a result of entrainment and deposition along the runout path help to determine the point at flow volume diminishes to zero. It also helps calculate the travel distance in this way. But in terms of hazard zoning this method has the limitation of being unable to determine any information on impact pressures and the potential damages (Barbolini et al. 2006).

Dai et al. (2002) while discussing the analytical approach of deriving dynamic parameters of landslides also emphasized the lump mass approach in which the debris mass is assumed as a single

point. Emphasis has also been laid on the model proposed by Hutchinson (1986) which assumes the material to be uniformly spreading and the basal friction as purely frictional.

Table 2.1: Various modelling approaches

Approach	Models/ Methods	Merits	Demerits	References
Empirical	Mass Change	Studies the influence of slope gradient, vegetation types and channel morphology by a multivariate regression analysis.	Does not explicitly account for the mechanics of the movement process.	Dai et al. 2002; Fannin and Bowman 2008; Prochaska et al. 2006.
	Angle of Reach	Derives a linear relationship between factors influencing the angle of reach and the volume of the materials.	The scatter of the data is too large for any reliable prediction. Only preliminary prediction of the travel distance is possible.	
Analytical	Lumped Mass Models	Simple approach. Can provide effective means for the calculation of runout distance, velocity and acceleration of the materials. Suitable only for comparing paths which are similar in geometry and material properties.	Keen analysis of the results essential because the calculated gravity centre is not always the geometry centre. Unable to determine complex patterns of failure and internal deformation of the sliding mass. Unable to account for the lateral confinement and spreading of the flow and also the resulting flow depth. Unable to identify basal elevation function pattern and downhill condition (such as obstacles). Unable to simulate the motion of the flow front or the momentum changes.	Chen and Lee 2004; Dai et al. 2002.
Numerical Methods	Distinct element method	Handling large displacements, fracture openings and complete detachments is straight forward. Able to understand mechanisms of segregation and deposition process encountered commonly in granular flows. Able to simulate runout distance and velocity	Determination of the location and geometry of the natural discontinuities Not yet amenable to be a general design tool in the estimation of the travel distance. Computationally intensive hence limited to modelling small 2D and 3D problems.	Chen and Lee 2004; Dai et al. 2002; Van Asch et al. Unpublished; Wong and Ho 1997.
	Continuum Models	With the application of the rheological equations it can best define the characteristics of boundary flow mixtures. Able to predict acceleration, velocity and runout distances.	Evaluation of the hydro-mechanical properties of the geologic materials unable to be determined in the laboratory	Chen and Lee 2004; Van asch et al. unpublished. Dai et al. 2002.

Chen and Lee (2004) on the other hand classified dynamic models into lumped mass models, distinct element models and continuum mechanics model (Section 1.2, Fig: 1.3), the former being approached analytically and the latter numerically.

In the lumped mass models the motion of flow is considered as a uniformly spread out sheet. The pore water pressure at the initial stages is assumed to be high and its dissipation is calculated by the 1D

consolidation theory thereby determining the runout distance. A similar model proposed by Sassa, (1986) is based on the principle of energy conservation, the primary assumption being that energy losses result due to dissipated friction during the movement. Thus the apparent friction angle is the measure of the fluidity and the friction losses during movement influenced by the internal frictional angle and the pore pressure, the former being measured by a ring apparatus.

Numerical methods of determining the runout behaviour include the distinct element method and the continuum methods. The distinct element model can be defined as the numerical technique that studies the mechanical behaviour of granular assemblages of materials subjected to gross motion. In other words, distinct element methods represent a continuous assemblage of blocks formed as a result of connected fractures in the blocks of the region under consideration. The equations of motion between these blocks are solved by the detection and treatment of contacts between these blocks (van Asch et al. unpublished). Hungr et al. (2005) has illustrated precisely an overview of the discrete and the continuum numerical methods as follows:

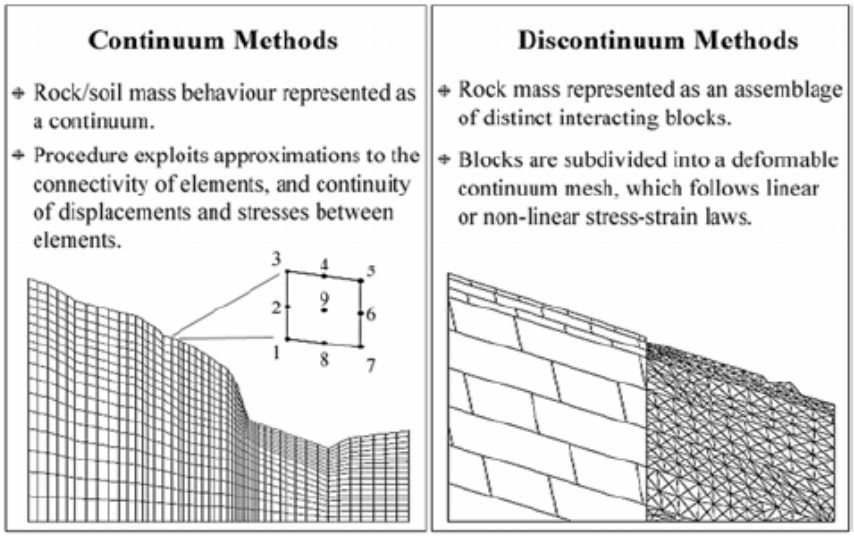

Figure 2.5: Continuum and Discontinuum or Discrete Methods of Numerical Modeling (Hungr 2001)

Continuum models are based on the mass and momentum conservation equations. When used with rheological equations these models can best outline the boundary characteristics of flowing mixtures as well as predict the flow properties like velocity, acceleration and the runout distance (Hungr et al, 2005). The time and space dimensions in these models are determined by the use of the following methods, namely, the limit equilibrium method (LEM), the finite element method (FEM), the boundary element method (BEM) and the finite difference method (FDM). As stated by van Asch et al. (unpublished) the LEM's do not consider the deformability of slope since they do not evaluate the stress and strain relations with the slope, whereas the FEM and the FDM are much flexible since they are able to handle material heterogeneity, non-linearity and boundary conditions. BEM's on the other hand highly simplify the input requirements because they require discretization at the boundary condition. They are hence unable to reproduce conditions where more than one materials are used nor in areas of spatial heterogeneity.

The continuum models are further classified into single phased models and two phased models depending upon the size and type of the materials, the viscosity etc. Referring to Takahashi (in Sassa et al. 2007) the single phased continuum models evaluate the stress and the rate of strain relationships on the basis of the empirical formulae or laboratory derived inputs or from back analyses of the model to similar events on the field.

In case of the two phased models the material is considered to have large interstitial spaces so that the saturated fluid is slurry or water having a liquid phase whereas the solid phase consists of a continuum medium. Hence these models have two equations of motions one for the solid and the other for the liquid phase. Thus according to Rickenmann (2006) in a continuum model the simulation allows the determination of the flow parameters and also deposition along the path where the material is considered as a quasi homogeneous material. Most of the models are hence based on the Bingham and viscoplastic fluid (Fraccollo and Papa 2000; Laigle et al. 1997; Takahashi, in Sassa et al. 2007).

Other methods of analysing the fluid motion are by using the Lagrangian and the Eulerian methods. The former method is the method analyses the trajectories of the fluid parcels while the latter observes fluid velocities at fixed positions (Price 2006). Thus in case of the Lagarangian system the two independent variables are time, t and the label for the fluid particle x0 which is considered as the position vector x0 at some time, t = 0 . Thus any flow variable has the is the function of F(xo,t) or x(x0,t) whereas Eulerian method emphasizes the flow at some spatial point x, so that the independent variables x and t are written as F(x.t) (Kundu and Cohen 2002).

2.6. Rheological Models

The word *Rheology* refers to the study of deformations and the resulting flow of matter on the surface due to applied stress (Rifai 2008). This deformation results from the force applied in the form of tension, compression, shear, bending, or torsion. The force applied is referred to as *stress* in Geology and the resulting deformation is termed as *strain*. The rheology theory is applied when the material is no more considered as a classical Newtonian fluid and being a Non-Newtonian fluid the characteristics motion of the material is determined by this property.

The rheological behaviour of solids can be classified as ***brittle*** (fracturing under stress), ***plastic***

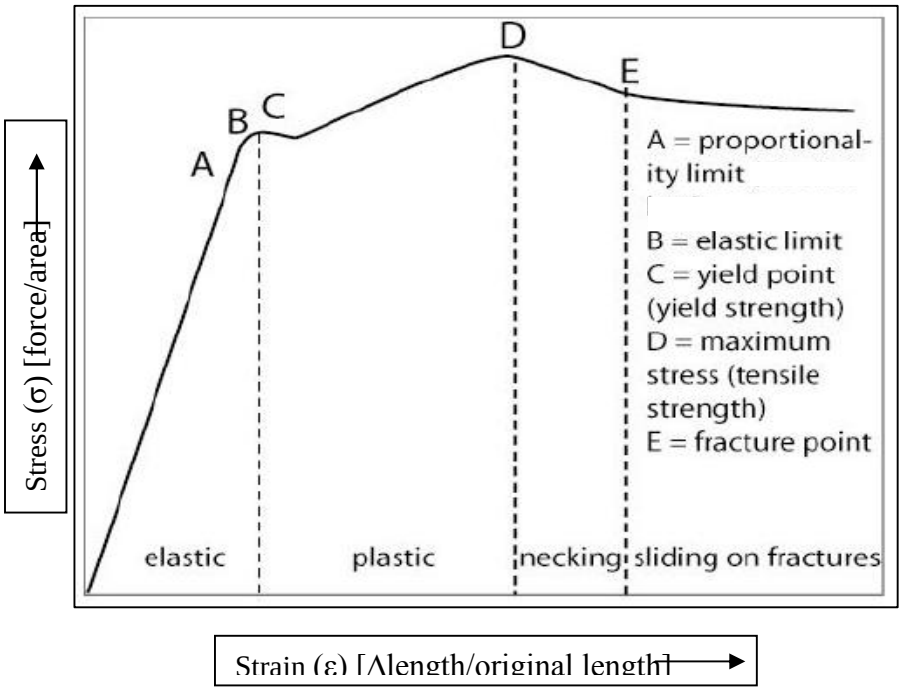

Figure 2.6: Rheological properties of Stress and Strain influencing deformation, (Elkins-Tanton, 2008)

(deforming under stress but not retaining the original form when the stress is removed) and ***elastic*** (deforming under stress but retaining the original form as soon as the stress is removed). In case of rock avalanches the rocks on the surface of the Earth are elastic to certain extent and fracture when the stress is increased. But in case of ductile substances with the increase in stress they deform plastically whereas

elastic deformations occur in a small stress range (Elkins-Tanton 2008). Figure 2.6 depicts that with the increase in the stress and the rate of deformation of the material from elastic to plastic and a small period of retention or the necking after which the material is dominated by shear stress.

Thus the key concepts that influence solid flow are viscosity and the material's resistance to deformation. Viscosity is the relation between the shear stress (σ) and the strain rate or the rate of deformation (ε), expressed as follows:

$$\eta = \sigma / \varepsilon \quad \text{Eq 3}$$

Hence the shear stress and viscosity are directly proportional. Materials with viscosities not dependent on stress are called Newtonian materials whereas those dependent on stress are called non-Newtonian materials. Whereas, those materials that are less viscous with response to shear stress are called thixotropic. Again there are materials that become highly viscous under the application of stress these materials are called dilatants. Mention must be made also of the Bingham plastics which deform only when the threshold shear stress rate is obtained.

It can be stated in this respect that the behaviour of a fluid can be Newtonian or Non-Newtonian. The Newtonian liquids have a linear relationship with shear stress and the angular deformation with a constant velocity, μ (Mu). Non-Newtonian fluids, on the other hand, have a non-linear relationship with shear stress and angle of deformation. The flow behaviour of the landslide mass considered as a Non-Newtonian fluid is governed by the following equations of mass and momentum:

$$\frac{\partial h}{\partial t} + \frac{\partial uh}{\partial x} + \frac{\partial vh}{\partial y} = 0 \quad \text{Eq 4}$$

Considering the equation in a Cartesian two dimensional framework it can be written as follows:

$$\frac{\partial h}{\partial t} + \cos \alpha\, x \frac{\partial uh}{\partial x} + \cos \alpha\, y \frac{\partial vh}{\partial y} = 0 \quad \text{Eq 5}$$

$$\frac{\partial h}{\partial t} + \cos \alpha x\, u \frac{\partial u}{\partial x} + \cos \alpha y\, v \frac{\partial u}{\partial y} + \cos \alpha x\, k \frac{\partial (\cos \propto x g h)}{\partial x} = -\cos \alpha\, x\, g(\tan \propto x + Sf\ qx) \quad \text{Eq 6}$$

$$\frac{\partial h}{\partial t} + \cos \alpha y\, v \frac{\partial v}{\partial x} + \cos \alpha y\, u \frac{\partial v}{\partial y} + \cos \propto y\, g \frac{\partial (\cos \propto y\, g h)}{\partial y} = -\cos \propto y\, g\ (\tan \propto y\, Sf\ qy) \quad \text{Eq 7}$$

where, h is the thickness or flow depth, *u* and *v* are the velocity vectors in the x and the y directions, *cos α x* and *cos α y* are cosine of the gradient of the bed in both the *x* and the *y* directions which help to transform the local reference system to the global one. *cos α* being the angle of the bed to the horizontal plane in both the x and the y directions. This takes the negative value if the flow is in the direction positive to the x and the y directions; *tan α x* and *tan α y* are the bed slope gradients in the x and the y directions. qx and qy are the coefficients where $|\mu|$ is the modulus of the velocity vector $\sqrt{u^2 + v^2}$ (m.sec):

$$qx = \frac{-u}{|\mu|} \quad \text{Eq 8} \qquad qy = \frac{-v}{|\mu|} \quad \text{Eq 9}$$

The momentum equation consists of three parts; the acceleration due to gravity denoted by g (m.sec2), a convective acceleration term both in the x and the y direction denoting the rate of change of acceleration with time, the second and third term of the equation and finally, a pressure acceleration term, the fourth term in the equation. The pressure acceleration is denoted by the earth pressure coefficient (active/passive pressure coefficient) k which is defined as the ratio between the tangential and

the normal stresses. It defines the internal flow friction brought about in the material due to changes in the well depicted by the Rankine Theory where:

$$\lambda = tan\,2\left(45^2 \pm \frac{\phi}{2}\right) \quad \text{Eq 10}$$

Here, ϕ is the internal angle of friction related to the angle of repose. Hence k_{act} and k_{pas} can be determined as follows:

$$k_{act} = \frac{1-\sin\delta}{1+\sin\delta} \quad \text{Eq 11} \qquad k_{pas} = \frac{1+\sin\delta}{1-\sin\delta} \quad \text{Eq 12}$$

with two extreme values, kact ≤ 1≤ kpas which is one for a perfect fluid and is greater than zero for a fluid with greater viscosity. The former applies to region of expansion and the latter regions of compression. In case of dry granular rock fragments the k act and k pas will range between 0.02 and 5.0 respectively making the slide mass more reluctant to spread or contract (Hungr 1995). The term Sf denotes the flow resistance term due to momentum dissipation resulting from frictional stress from the bed (Begueria et al. 2009b). This is determined by the rheologies used in the model. Different types of rheology will determine the different types of material characteristics and hence help determination of the movement of the material.

Obtaining the apt rheology that influences the motion mechanism of landslide can be described as follows depending upon the stress and strain relations:

2.6.1. Visco-plastic Fluid Model

Landslide blocks that move under the influence of water and that after moving a considerable distance stops. This contributes to the fact that the material consists of shear stress that is more than the yield strength which aggravates motion and when the stress is reduced considerably the motion halts (Jakob and Hungr 2005). Hence the material is considered as a viscous fluid having some strength and can be numerically explained in 1D as follows:

$$\tau_{shear} = s_f + \mu\, dv_x/dz \quad \text{Eq 13}$$

where, s_f is the shear strength or the yield strength and dv_x/dz is the 1D shear deformation rate, v is the velocity of the material at height z. (Iversion in Jakob and Hungr 2005)

The Bingham Fluid model is the simplest visco-plastic model where the stress and the strain relations are portrayed as follows and considering n=1.

$$\tau = \tau_y + K\,(du/dz)^n \quad \text{Eq 14}$$

where, τ_y is the yield stress, u is the velocity at the height z and K and n are the numerical coefficients. The resisting shear stress depends on the constant yield shear strength and a viscous term that is dependent on the velocity and the inverse of the thickness of the material sheet (Hungr and Evans 1996). As Mckinnon (2008), has stated that the Bingham model may produce simulations of highly plastic materials primarily involving clayey material in a much better way.

The modification of the model led to the Coulomb-Viscous model expressed as follows,

$$\tau = c + \sigma_n \tan\varphi + \mu_b(\, du/dz) \quad \text{Eq 15}$$

where, σ_n is the internal normal stress and μ_b is the Bingham viscosity. This equation has been derived from the Coulomb friction model which states that the bulk intergranular shear stress on the plane of shearing is proportional to the bulk intergranular normal stress irrespective of the area of grain

contact, the magnitude of the stress components and the rate of shearing. Modification of the equation using the Bingham viscosity helps interpret granular viscous flows.

The Herchel-Bulkley fluid model where n<1 (Coussot 1995), details of which are available in Section 3.8, are also frequently in use to determine the motion of landslides where the materials are highly viscous.

The only drawback in all the above stated models is that it is fairly difficult to determine the τ_y and μ_b. Even laboratory experiments that help derive the values are seldom able to accurate simulate and account of the changes that may occur due to saturation of the material.

2.6.2. Dilatant Fluid Model

Materials that consist of grains larger than gravel size reach an area less than 4^0 with a very high mobility. Thus the resistance is said to be low due to the collision of grain particles providing stress-strain relationships in inertial and viscous regimes and expressed by the following two equations. Bagnold was the first to determine this model further details of which can be availed from Sassa et al. (2007).

$$p = a_i \cos\alpha_i . \sigma \lambda^2 d^2 (du/dz)^2 \quad \text{Eq 16}$$

$$\tau = p.\tan\alpha = a_i \sin\alpha_i . \sigma \lambda^2 d^2 p (du/dz)2 \quad \text{Eq 17}$$

where, p is the dispersive pressure in flow, a_i is the numerical coefficient, α_i is the collision angle and λ the linear concentration of grains.

The significance of this discussion is that these models help determine the resistance factor which in turn determines the yield stress which once overcome initiates the flow of the landslide (Coussot 1996). Some of the formulas to determine the resistance factor Sf have been explained in detail in Naef et al. (2006) illustrated in Figure (2.7).

Descriptor	Flow resistance relation	Flow resistance term S_f
A	Full Bingham	$S_f = \frac{\tau_0}{\rho g h}$ τ_0 can be determined by: $2\tau_0^3 - 3\left(\tau_y + 2\frac{\mu_B q}{h^2}\right)\tau_0^2 + \tau_y^3 = 0$
B	Simplified Bingham	$S_f = \frac{\tau_0}{\rho g h}$ with $\tau_0 = 1.5\tau_y + 3\frac{\mu_B q}{h^2}$
C	Voellmy	$S_f = \frac{q\sqrt{q^2}}{h^2 C^2 h_r} + \cos\alpha \tan\delta$
D	Turbulent & Coulomb	$S_f = \frac{n^2 q\sqrt{q^2}}{h^{\frac{4}{3}} h_r} + \cos\alpha \tan\delta$
E	Turbulent & Yield	$S_f = \frac{n^2 q\sqrt{q^2}}{h^{\frac{4}{3}} h_r} + \frac{\tau_y}{\rho g h}$
F	Turbulent, Coulomb & yield	$S_f = \frac{n^2 q\sqrt{q^2}}{h^{\frac{4}{3}} h_r} + \frac{\tau_i}{\rho g h}$ with $\tau_i = \min(\tau_y ;\ \rho g h \cos\alpha \tan\delta)$
G	Quadratic	$S_f = \frac{n^2 q\sqrt{q^2}}{h^{\frac{4}{3}} h_r} + \frac{\kappa\eta q}{8h^3\rho g} + \frac{\tau_y}{\rho g h}$
H	Coulomb viscous	Full Bingham with $\tau_y = \rho g h \cos\alpha \tan\delta$

Figure 2.7: Frictional Resistance for Various Rheologies (Naef, et al., 2006 in Rifai, 2008)

But according to Naef et al. (2006) there are no methods for determining the bulk representative parameters that is the viscosity or the yield strength of the material, so, these parameters have to be back calculated and calibrated to provide values that are generalized. The following overview of the research carried on so far provides a glimpse of it.

2.7. Overview of Numerical Models

Literature reveals evidence for the scope of work done in the field of assessing the dynamic characteristics of runout of landslides be it the runout distance, the extension of the area, the deposit depth, the front velocity or the surge. Application of various models and empirical methods has been discussed in detail below providing a glimpse of the current state of progress in landslide dynamic modeling. The following discussion also gives a preview of the availability of the different dynamic models, their strengths and limitation considering the different case scenarios. Moreover it provides a brief preview into the progress in research in this field.

Hungr (1995, 1996,); Hungr and Evans (1996); Mc Dougall and Hungr (2004, 2005); have carried out immense work in the field of dynamic modeling working intensively with the DAN-W model, which was improvised as the quasi 2D model, DAN-2D and then later into a three dimensional, DAN-3D model. Applications of different rheologies to this model have revealed valuable outputs of significance not only for the back analyses of parameters for calibration of the rheological model but also provided prediction of the landslide runout velocity, length, depth etc. Moreover the applicability of the model in different types of landslide events be it rock avalanches as well as debris flow and rock slide debris flow have provided insight into the functionality of the model to predict the runout characteristics of a wide variety of phenomenon.

A comparative study of two well known events in the Cortina d'Ampezzo region, Eastern Dolomites, Italy have been conducted by Armento et al. (2008) using two different single phased, non Newtonian models, FLO-2D (FLO-2D software, 2000) and DAN-W (Hungr, 1995). The former is a two dimensional model while the later is a single dimensional model used to test the simulation of the model to events with limited range of input parameters. The model if calibrated well could be used for the prediction of the future events in a similar scenario. The analyses resulted in the determination of the runout distance, velocity and thickness of the terminal deposits. Using DAN-W back analyses of the events providing best fit parameters for friction and turbulence coefficient was conducted. Frictional and Voellmy rheologies were used and the latter was found to be applicable in case of DAN-W and absence of rheological parameters led to the estimation of viscosity and yield stress parameters in case of FLO-2D.

Santolo and Evangelista (2008) have carried a detailed study of the post-failure behaviour of rapid landslides using 2D DAN-W code (version 2003). They are of the opinion that though the empirical methods of depicting the dynamic parameters of landslides (velocity, volume, angle of reach, etc.) have been used for existing predictions, a better forecast can be availed from dynamic modelling of the runout areas. They carried out a detailed study of the debris flow in the pyroclastic region of Campania, Southern Italy comparing the rheological models Voellmy and frictional for indicative prediction of the dynamic parameters of probable flows in Campania. They also carried out a calibration of the model using case studies from fifty seven studies in the region in order to back analyse for the parameters under consideration.

A detailed comparison of three runout models is availed in Begueria et al. (2009) where the applicability and limitation of the models to Turnoff Creek rock avalanche, British Columbia has been enumerated. The models DAN-W, DAN-3D and MassMov2D are able to simulate velocity, deposit depths and the shape and extent of the deposition zone. The DAN-W model though unable to simulate direction changes was able to determine the deposit depth and the velocity reasonably whereas the other two models were able to simulate the lateral expansions considerably. The common limitation of all the three models being assumption of the rheological properties and thereby the parameter values during the

simulation. Keeping in mind the dynamic characteristic of landslides and debris flow changes due to water pressure dissipation along the runout path these limitations are a hurdle in the determination of the hazard.

Owing to the limitation of parameters for the rheological model Bertolo and Botini (2008) carried out back analyses using three simulation models in Frangellino Stream-Susa Valley, Italy. Considering that the three models used different codes with similar parameters the same parameters were used to evaluate the output. The parameter values were obtained by detailed literature review and Bingham, Voellmy fluid and Quadratic rheology (obtained by adding collision and turbulent stresses to Bingham law) were used. Boss DAMBRK, DAN-W and FLO-2D were calibrated and back analysis was conducted to obtain the best parameters. It was concluded that no single unique model can represent the complexity of the flow hence different rheological models are required in order to evaluate the varying characteristics of the flow.

Chen and Lee (2003) in their study of the rainfall induced landslides in the Lantau Islands, Hongkong, emphasized the determination of the dynamic characteristics and the runout mechanics for landslide hazard assessment. The study revealed that the use of a quasi three dimensional model, DAN using Lagrangian framework with an appropriate rheology would be able to simulate reasonably correct runout behaviour. The Voellmy rheology was chosen in this case and was used to derive information of the depth, the travel distance, the velocity and the footprint area. The Lagrangian method was flexible to fit in with any rheology depending upon the sediment properties and was able to detect accurately the topographic surface changes. Hence in the words of Chen and Lee (2003), the method being '*straightforward, efficient and easy to implement*' can enhance the preliminary hazard zoning and risk management in the mountainous terrain.

Similar works were also undertaken by Sosio et al. (2008) and a first time attempt was made to back-analyse and calibrate the rheological parameters by using the front velocity of the Thurweiser rock avalanche, Italian Central Alps, its runout extent and the deposit depth. The DAN3D model was used in this respect after having derived the parameters from the calibration of DAN and the quasi-2D model. It was found that the frictional rheology could best simulate the granular path over rough terrain except for the glacial ice. The downward thickening was approximated by the Voellmy rheology though the geometry of the deposit was found to be erratic. The study emphasised the importance of applying these models for forward prediction with an extra effort on a detailed back analyses of well-observed cases.

The Table 2.2 below provides an overview of the different models and their characteristic features The table includes the research work in the field of dynamic modelling from earlier times. But the latest developments in the field of dynamic modelling and progress in landslide science can be availed from the proceedings of the International Forum on Landslide Disaster Management held in Hongkong (2007), in which various benchmarking exercises were conducted on landslide debris runout and mobility modelling where a large number of models were used namely Wang, TOCHNOG, MADFLOW, FLO2D, etc. The applicability of these models was tested in case scenarios from around the world details of which can be availed form Ho and Li, (2007). Moreover the rheological parameters were back calculated for certain events and the models were tested in case scenarios determining the significance of these models in the application of forward prediction of landslides. The results for all the models were compared to understand the how each model behaved in a particular circumstance. It is here that the MassMov2d model gains significance as a physically based dynamic model which has been discussed below.

Table 2.2: Dynamic Models and their characteristic features

Models	Rheology	Analyses	Limitations	References
DAN-W	Voellmy	Accurate representation of runout distances and velocity. Underestimates deposit depths (details can be availed fro reference). Unable to provide satisfactory results along flow path. Able to predict maximum extension and deposit thickness. Modelled velocity was close to Hungr's equation and slightly lower than Evan's equation.		1. Armento, et al., 2008. 2. Begueria, et al Comparison of three runout models in the turnoff creek. 3. Geertsema et al, 2006. Chen and Lee, 2003
	Frictional Bingham	Application in the source area did not provide satisfactory results. Excellent simulation of the observed longitudinal distribution of deposits include a thick deposit at the toe region of the source scar, a uniformly distributed sheet like deposit along the path and some thickening at the distal area.	Determination of the Bingham properties of viscosity and yield shear strength through 'trial and error'.	
FLO- 2D	Three-term	Accurate representation of the hazard area with respect to flooded area. Results of runout distances and deposit thickness are similar to DAN-W. Maximum velocities have been underestimated to that of actual ones.	Unavailability of detailed topographical, rheological and hydrological data.	Armento et al, 2008.
DAN3D	Voellmy Frictional	Estimated the shape of the deposition well. Maximum thickness of the deposit underestimated. Maximum velocity was found to be higher after the turbulrnce coefficient was lowered unlike DAN-W.		Begueria et al Comparison of three runout models in the turnoff creek Sosio et al, (2008)
Mass Mov 2D	Voellmy	Able to correctly predict the extension of deposits. Slight under prediction of deposit depths. In order to obtain the accurate extent of the deposition the frictional angle was lowered which under predicted the extent of runout. Unlike others deceleration of the material along the slope was observed.		Begueria et al Comparison of three runout models in the turnoff creek

2.8. MassMov2D Model

The model is based on the assumption of a single phase homogeneous material on the basis of the classical Savage and Hutter Theory (Savage and Hutter 1989). The flow is modelled in two dimensions using the depth-integrated form of the Navier Stokes Equation. The shallow water assumption is based on the Saint Venant's equation which states that the horizontal length of the flowing mass is greater than that of the vertical length and hence the velocity of the fluid is small. The depth is measured in the *z* direction being normal to the bed. It is also assumed that no shearing deformation takes

place at the top surface and the flow moves with a velocity constant over the depth *h*. Shear deformations are assumed to exist at the base of the moving mass and is very small in comparison to the flow height.

The deformation of and the flow of matter with applied stress is referred to as rheology. This concept is applied when the classical theory of fluid mechanics and the Newtonian theory of fluid mechanics together are unable to define the kinematic behaviour of materials. The model uses a set of rheologies namely, Voellmy, Bingham and the Herschel-Bulkley.

The **Voellmy rheology** uses the frictional-turbulent rheology and is a two parameter model developed by Voellmy (1955) for use in determining snow avalanches (Hungr and Evans 1996). It consists of a friction coefficient (μ) and a turbulent term which is dependent on the square of the velocity and the density of the material and can be stated as follows:

$$T = A_i\left[\gamma H_i\left(\cos\alpha + \frac{a_c}{g}\right)\tan\emptyset + \gamma\frac{v_i^2}{\varepsilon}\right] \quad \text{Eq 18}$$

Where A_i= area of the base of the block, $a_c = \frac{v_i^2}{R}$ centrifugal acceleration dependent on the vertical curvature radius of the path *R* and $tan\,\emptyset$ is equivalent to (1- r_u) $tan\,\emptyset$ a frictional term where r_u refers to the pore pressure co-efficient (ratio of pore pressure and the total normal stress applied at the base of the block) (Hungr 1995). This $tan\,\emptyset$ is equivalent to the dynamic frictional coefficient Coulumb type where the shear force is proportional to the normal force, where $\emptyset$, is the basal frictional angle of flow. The internal pore fluid pressure on the other hand being a transient term coupled to the normal stress dissipates during the motion of the material and is very difficult to estimate (Begueria et al. 2009b). The pore pressure parameter is hence assumed constant and the frictional dissipation is lumped into a single parameter $tan\,\emptyset$. The turbulence coefficient ε determines the flow velocity and the density of the materials. It has the dimensions of acceleration and is of viscous type where the drag is proportional to the square of the velocity. Thus the model contains two resistance terms one of Coloumb type and the other the Viscous type the values for which depend on the size, type and ground condition and the shape of the runout track (Kocyigit and Gurer 2006). The model is used to determine the behaviour of granular solid materials (Naef et al. 2006).

The **Bingham model** is a combination of both the plastic and viscous behaviour with a laminar flow regime (Hungr 2007). A Bingham fluid with a constant yield strength and viscosity behaves as a rigid body below threshold yield strength and follows a linear stress-strain relationship when the yield stress exceeds threshold (Begueria et al. 2009). The shear stress is dependant on this constant yield strength and the viscous term is dependent on the velocity and the inverse of the thickness of the material (Hungr and Evans, 1996). The model can be described by the following relationship

$$r = r_c + \mu\left(\frac{\partial v}{\partial \tau}\right)^{\beta} \quad \text{Eq 19}$$

Where, r is the total resistance by the shear stress in the flow depending upon the yield strength due to cohesion (r_c) and the viscosity (μ) depending upon the shear rate, $\frac{\partial v}{\partial \tau}$. The viscosity of the flow is also found to be related to the concentration of solids with a value ranging between 10^{-2} and 10^{3} (O'Brien and Julien, 1988; Parsons et al, 2002in Begueria et al, 2009) while the exponent β is an empirical parameter and equals one in the Bingham model (Begueria et al, 2009).

Replacing the above equation with the cohesive frictional component the **Herschel-Bulkley model** is derived where the fine fractions are large enough to lubricate contacts between grains (Rickennman, 2006). Coussot (1996) states that a clay fraction with particle size of less than 40 μm or 10 % is required for the materials to behave like the Herschel-Bulkley fluid. The following Coulomb-viscous model is obtained by incorporating the cohesive-frictional component.

$$\tau = \tau_c + (\sigma - u)\tan\varphi + \mu\left(\frac{\partial v}{\partial z}\right)^{\beta} \quad \text{Eq 20}$$

Here the frictional component (σ) depends on the bed normal stress and is equal to the density of the material, the pore pressure and the basal frictional angle. The pore pressure ratio (μ/σ) being difficult to estimate is considered as a constant and the apparent frictional angle is lumped with the frictional dissipation of the material.

Depending upon the rheology the S_f or the frictional resistance terms can be determined as follows; Voellmy:

$$Sf = g\left[\cos^2\alpha\tan\varphi' + \frac{u^2}{\xi h}\right] \equiv g\left[\cos^2\alpha\tan\varphi' + \frac{u^2}{C^2 h}\right] \quad \text{Eq 21}$$

Simple Bingham and coulomb-viscous Herschel-Bulkley :

$$Sf = g\frac{1}{\rho h}\left(\frac{3}{2}\tau_c + \frac{3\eta}{h}u\right)$$

$$Sf = g\left[\cos^2\alpha\tan\varphi' + \frac{1}{\rho h}\left(\frac{3}{2}\tau_c + \frac{3\eta}{h}u\right)\right] \quad \text{Eq 22}$$

Thus from the above equations it can be summed up that for a particular simulation the rheology of the moving material is defined by the (ρ, r_c, μ) ,(ρ, φ, r_c, μ) and (ρ, φ, α, r_c, μ) for Bingham, Coulomb-viscous and Voellmy rheologies respectively, where ρ is the density of the material, r_c is the constant yield strength due to cohesion of the material, μ is the dynamic viscosity of the moving material, φ is the apparent or the basal frictional angle and α is the angle of internal friction. Owing to the constraints in the availability of the data these parameter vectors are availed from best fit parameters for calibration of past events. This is obtained by the back analysis of events to obtained observed values of runout length, deposit depths, extent of deposit, etc. Hence these parameters are not the actual parameters but only apparent estimates from the back analyses of similar scenarios. These are used for calibration purposes of events similar in occurrence or events that have occurred in the same area for a particular case. The rheological parameters for Voellmy rheology have been back analysed for many events and in different regions and hence values of bet fit area available from literature. They were actually applied in case of snow avalanches and rock avalanche runout modelling. Thus it can be stated that these apparent rheological parameters are not free from natural variability. The actual range of these parameter values is unknown and determining the range of parameters best suitable for a particular scenario requires research. Back analyses and calculation of the results hence is important in this case. This may influence the uncertainty in the model output as well. If the range of parameters for a particular event is known and events in the area successfully back calculated the range of parameters can be used for the forward prediction of an event. The input parameter required by the present model has been detailed below. Most of these are in the form of maps the most significant of them being the Digital Elevation Map.

2.8.1. Model input parameters

The input parameters required by the model are as follows

Table 2.3: Inputs requirements of MassMov2D

Input parameters	DEM subtracted by soil depth at the initiation zone, Soil depth at the initiation zone and initial volume, Initial area where initiation zone includes secondary slides along the runout zone, Soil depth along the runout and deposition zone.
Rheological Parameters (Frictional)	Turbulence co-efficient (ξ) measured in m.sec-2 Angle of basal friction (μ) measured in degrees Angle of internal friction (λ) measured in degrees Density of the soil (Pa) measured in kg.m3 Resisting strength of the soil (Pa), Cohesion of the soil (c) Fluid rate measured in m.sec-1
Others	Scouring rate measured in m.sec Number of timesteps in seconds

2.9. Scientific Rationale

Though immense work has been carried out previously and currently in the field of dynamic modeling of landslide, in all the analyses, depicting the parameters for the rheological models has been a difficult task which has been overcome by calibration and back analyses of the models to scenarios with similar geological setup. This has contributed largely to the uncertainty in the derivation of the accurate parameters for the prediction of landslides. The current study tries to explore this aspect of dynamic modeling with a view to improvise on the probability of occurrence of the simulated results in regions where very little knowledge of the parameters remain.

Analysis of past events provide us with useful indications of the future but a more detailed prediction of their effects can be simulated using mathematical models which are applied in order to derive quantitative estimates of the dynamic characteristics (Ayotte and Hungr 2000; Arattano et al. 2006). These dynamic characteristics of landslide phenomena are specifically important to the planners; land administrators etc. who are responsible for the protection of life and property in the hazard prone areas. But it must be emphasized that although these models have gained immense significance in detailed hazard assessment with growing complexity in undergoing the latter there are inherent uncertainties in the input data specifications, as has been discussed, which is not explicitly incorporated into the analyses nor is it portrayed in the maps (Barbolini et al. 2006).

Moreover each of these models uses a different numerical technique in the approximation of the governing equations which leads to considerable uncertainty in the comparison of the results (Naef et al. 2006). The determination of the most applicable rheology for various events is a tedious task. But what is more difficult is the determination of the friction coefficients for each of the rheological models that can be estimated by means of calibration. Barbolini et al. (2006) stated that well established calibration were found to exist in the Swiss guidelines for the Voellmy-Salm model but there are difficulties in extending to other dynamic models.

In this respect it can be stated that uncertainty analysis is a tool productively used to test a model concept that enhances confidence in the model output (Zhang et al. 2008). This uncertainty being generated from a variety of sources such as input data, parameter estimation and prediction of a real world output. . Barbolini et al. (2004) have tried to determine the uncertainty in the rheological parameters using a 1D dynamic model applying PDF derived from regional analyses. He has further determined in his study (2006) the release condition uncertainty with respect to the volume and the velocity of the material. But is more important as well is the determination of uncertainty in the depth of the deposited debris, the velocity of the material in motion and the extent of the runout that may help in future mitigation of such events.

This study provides to study the method of quantifying this uncertainty and the variability in the various parameters used for the purpose of calibration of the model.

3. Methodology and model parameterization

The research work was conducted in three phases:

- Firstly an intensive literature review was made in order to answer the research questions 1, 3 and 4 mentioned in *Chapter1, Section1.8*. This was further incorporated in the Literature Review *(Chapter2).*
- The second phase included determining literature derived values for the calibration of the model and back analysis of the result with that of the observed values. This phase also included sensitivity analyses of the model parameters and fulfilment of research question 3.
- The third and the final phase lead to the uncertainty analyses of the model in terms of area, depth and volume. Keeping in mind the fairly large modeling time taken by the model for each runs (approx. 15 minutes) and considering the fact that availability of data for the study was not a hindrance no field work was conducted. Rather a much more emphasis was give to the analyses of uncertainty.

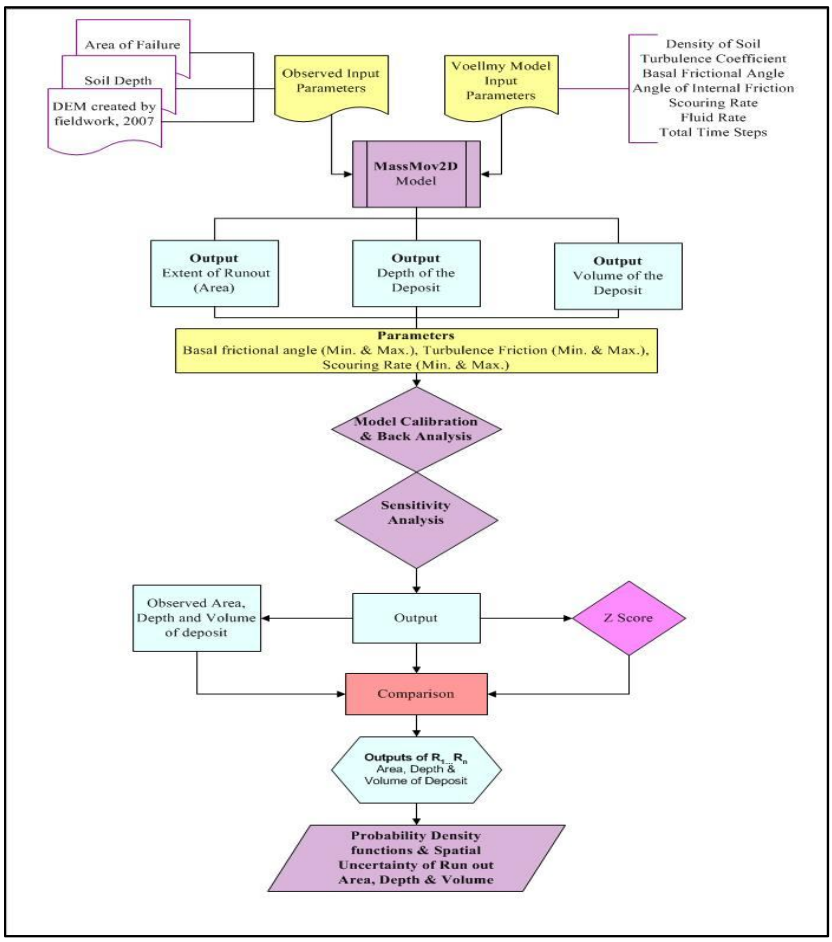

Figure 3.1: Methodological Framework

Thus the present study intends to determine the landslide dynamics and the inherent uncertainty in the model output with the help of MassMov2D model. The fulfilment of the objective was possible by progressing along a simple methodological framework which has been illustrated in Figure 3.1. The time utilization framework of the study is provided in Appendix I.

The entire project comprises of a cyclic methodology where frequent comparison of the model simulated result was made with the observed values for area, depth and volume. The first section of the study involved the model structure identification and deriving parameters for the model. This was followed by running the model MassMov 2D for the various scenarios chosen on the basis of the observed data available for each of the scenarios. This resulted in outputs for runout area, depth and velocity of the landslide deposit. The second section of the work involves the model calibration, back analyses of the simulates results with that of the observed and sensitivity analyses using the Z Score method which led to the determination of the most uncertain inputs, and provided appropriately calibrated values of the chosen parameters.

The second section of the work laid emphasis on the derivation of the Z Score graphs for deposit depth. The model simulated result of deposit depth from which the actual deposit area was clipped. The mean and standard deviation for deposit depth was derived for the deposit area. This was done for all the calibration results to determine the variability of the deposit depth. But the calculation of the mean and standard deviation alone cannot determine the variability of the results from the observed depth value. Hence the Z Score method was used where the values were standardized around the observed mean to derive a normalised distribution curve. Owing to the large number of pixels in the dataset preparing a graph with all the values was not an easy task. As a result the Z Score values for the deposit depth in the deposit area were put in frequency bins ranging between -2 to +2 at an interval of 0.5 units to derive a graph for the deposit depth. Thus the graphs prepared using the frequency bins show the frequency values on the y-axis and the Z Scores on the x-axis. Further quantification of the variability was made by deriving the coefficient of variation with the mean and standard deviation of the depths obtained for each simulation using the calibration values (c.f. Chapter 6).

The back analysis was conducted for determining the predictive accuracy of the model for observed area, depth and volume. Once the model was appropriately calibrated and back analysed, the third and the final stage was focused upon. In the final stage of the study spatial and graphical representations of the uncertainty was derived. This was done first by deriving random values from the range of maximum and minimum values for the parameters calibrated, turbulence coefficient and basal frictional angle using the Monte Carlo Technique. Emphasis was laid on the determination of the probability of occurrence of the runout in the particular pixel for each of the calibrated results. This would determine the spatial uncertainty of the occurrence of runout in the particular area. Details of the approach are found in the forthcoming Chapters.

3.1. Model parameterization

Model parameterization led to the initialization of the study to achieve the farsighted goal of quantifying uncertainty. Setting up the model with all the preliminary requirements required a set of data in the form of maps and knowhow of the basic requirements of the model the details of which are discussed below;

3.1.1. Basic Requirements of the Model

The model chosen for the study is the physically based dynamic model named MassMov2D (See Chapter 1 Section 1.4). The core part of the model has been implemented using PCRaster, a GIS scripting language.

The executable file of the model available freely at the digital website of CSIC (*http://hdl.handle.net/10261/110804*) requires the working installation of the PCRaster spatial modeling software also available freely at the website *http://pcraster.geo.uu.nl*.

Table 3.1: Components of PCRaster used to run MassMov2D Model

Components of PCRaster for running MassMov2D	Description
Aguila	The visualization software in PCRaster used to display model outputs available with PCRaster.
Partdiff	The vector calculus functions are stored in this dynamic library.
pcrcalc.exe	It is the core command in used to call each function in PCRaster.
oldcalc.exe	The command used in older versions of PCRaster to make all the programs run in the older versions compatible with the upgraded versions of the software.
Nutshell	The user interface of PCRaster with the command prompt window on the upper left where the PCRaster commands can be given. To the lower left is the explorer window and to the right is the model editor which is a regular text editor with syntax highlighting for the PCRaster language used edit changes in a script. The Nutshell was developed independently of PCRaster and needs to be accessed via the Aguila visualization software.

The following procedure is necessary to setup the MassMov2D model which is embedded in PCRaster (the details of the components are available in Table3.1)

- It is recommended that the latest version of the software with the updates along with the *Aguila* visualization software should be installed which will help display the outputs.
- Moreover the *Partdiff* dynamic library, the vector calculus functions should also be installed into the PCRaster applications file since it is not the core part of PCRaster installation. It can also be incorporated into the same directory as that of the model.
- The command old calc instead of the *pcrcalc* must be used for the running of the model due to compatibility issues with the dynamic library.
- With PCRaster finally setup the model is incorporated within any of the executable directories along with the input map parameters which can then be simulated using Nutshell, the PCRaster user interface. This can directly be run from the prompt window with the expression nutshell and appears as in Figure3.2.

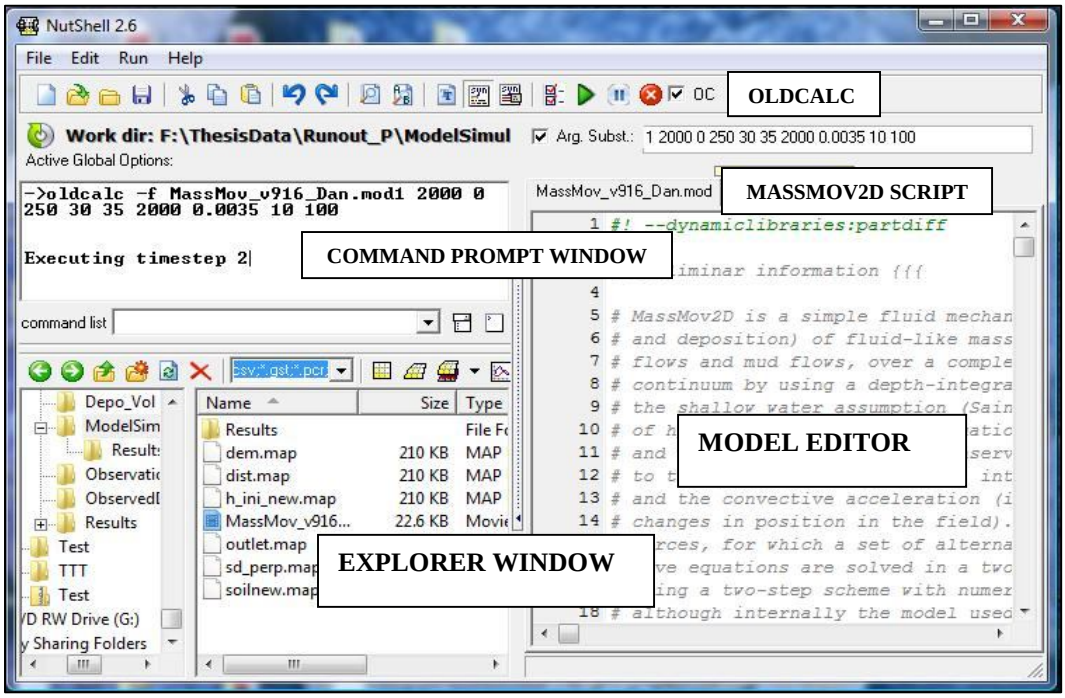

Figure 3.2: User interface of PCRaster, the Nutshell

3.1.2. Maps required for simulation of the Model

In order to run the model successfully several input parameters are required as described in *Chapter 2, Section 2.8.1, Table 2.3*. The global input parameters require maps as inputs and they are as follows:

- **Digital Elevation Model**

The DEM (Digital Elevation Model) stands as the major deciding factor for the outputs. The model accepts the detailed complexity of topography via the DEM and can simulate results of field case studies. Hence the simulation of the result depends strongly upon the resolution and the accuracy of the topographic input data. The original DEM was prepared by interpolation of field derived GPS data outside the field area at 1m and the contour map of 20m interval. The DEM optimization operation in ILWIS was used to 'burn' existing drainage and road features into the DEM so that the subsequent flow direction on th output DEM will follow the existing drainage pattern and road as well. The road was

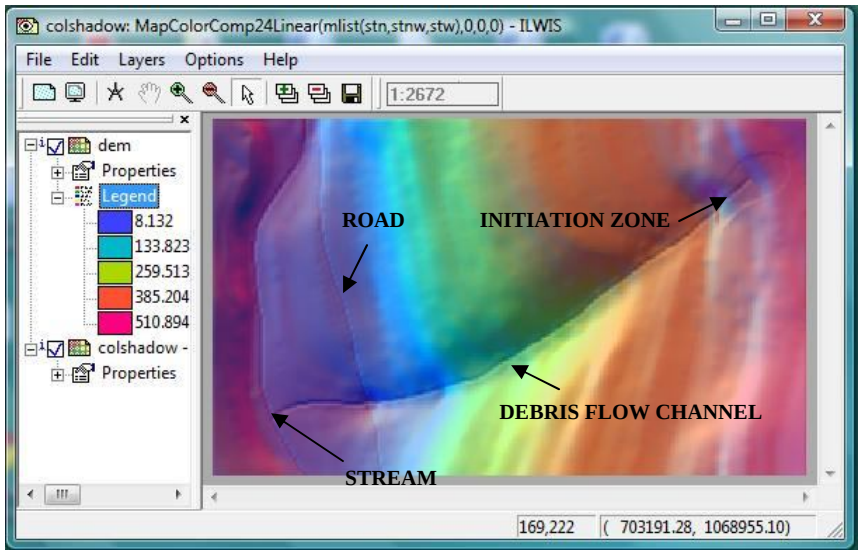

Figure 3.3: The DEM map with the stream and road map embedded and reduced soil depth at initiation

buffered at a distance of 4.5m (width of the road) and the stream at a distance of 2m to indicate the area that will be affected by the drop or raise which should be greater than zero. Thus the segments of the stream and road were embedded into the DEM with a final smooth and sharp drop height of 1m indicating the height at which the segments were additionally dropped to burn the stream and the road into the DEM. Thus the DEM was enhanced to create a direction of flow confined within the channel. The road along the channel was also demarcated to observe the affect of the model simulations for debris flow. The zone of initiation was finally reduced from the original DEM with the help of the soil depth map perpendicular to the slope. This map was then converted to the map format in PCRaster as a significant input map. The derived map has an elevation gradient of 5m- 515m which shows that the region is an undulating terrain with shallow landslides.

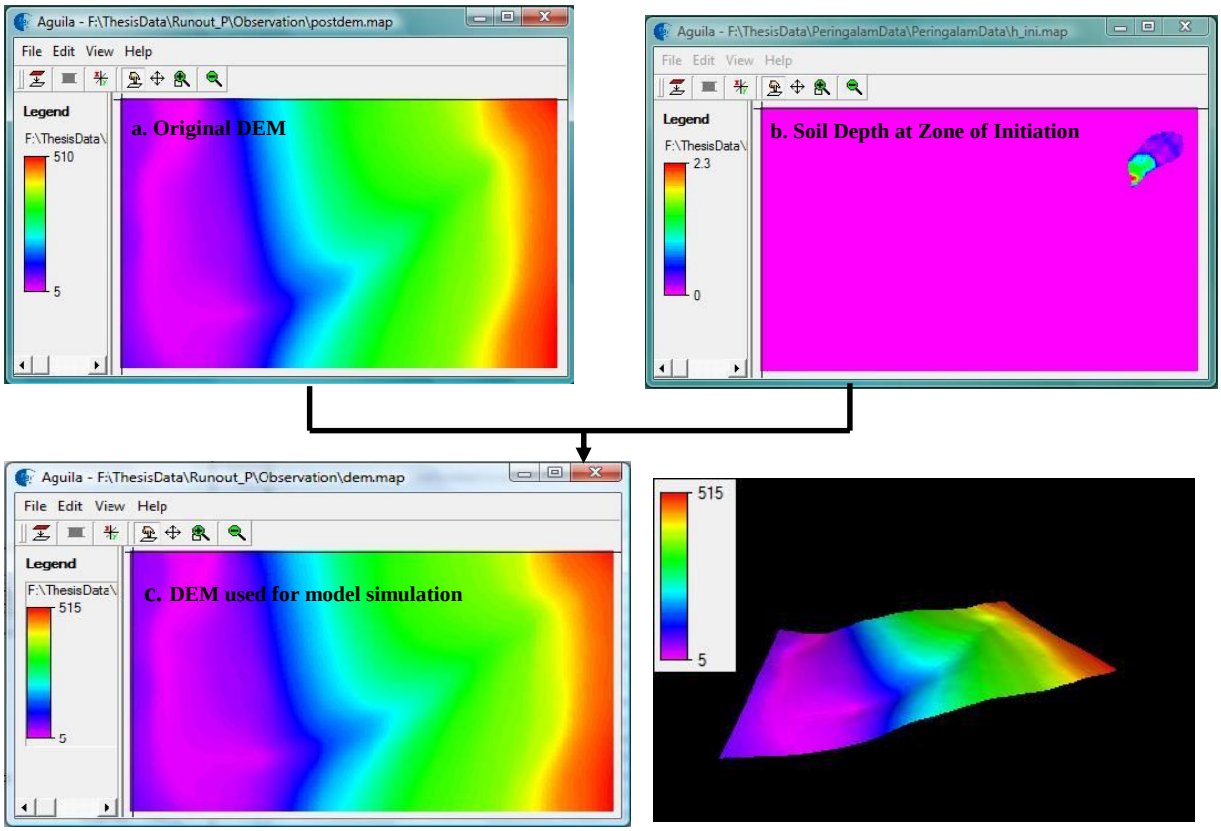

Figure 3.4:a: Original DEM map and b: Soil depth initial zone used to create the c: DEM map used for the model simulation, Bottom left:DEM in 2D Format as in Aguila

- **Soil Depth**

Soil Depth at Zone of Initiation: The model requires the initial values of soil depth that is derived from the *h_ini.map* (Fig.4.5).This map is the soil depth map perpendicular to the slope found at the zone of initiation and is required for the initial movement of the material in the release zone within the model. This map is clipped from the *slideparts.map* (Fig. 3.8) for the release area and then from the *sd_perp.map*, which is the map for the perpendicular soil depth in the region derived

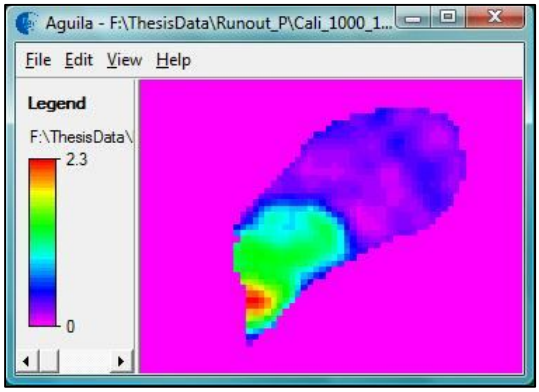

Figure 3.5: The soil depth at the release area or initiation zone

from a field derived vertical soil depth map, in order to determine the initial soil depth (Figure 4.5).

Depth of the Soil for the entire area prior to the landslide: This data was available in map format for the modeled area and is derived from the *soil.map (Fig.4.6)*. It is the pre-event soil depth map generated by subtracting the pre-event DEM and the post event DEM to derive the soil depth of the modeled area. The resulting map was the soil depth at the initiation zone. Then the soil depth was converted perpendicular to the slope thereby deriving the soil depth map perpendicular to the slope (Figure 4.6) that helps derive information of the scoured material during the motion of the landslide mechanism. The spatial variation of the soil depth is captured with the help of the pre and post event DEM of the modeled area. The map accounts for information only in the area of the slide and to about 5m and the surrounding area has information derived from interpolation.

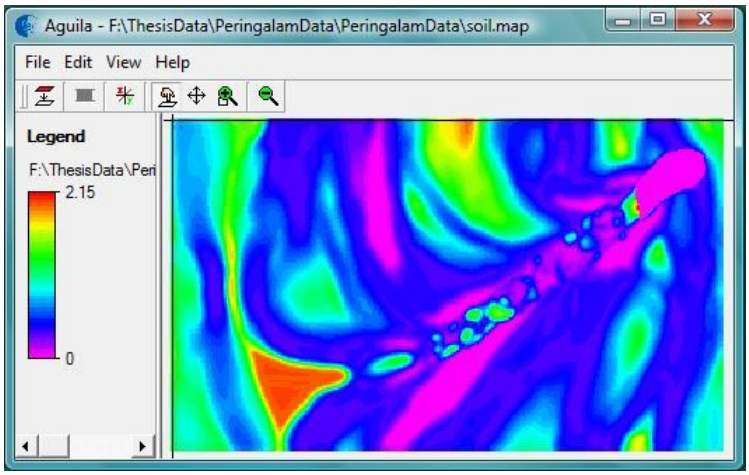

Figure 3.6: Soil depth map for the simulated region

- **Distance to fluidized toe**:

The distance from the zone of initiation of the landslide to its toe created using the spread function in PCRaster generating the *dist.map* . The zone of initiation, the entire area here is considered as a point from which the distance to the toe of the landslide is measured.

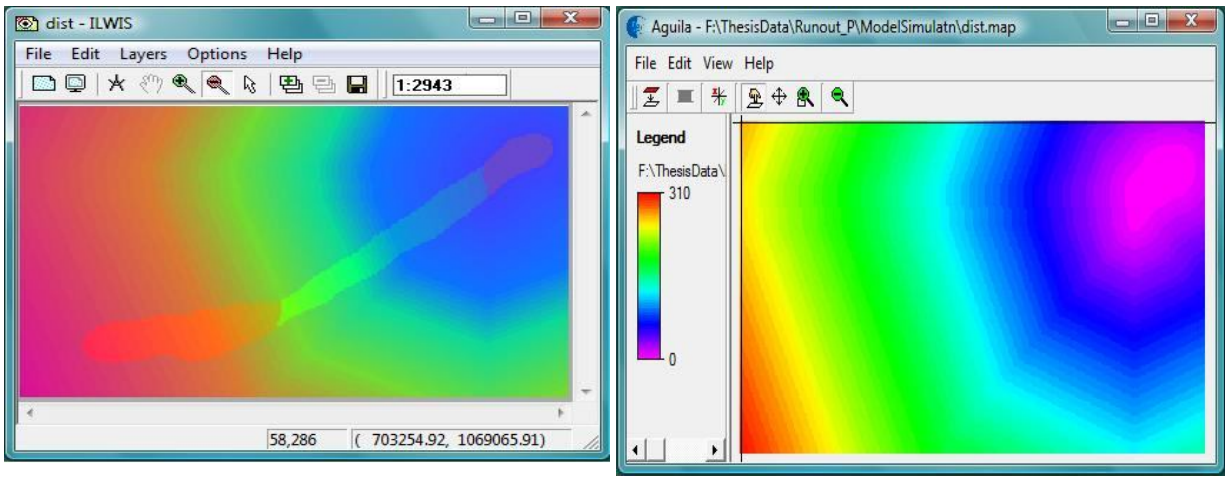

Figure 3.7: Left:The distance map overlaid with the slideparts map and Right: the fluidized distance to the toe

- **Domain boundary map**:

This is the *outlet.map* which represents the boundary domain and the area from which the material may exit. This map is generated keeping in mind the lowest point in the DEM and uses the lddcreate function of PCRaster. This function helps create a local drain direction in the map along the channel from each cell to the steepest neighbour down the slope (Inset Figure3.9) thereby determining each cell in its neighbour to which the material will flow. The domain boundary is required in order to direct the material along the flow using this as a base map.

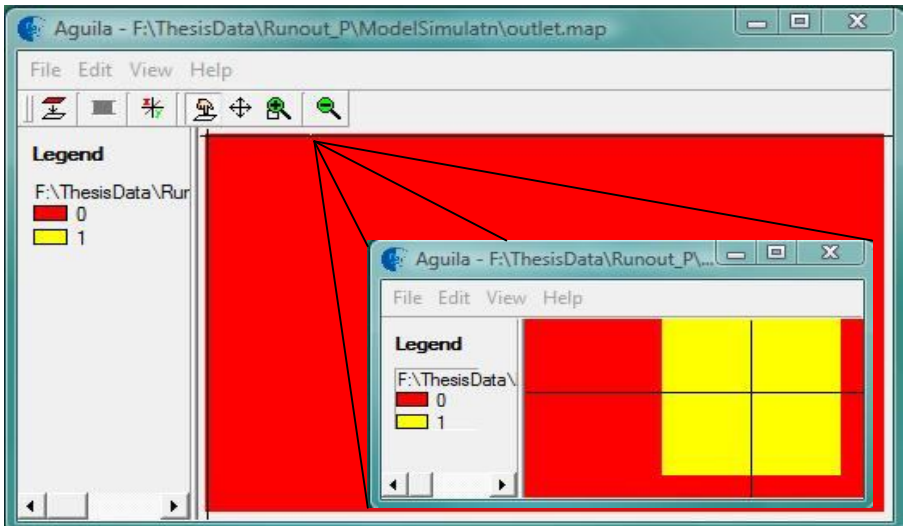

Figure 3.8: The outlet map displayed the lowest point of the DEM in the subset

The four maps DEM map, the initial soil depth map, the soil map for the entire area, the distance map displaying distance from the zone of initiation to the toe of the landslide and the outlet map that forms the domain boundary are the basic requirements for the running of the model. All the numerical calculations are conducted with a combination of these maps resulting in the output maps.

3.1.3. Maps required for back analyses of the Model

For the back analyses of the results in order to compare the deposit extent, deposit depth and volume the following maps were used. They were further used to derive the observed area the deposit depth and the volume details of which can be found in the Section 3.1.7.

- **Individual parts of the slide**:

This map is represented as the *slideparts.map* and represents the individual interpreted parts of the slide area digitized from the Cartosat I, data of 2007. The slide is demarcated into the initiation zone (depicted in green), the scouring area or the zone of erosion and deposition of debris (depicted in cyan) and finally the distal zone of deposition or the region of accumulation of debris (depicted in red). It should be noted that the region of accumulation has been termed the deposit area or the area of runout in the entire study. The uncertainty analysis has been done in this region and the all the observation for model calibration has been observed for this part of the slide.

Figure 3.9: Parts of the slide interpreted as the Initiation zone, the Scouring region and the Deposition Zone

- **Post event DEM**:

The post event elevation information is derived from the Post-DEM map which was prepared using the field derived GPS data at 1m (c.f Figure) and the contour map with an interval of 20m. It is to be noted that outside the landslide area the entire region has elevation values similar to values prior to

the event as tehse are the interpolation values. The map was interpolated using the Integrated Distance Weighted method using Nearest Neighbour as the criteria for interpolation. Thus the DEM map so generated has a coefficient of determination 0.8. This map is essentially used for deriving the observed deposit and volume which has been compared with the calibration results.

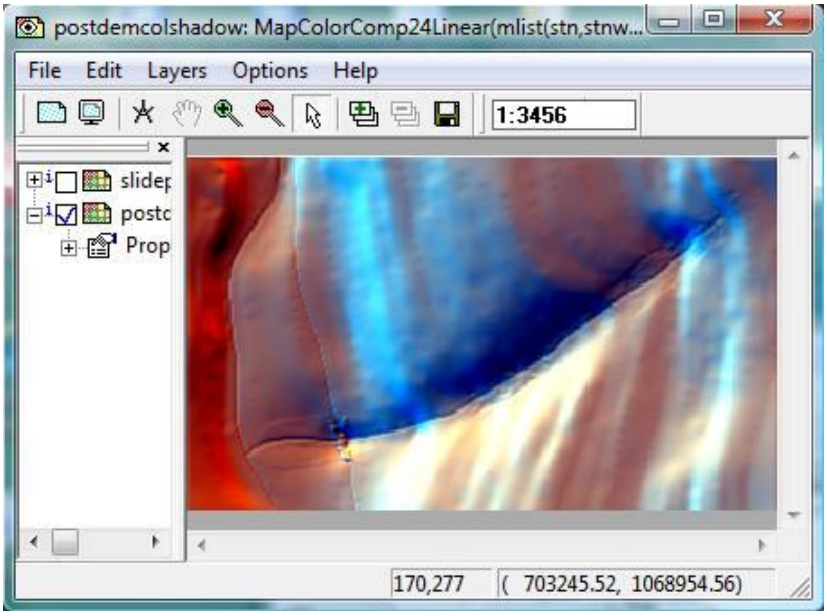

Figure 3.10: Post event DEM visualized in ILWIS with the evident deposit area

- **Other input maps**:

Apart from the Cartosat I image (dated November 8th, 2007) that was used to determine and interpret the distinct parts of the slide various vectorised ArcMap files in the *shapefile* format were used. The *shapefiles* for the individual interpreted slide parts, the boundary *shapefile*, clipped for the area simulated along with the stream and river *shapefiles* were all used for representation of the outputs in various forms. Apart from all the above maps used either as global input parameters or for the purposes of validation and as reference maps for presentation purposes there are other parameters to be determined as well for numerical modeling. The values for the input parameters in the model like the density of the soil and the angle of internal friction were available from previous research in the area conducted by Kuriakose (2006); Kuriskose et al.(2009b); Kuriakose et al. (2009c). The turbulence coefficient, the basal frictional angle and the scouring rates were calibrated and derived through trial and error method.

Table 3.2: Other parameter values for simulating the model

Density of the debris at the initiation zone	2000 kg/m^3 (Kuriakose 2009c)
Angle of Internal Friction	35^0(Kuriakose 2009c)
Basal Frictional Angle	Denoted by φ measured in degrees
Turbulence Coefficient	Denoted by ξ units of measurement is m.sec^{-2}
Scouring Rate	Determined by synthetic range and calibration
Fluid Rate (Transition from solid to fluid)	10 m.sec (Kuriakose 2009c)
Total Timestep	100 sec (Time taken for the debris flow from the initiation zone to the toe of the landslide)

3.1.4. Reliability of the Maps required for simulation and back analyses of the Model

The present study deals with the determination of uncertainty that needs to be quantified. As a result the reliability of the maps used in the analyses is significant some of the maps have been created in PCRaster depending on the DEM as the base map.

3.1.5. Metadata of the maps used in the Model simulation and back analyses

In order to study the uncertainty derived out of the model prediction it is important to know the reliability of each of the maps.

Table 3.3: Reliability of the input maps

Maps	Reliability
DEM map (post event, c.f. Figure 3.3)	The DEM map was created with the field derived GPS location at 1m and the contour map at aninterval of 20m. The coefficient of determination of the DEM is estimated at 0.8
DEM map used for model simulation (c.f. Figure 3.3, 3.4 Bottom Left)	This map was generater from the post event DEM with the stream and the road embedded into it. The initial soil map was reduced to provide the direction in which to direct the flow of material in the model, Thus the coefficient of determination is similar to the above DEM with information along the channel at a buffer of 2m and along the road at 4.5m. The map is reliable for information along the slide area with the coefficient of determination similar to the DEM.
Soil map (perpendicular soil map of the modelled area, c.f. Figure 3.6)	This map was created with the above subtracting the above two DEM to derive the spatial variability of soil depth with reference to the DEM and thus has the same coefficient of determination as the DEM. The initial soil depth was reduced from the area to get the resulting map which is reliable for information upto 5m along the slide area. The area outside the slide has information from interpolation of the DEM.
Distance map (distance from the zone of initiation to the fluidized toe, c.f. Figure 3.7)	This map was generated in PCRaster using the spread function that helps to identify the shortest accumulated friction path to every cell centre along the flow. The distance is determined as 1m depending on which the a path is followed over the consecutive neighbours and theis path distance increases. The friction value of 1m determines the friction distance per unit distance as the average of the source cell and the destination cell (PCRaster Manual).
Boundary Map (determines the material outlet from the modelled area, c.f. Figure 3.8)	This is the outlet map that is created using the lddcreate function of PCRaster that is the local drain direction map that directs the flow towards each cell in the lowest downslope drain direction.
Slide parts map (c.f Figure 3.9)	The slideparts map is digitized from the Cartosat I image of 1m resolution and converted to the PCRaster map format.

3.1.6. Model output

The model hence set up with all the input requirements was then simulated for the case study area and the resulting simulation was used for deriving the observed deposit depth, the velocity and the extent of the runout. The model output resulted in timeseries maps for each of the hundred time step considered here because the debris took an approximate time interval of around one minute and fifty seconds to dislocate from the zone of initiation to the zone of deposition or the runout zone which was approximated as 100 seconds. This is the considerable amount of time taken for the displaced mass to

move from the zone of initiation to the zone of deposition details available from a survey conducted in the area in 2007. This time was used as the fixed timestep in all the simulation and the required system time to run the model with a high configuration (processor speed 2GHZ, 2Gb RAM) was approximately 15 minutes for each model simulation. A total of around 730 model runs were done for the calibration of the model and another 100 were done with the random parameter values generated by the Monte Carlo Random number generation. The available output is a map series for each timestep for deposit depth which was used for the uncertainty analysis.

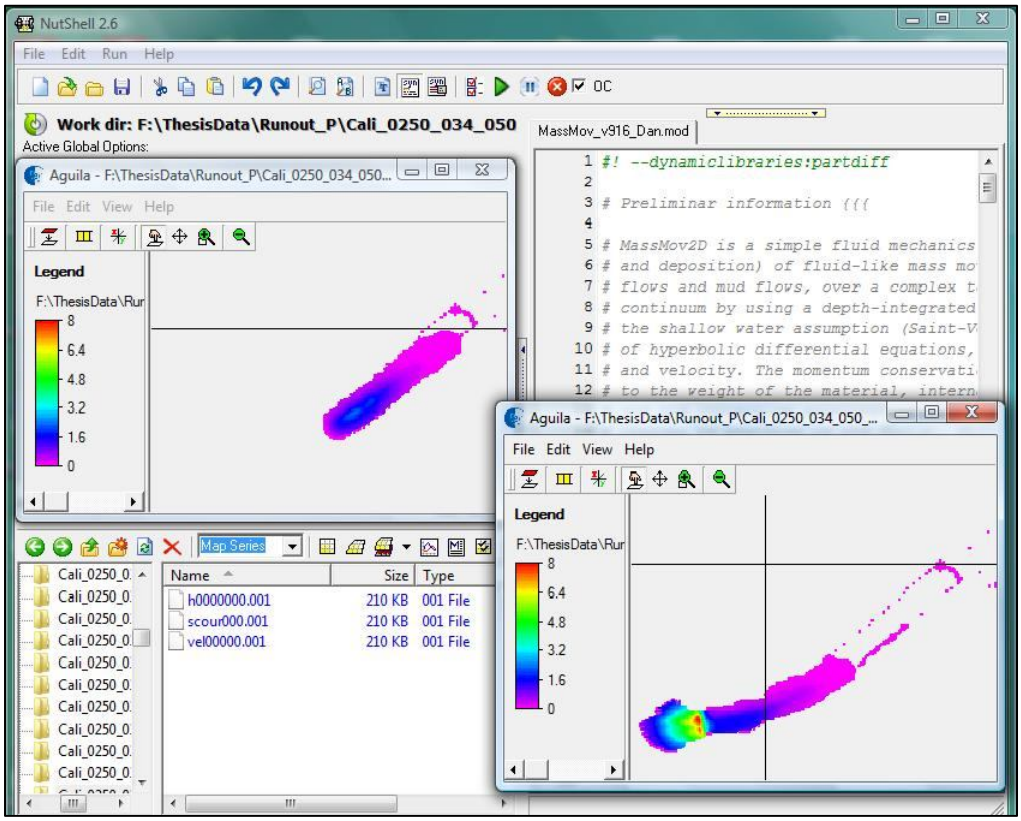

Figure 3.11: Model out above at timestep 20 and below at timestep 100

3.1.7. Derivation of observed area, deposit depth and volume

The model produced results for deposit depth in a mapseries where a map is generated for each of the timestep. Mapseries were generated for each of model run with the calibration parameters. These results had to be compared with the observed deposit depth. Assuming that the highest deposit depth would be found in the deposition area the observed depth was derived for this region and the area for the dposit zone was also derived. The determination of the deposit area was essential to determine the affect of the debris flow in the zone of deposition. This output was generated by subtracting the Digital Elevation Model (DEM) (c.f. postdem.map, Figure 3.10) and the original DEM (c.f. originaldem.map, Figure 3.3) and finally clipping the deposit area (with reference to slideparts.map, Figure 3.9). Thus the extent of the material deposited was determined. This has been illustrated below in a stepwise sequence The area hence derived was approximately 2686sq m and the maximum depth of the deposit was 6.4m. The mean and the standard deviations were simultaneously derived for further analysis of the observed deposit and were 0.58 and 0.89 respectively.

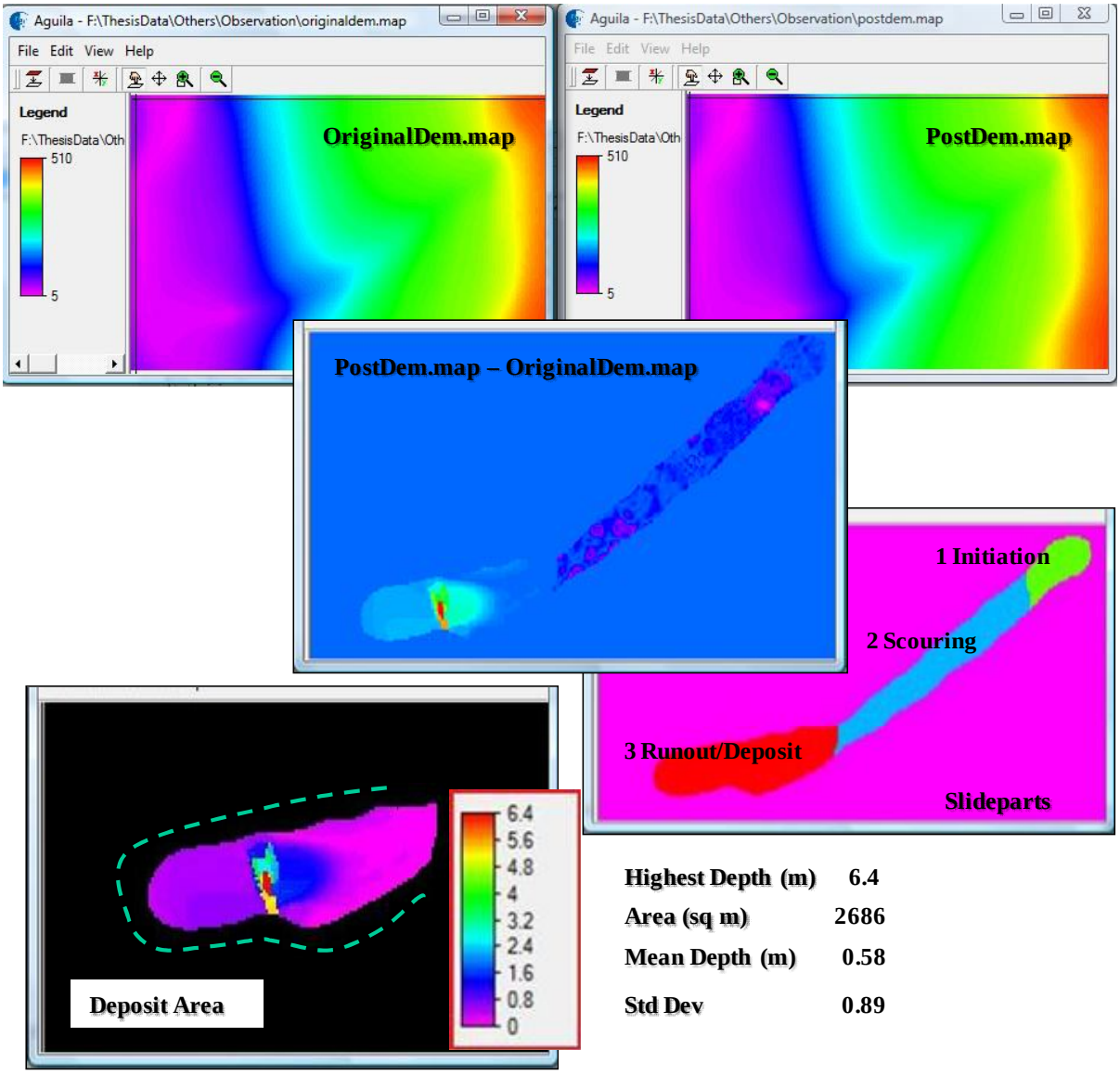

Figure 3.12: Derivation of the deposit area and the deposit depth for validation.

The final deposited volume was estimated from the deposit area, observed by the summation of the values. Since the pixelsize is one meter and the height of the deposit in the map is the amount of soil that has been entrained along the path from the zone of initiation to the zone of deposition the volume was derived by the simple summation of the values for soil depth. This value was derived by a simple conversion of the map in ASCII file format using PCRaster map2column function. The volume for the initiation area was derived from the initial soil map of the region (c.f. Chapter 3, Section) and was estimated at 437 m^3 while that at the final runout area was estimated at 1553 m^3. These values were further used to assess the simulation results to that of the observed results. The error in the prediction of the area of runout was determined simply by subtracting the values for area derived by the simulation of the model with varying calibration parameters and the observed values.

4. Calibration

4.1. Calibration: Significance in Dynamic Modelling

The adequacy of the model is determined by answering the question '*was the range of parameter values used to derive the model components for process simulation wide enough to include our conditions?'* (DEQ 2009).These simulations are needed to narrow the range of variability in model input data since there are numerous choices of model input data values that may result in similar results. Thus to know the parameter range suitable for the present case study is significant. Donatelli and Stöckle (1999) have emphasized the main reasons for conducting model calibration as follows,

- It allows the description of the system under study. Though referred to as calibration it requires the selection of correct input thereby characterizing the system under study.
- Moreover no universal model exists that may account for unaltered set of parameters applicable to all conditions.
- Adjustment of parameter values within the chosen range of parameter avoids any degradation of a process based model to a statistical regression.

In a nutshell model calibration refers to the systematic adjustment of model parameters in order to determine estimates for the model parameters through comparison of field observations and model predictions (Himesh et al. 2000). This procedure can be carried out by identification of the model parameters to be calibrated and selection of the method of calibration to form a calibration cycle as illustrated below,

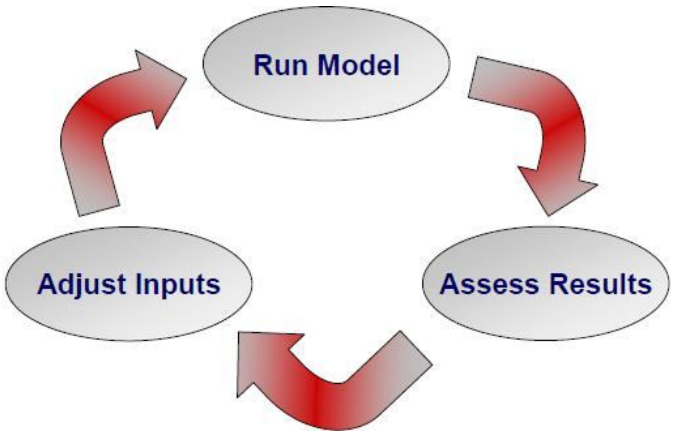

Figure 4.1: Calibration Cycle (Taylor 2007)

Hence calibration of the model in order to derive the material properties and the characteristics of the movement of the material was accomplished through back analysis. This was actually based on the trial and error adjustments of the input parameters that define the flow resistance. This is because of the fact that the rheological properties affect the dynamic characteristics of the flow mechanism in a landslide and the application of the most appropriate rheology is an object of research. Arrattano and Franzi (2006) have pointed out that the resistance terms are related to the rheological behaviour of the material mixtures and are important in the estimation of the rheological parameters accurately. As a

result a detailed literature study was conducted in order to derive the parameter values used for the calibration of the model discussed below.

4.2. Parameters chosen for the Calibration

The Voellmy model has been widely used for snow avalanche models and the empirical model was built combining the Coulomb frictional and the turbulent term (Chapter 2, Section 2.8, Eq 14). The application of this rheology to rock avalanches and debris flow has been implemented successfully (Hungr and Evans, 1996; Hungr 2003).Though this rheology requires the estimation of the two significant parameters (μ and ξ) (Bertolo and Wieckzorek, 2005) for calibration, the most appropriate values of these parameters are still an object of research. Calibration of these parameters will help to determine the range of the appropriate Voellmy coefficients that can be applied for prediction in the region.

In the present study only the rheological parameters that were varied include the basal frictional angle (μ) and the turbulence coefficient (ξ). An attempt was also made to calibrate the scouring rate because a debris flow or be it any form of mass movement is not free from material entrainment. The scouring rate determines the amount of material entrained by the model. It is the measure of erosion at the base of the flow. Calibrating this parameter is generally not attempted because it is dependent on the apparent angle of internal friction that changes at every timestep depending upon the addition of saturation in the soil. Changing the scouring rate would entail addition of volume at each timestep and lead to high rates of final volume. Further details of the parameters values for scouring rate have been detailed below. The criteria chosen to estimate the prediction accuracy were the extent of the runout, the volume displaced and the deposit depth. The density of the soil being field derived was not considered for calibration. Whereas the angle of internal friction keeps changing for every timestep cannot be measured for the moving material. As such angle of internal friction was not calibrated and kept at a constant of $35^{\mathbf{0}}$ (Kuriakose et al. 2009c). Moreover previous studies in the same region reveal that the angle of internal friction ranged between $25^{\mathbf{0}}$- $39.9^{\mathbf{0}}$ (NBSS and LUP 1999 in Kuriakose et al. 2009a) for different soil types in the area hence tweaking it would have affected the ambiguity of the output.

4.2.1. Turbulence Coefficient

Turbulence Coefficient has been expressed in Equation 10(Chapter 2, Section 2.8). The equation reveals that the 'turbulent' term is dependent on the square of the flow velocity of the debris. Voellmy introduced this term to determine all the velocity dependent factors of flow resistance. It accounts for the rate dependent resistance that is due to change in the material behaviour of the high-shearing strain rates (Sosio et al. 2008). This term is dependent upon the overburden stress and influenced by the flow height. Field measurement of this parameter is not possible and only laboratory derived values of shear straining rates can be determined. In the absence of laboratory measurements of this value literature derived values have been used. Hungr and Evans (1996) have compiled well documented case histories for calibration of the Voellmy turbulence coefficient parameter suitable for back analysis (c.f. Table 4.1).

According to Bertolo and Wieckzorek (2005) calibration of the debris flow in the Yosemite Valley in California resulted in a range of values for Voellmy turbulence coefficient ranging between 500-600 $m.sec^{-2}$. Similarly Cipeda et al. in Ho and Li (2007) in order to conduct the benchmarking exercise for the Tate Cairns debris flow have also used 500 and 1000 $m.sec^{-2}$ as the turbulence coefficient values for calibrating the Voellmy model using DAN3D. It can be summarised that there is an inherent uncertainty regarding the range of values to be chosen for the calibration of the model.

Table 4.1: Turbulence Coefficient values used for Calibration of the model, (Hungr and Evans 1996)

Case scenarios	Turbulence Coefficient ($m.sec^{-2}$)
Pandemonium Ck	1000
Frank	700
Avalanche Lake N.	700
Avalanche Lake S.	500
Hope	500
Dusty Creek	200
Rubble Creek	100
Turbid Creek	300
Kennedy River	300
Mystery Creek	600
Lake of the Woods	200
Mt. St. Helens	500
Madison Canyon	500
Sherman Glacier	1000
Gros Ventre	500
Val Pola	500
Mt Granier	1000
Diablerets	450
Elm	500
Goldau	500
Flims	500
Ontake	200
Mayunmarca	500

The range chosen here for the turbulence coefficient parameter was between 100-1000 $m.sec^{-2}$ to observe the changes that these values have on the deposit depth, area and the volume. Generally rock avalanches have values of turbulence coefficient between 500-1000 $m.sec^{-2}$ (McDougall and Hungr 2005) whereas debris flow or flow in a torrent have values between 100-400 $m.sec^{-2}$(Hungr and Evans 1996). In order to observe the influence that such a wide range of parameter values have on the observed parameters such a range was chosen. Moreover with a wide ranging parameter values the behaviour of the model in the prediction can be observed in greater detail. Again for this would help in determining the range of values significant for the present case study too. Thus model runs were conducted by varying the turbulence coefficient values for each simulation. It was found that when the model was simulated keeping the basal frictional angle at 30^0 and scouring rate at 0.0035 m.sec by choosing a synthetic range the following results were obtained.

Table 4.2: Results for Calibration by varying values for Turbulence Coefficient

Turbulence Coefficient ($m.sec^{-2}$)	Deposit Area (m^2)	Deviation from observed area (2686 m^2)	Maximum Depth (m)	Deviation from observed depth (6.4m)	Final volume (m^3)	Deviation from observed volume (1533 m^3)
100	1634	1052	8.25	-1.85	2904	561
200	1836	850	7.40	-1.00	3188	-1635
300	1833	853	4.23	2.17	2634	-1081
400	1689	997	3.30	3.10	2065	-512
500	1616	1070	2.34	4.06	1573	-20
600	1687	999	2.26	4.14	1570	-17
700	1687	999	2.32	4.08	1545	8
800	1654	1032	2.39	4.01	1217	336
900	1661	1025	2.22	4.18	1026	527
1000	1611	1075	2.37	4.03	1045	508

The results reveal considerable variation in the outputs. Table 4.2 reveals that all the values for deposit area are under predicted. The amount of deviation from the observed deposit area 2686 m^2 as tabulated above shows a considerable discrepancy in the prediction of the area. Similarly for deposit depth varying the model with turbulence coefficient values of 100 and 200 $m.sec^{-2}$ results in maximum deposit depths of 8.25 m and 7.4 m respectively that is a little higher than the observed deposit depth of 6.4 m. But the resulting maximum deposit velocity and volume is much higher with the same values. A trend is observed by varying the values of turbulence coefficient. With increasing values of turbulence coefficient the volume decreases with the exception of the value 200 $m.sec^{-2}$ that predicts the highest volume. Similarly in case of velocity increasing the turbulence coefficient values lead to increase in the resulting velocities. The model hence is able to predict the deposit depth with slight variations from the optimum value within the parameter range of 100-200 $m.sec^{-2}$ when all the other parameters were kept constant. In the rest of the cases the model showed results far deviating from the observed values. Moreover with extreme high values of turbulence coefficient the model under predicts deposit area, depth and volume. From the overall table it is observed that the varying turbulence coefficient values have little effect on the deposit area predicted. But varying a single parameter alone cannot truly depict the range of values required for prediction of the landslide. Further details of the values for deposit area, depth, velocity and volume are comparable in Section 4.3.

4.2.2. Basal Frictional Angle

The apparent frictional angle used in the Voellmy model determines the fact that the basal shear stress opposes motion and depending upon the chosen reference coordinate system is always negative (Hungr and McDougall 2007). Thus the movement of the mass of the material is determined by a basal rheology which may be very much different from the internal rheology of the material under consideration. It accounts for the momentum dissipation. In the Voellmy rheology as stated in Chapter2, Section 2.8, the pore pressure ratio is assumed as a constant since it is extremely difficult to estimate being dynamically related to the changing levels of normal stress in the material and being influenced by time dependent diffusion at the same time (Begueria et al. 2009). Thus when the pore pressure ratio (u/σ) in Equation 18 (Chapter 2, Section, 2.8) is kept as a constant the total normal stress and the shear stress become proportional and the referred Equation is simplified. It only has a single independent variable, the basal frictional angle, which assumes loading response intermediate between totally drained

and undrained responses and needs to be validated by calibration. With reference to the Benchmarking Exercise on Landslide Debris Runout and Mobility Modelling conducted at the International Forum on Landslide Disaster Management a range of basal friction angle values were chosen for model calibration (Ho and Li, 2007).

Using the values of basal frictional angle listed in Ho and Li (2007) and keeping the turbulence coefficient, the angle of internal friction and the scouring rate at a constant of 250 $m.sec^{-2}$, 35^0 and 0.0035 m.sec respectively the following results were obtained.

Table 4.3: Results for Calibration with varying values for Basal Frictional Angle

Basal Frictional Angle (^{0})	Deposit Area (m^2)	Deviation from observed area (2686 m^2)	Maximum Depth (m)	Deviation from observed depth (6.4m)	Final volume (m^3)	Deviation from observed volume (1533 m^3)
9	2017	669	2.38	4.02	2454	-921
14	2064	622	2.61	3.79	2523	-990
16	2026	660	2.91	3.49	2604	-1071
20	1993	693	3.43	2.97	2768	-1235
24	1998	688	3.71	2.69	2718	-1185
25	1959	727	4.13	2.27	2874	-1341
26	1960	726	3.99	2.41	2711	-1178
30	1813	873	5.58	0.82	3126	-1593
32	1782	904	7.19	-0.79	3263	-1730
34	1754	932	7.99	-1.59	2982	-1449

The above table vividly depicts the influences of the basal frictional angle inhibiting the movement of the materials by hindering the velocity. The values for the volume were seen to have little changes with increasing basal frictional angles of 9^0-26^0 after which the volume increases drastically. But basal frictional angles provide resistance to the movement of material forward so values of basal friction of 32^0 and 34^0 provide uncertainty in the prediction of volume. Depths for these values also seem to exceed suddenly determining the uncertainty in the value range. It was observed that with low values for basal frictional angle keeping the turbulence coefficient and all the other parameters at a constant as mentioned above though the area of the runout was underestimated, the depth values were in a considerable range of 5.58 m to 7.19 m with basal frictional angles of 30^0 and 32^0 whereas the observed depth was 6.4 m at the runout area. The model also overestimated the final volume. But a more precise estimation of the range of values for basal frictional angle can be found by simultaneous variations of scouring rate and the turbulence coefficient values to get a clearer picture (c.f Section Inter and Intra parameter).

4.2.3. Scouring Rate

The model requires values for the parameter scouring rate which determines the rate at which the erosion of the material occurs at the base of the material being transported. The scouring has occurred is vivid from the fact that the material entrainment leads to increased volume at the far end of the deposit. The initial volume of Peringalam landslides was 437 m^3 and the deposit volume was 1533 m^3 which reveals the fact that there must have been a substantial amount of scouring that lead to an increased volume. As stated earlier calibration for the correct scouring rate value is generally not done keeping in mind that its dependence on the angle of internal friction. But in this study an attempt has been made to

determine the influence of scouring rate on model simulation. A synthetic range for the estimation of scour rate was estimated. The calibrated results keeping the other parameters at a constant were as follows.

Table 4.4: Results for calibration with varying values for Scour Rate

Scouring Rate (m.sec)	Deposit Area (m^2)	Deviation from observed area (2686 m^2)	Maximum Depth (m)	Deviation from observed depth (6.4m)	Final volume (m^3)	Deviation from observed volume (1533 m^3)
0.005	1850	836	5.71	0.69	3215	-1682
0.0065	1836	850	4.73	1.67	2950	-1417
0.0095	1879	807	5.38	1.02	3203	-1670
0.0125	1930	756	7.17	-0.77	3702	-2169
0.0196	1931	755	7.49	-1.09	3754	-2221

The results show variability in the nature of the extent, the deposit depth and the volume of the material. The above table depicts the deposit depth in a range of 5.71 to 7.17 m with scouring values of 0.0050- 0.0125 m.sec when the turbulence coefficient was at a constant of 250 $m.sec^{-2}$, angle of internal friction at 35^0 and basal frictional angle at 30^0. But it is absurd to keep values of scouring rate as high as 0.0125 and 0.196 m.sec because it will add exceeding volumes as visible in the above table. The volume with a scouring rate value of 0.0196 m.sec is 3754 m^3 due to the influence of various factors like water content, apparent angle of friction, the runout path etc. Such higher values of scouring rate are not feasible for a debris flow characteristic of the present study area where the materials are more granular in composition and confined within a channel. In this case it will produce overestimated volumes. This shows that there lies an intrinsic uncertainty in determining the appropriate range of parameter value for the present study area.

In all the above calibration keeping one or either of the parameters as a constant the model over estimated the volume of the deposit. The values for deposit depth were found to match the optimum values. But the extent of the deposit area was under predicted by the model. In order to observe the influence of the minute changes as a result of calibration the parameter values were both inter and intra varied.

4.3. Inter and intra varying of parameters

Each of the parameters were not only varied with some constants but were also varied interchangeably to compare results with the observed parameters for the runout. This involved varying each value for the turbulence coefficient with that of the values for basal frictional angle maintaining the constant values for angle of internal friction and scouring rate as previous in order to find the combined influence of both these parameters on the runout. The Table 1 (Appendix II) reveals the results of the calibration.

It can be stated after observing the results from the above mentioned table that the model prediction with lower values of turbulence coefficient and basal frictional angles ranging between 200-300 $m.sec^2$ and 25^0-30^0 respectively provides the possible range for prediction of the deposit depth. With turbulence coefficient of 300 $m.sec^2$ and 34^0 the deposit depth was 7.31m deviating from the optimum of 6.4m by 0.91m. The rest of the combinations with this turbulent coefficient values showed below optimum results. Similarly in case of turbulence coefficient of 100 $m.sec^2$ lower values of basal frictional angles of 9^0 - 24^0 predict the deposit depth in the range of 5.58 m - 7.78 m and higher values predict results far deviated from the observed 6.4m. Considering the overall trend of deposit depth with varying

basal frictional angles it is vivid that turbulence coefficient influences the deposit depth considerably. Increasing the values of turbulence coefficient to 1000 m.sec^2 the lowest prediction for deposit depth (1.65m) was observed with the highest value of basal frictional angle (34^0). This signifies that the higher values of turbulence coefficient and basal frictional angle influence the flow height. A higher basal frictional angle retards the movement of material forward together with a turbulence coefficient the affect of overburden stress of the material is reduced considerably.

Again considering the values for area near optimum predictions were found with turbulence term of 250 m.sec^{-2} and basal frictional angles 9^0- 16^0 but deposit depth values are much deviated from the optimum. Similar influence of both the TC and BFA parameter values has been observed with volume output predictions as well. With increasing TC (600-900 m.sec^{-2}) and BFA (14^0-20^0) the volume predicted matches well with the observed final volume of 1533 m^3.

A similar approach was taken by varying the turbulence coefficient, the basal friction angle and the scouring rate simultaneously. The detailed results for it can be found in Appendix II. The values generated thereby show that the model overestimated the final volume of the material.

4.4. Back Analyses of the calibration to observed values

Validation refers to the testing of the model to sets of field data that are preferably under different or varying environmental conditions. This helps in the examination of the range of validity of the calibrated model and is a necessary requirement for model application. But what should be borne in mind is that the calibration data should be independent of the validation data. Validating the results of calibration to various output variables helps strengthen the predictability of the model under a possible range of perturbed environmental conditions that are difficult to predict. Hence it can be stated that model validation is necessary for the application of the model to various scenarios.

But in case of numerical modelling owing to the presence of a single event validation of the result becomes difficult. As such the method applied here is known as back analyses. Back analysis refers to the comparison of the model output with the calculated values which are referred as observed values (c.f. Chapter 3, Section 3.1.7) and simultaneous varying of calibration values until the optimum observed value is reached. The following Figure 4.2 shows the area modelled and also demarcates the

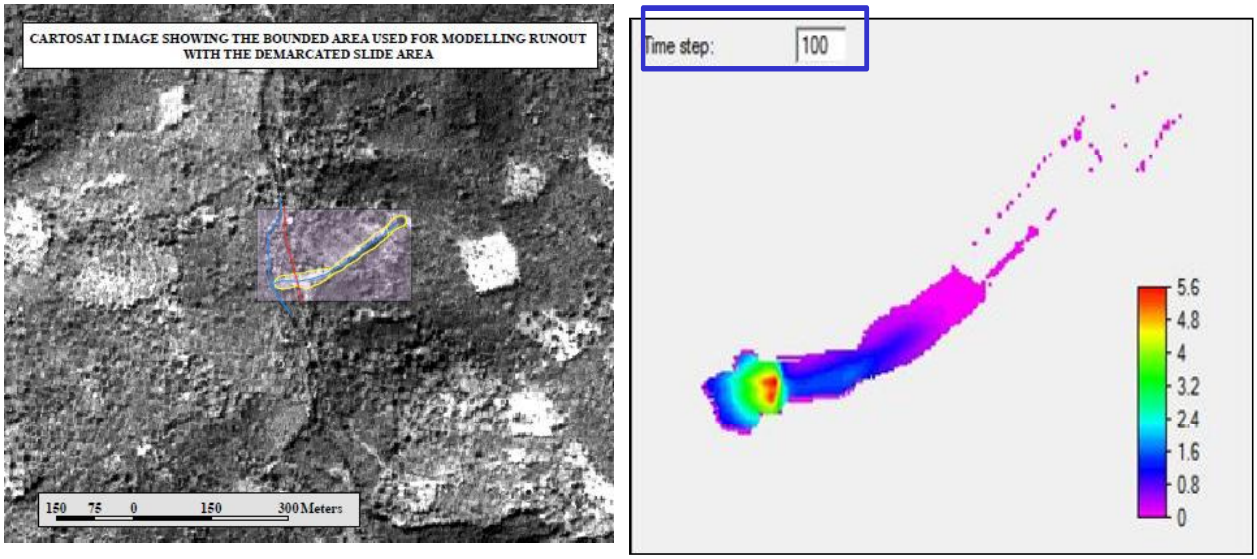

Figure 4.2: CARTOSAT I showing the landslide, the road affected by the landslide and the stream into which the slurry part of the debris drained with the demarcated channel and road affected

stream that flows along the debris flow. The road affected by the debris flow is also visible. To the right is the simulated result for the 100th timestep for the calibration value mentioned below.

The model was calibrated with a set of parameter values that were varied for each model simulation to match the observed results. The simulated result for each calibration value was compared with the observed values of maximum deposit depth at the deposition zone, the total deposited volume and the area. The Figure (5.3) depicts the back analyses of a simulation with turbulence coefficient values of 250 m.sec^{-2}, basal frictional angle of 30^0 and scouring rate of 0.0035 m.sec reveal the deposit depth of 5.6 m, an area of 1813 m^2 and a final volume of 3126 m^3.This was validated with the demarcated actual landslide runout zone from the Cartosat I image (date of pass, 18th November, 2007). It can be seen from the Figure5.4 that the runout matched the runout zone upto a considerable limit. There are areas in the deposit zone for which the runout is not certain. They comprise the outer edge of the deposit area and the front. Moreover the parameter combination does not accurately predict the deposit depth. The area is also under predicted whereas the volume is over predicted.

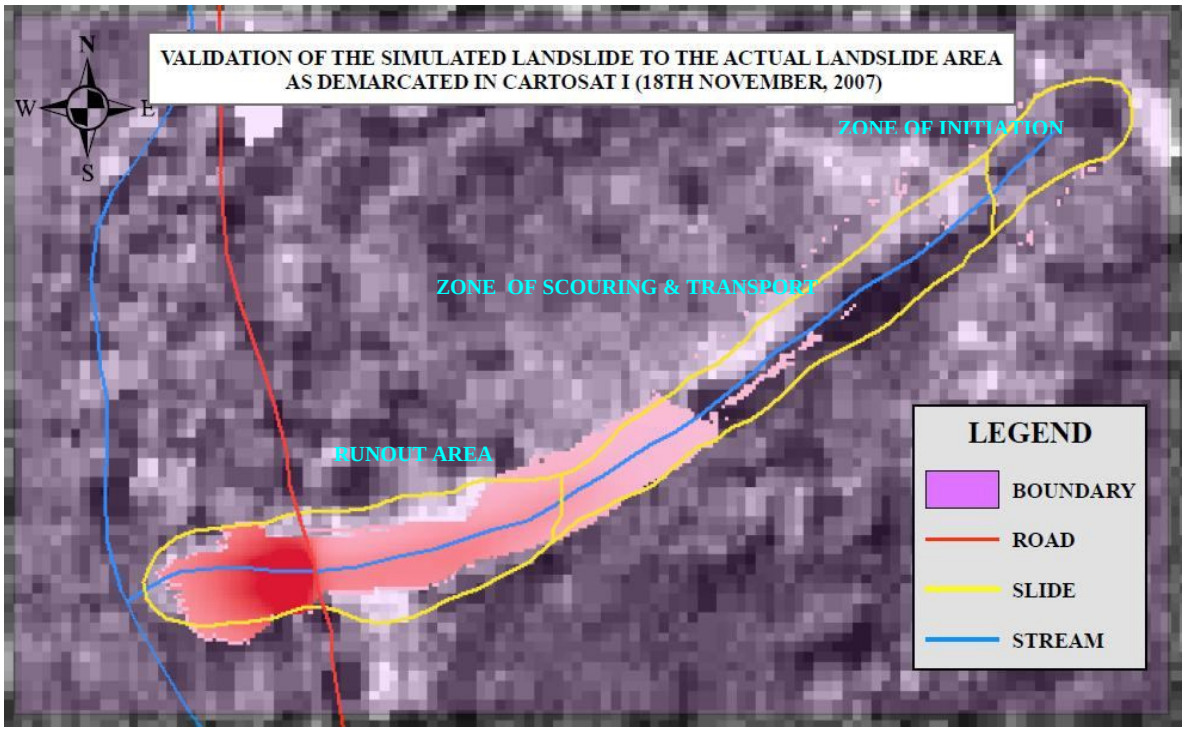

Figure 4.3:Validation of the simulated area to that of the observed

Similarly the values for deposit depth, area and volume were compared for each of the calibrated result. This shows the amount of variability from the observed values for each of the calibrated parameters. Hence it is possible to determine the how much the simulated values differ from the observed values. The results of this varying amount of deviations from the observed area, the deposit depth and the volume have been tabulated in Tables 5.1, 5.2 and 5.4.

It is clearly visible in Table 5.2 that the amount of variation from the observed depth was found to be lowest when the turbulence coefficient was 200 m.sec^{-2} wheras the area was under predicted with an error of (2686 (observed) – 1836 (simulated)) m^2 = 850 m^2 . Similarly the error in the prediction of final volume was estimated as (3188 m^3 (simulated) -1533 m^3 (observed) = 1635 m^3 of over predicted volume. Thus the calibration of the model and back analyses of the simulation resulted in the variations and derivation of errors that has been shown in the Appendix (II).

5. Sensitivity Analysis

Many synonyms can be encountered in literature sensitivity analysis such as geographical sensitivity analysis (Lodwick et al. 1990), sensitivity analysis or variability analyses (Lowry et al. 1995; McKinney et al. 1999), etc. But the dominating query that lies beneath all these synonyms is how the application of sensitivity analysis can be significant in the analysis of uncertainty.

Determination of the amount and kind of change produced as a result of model predictions due to changes in the model parameters is referred to as sensitivity analyses (Scott 2004). It is the study of how variations in the model simulation results can be contributed, be it quantitatively or qualitatively, to various sources of variation. This emphasizes on the variability of the model output depending upon the information fed into it. Though seldom confused with the term uncertainty, sensitivity considers uncertainty via back analysis (from the output back into the input) determining the amount of individual uncertainty contributed to the output uncertainty (Tarantola and Crosseto 2001). Sensitivity is related to the model and its dependence to the variations of the input factors.

Thus sensitivity analysis has gained importance as it provides answer to the following aspects:

- the factors that contribute to the variability in the output,
- the possible range of parameters for which estimates have to be made,
- the input factors for which the model variability is the maximum, and
- the influence of factors that interact among themselves (Scott 2004).

Thus according to the European Commission handbook for extended impact assessment, a working document by the European Commission (2000) it can be inferred that, "*a good sensitivity analysis should conduct analysis over the full range of plausible values of key parameters and their interactions, to assess how impacts change in response to changes in key parameters*" emphasizing the need for uncertainty and sensitivity analysis (in Saltelli, 2005).

In this study sensitivity analyses was conducted so as to determine the variability in the range of parameter by observing the output results obtained by changing the inputs. In a dynamic runout model there are many parameters representing quantities that are difficult to determine and sometimes even impossible to measure and if possible it is a tedious task to measure it with a great deal of accuracy. Hence there are estimates used for the parameters and sensitivity analyses is required involving the turbulence coefficient and the basal frictional angle to determine the influence they bear on the level of accuracy necessary to make the model useful and valid. A sensitivity analysis in this case is able to indicate the range of parameter values that can be reasonably used in this particular shallow landslide debris flow. A wide range of parameter values can best indicate the behaviour of the model in extreme situations. The following graphs depict the sensitivity of the extent of the deposit, deposit depth and volume resulting from calibration of parameters. It also accounts for the amount of variability for a particular parameter.

An approach for standardization of the deposit values was undertaken using the Z- Score method discussed in Chapter 1 & 2. Z Scores are used to provide a way of standardizing data across a wide range of experiments or results. Data once normalized using Z score transformations can be used directly to determine the significant changes between two parameters. An advantage of the Z Score method is

that it provides a profile of the observed deposit directly from the Z distribution curve. The complete picture of the whole distribution of the deposit depth is available for each of the simulated results. Thus when the Z score transformation is applied it determines here the values of individual simulation result expressed as a number of standard deviations above or below the mean value of the observed deposit. It accounts for the measure of variability for each simulation. Not only that the mean and the standard deviation values help determine the deviation from the mean and the amount of deviation is determined by the standard deviation. Thus it is not only comparable to the observed deposit depth but also for each of the simulations relatively. Thus Z score method are advantageous because of the increased statistical power they possess being a continuous variable. Used as an index of severity it can portray the extreme variability in the simulations results with visual clarity. Another advantage is the calculation of useful statistics like the coefficient of covariation that can help quantify the amount of variability in the simulated results.

The amount of variation of deposit depth when the turbulence coefficient values were varied can be depicted from the graph below (Figure 5.1). The turbulence coefficient parameter was varied and it was found that varying the parameters with turbulence coefficient (TC) values while keeping all the parameters as a constant variability with respect to higher values of Turbulence coefficient were less than those observed with lower values of turbulence.

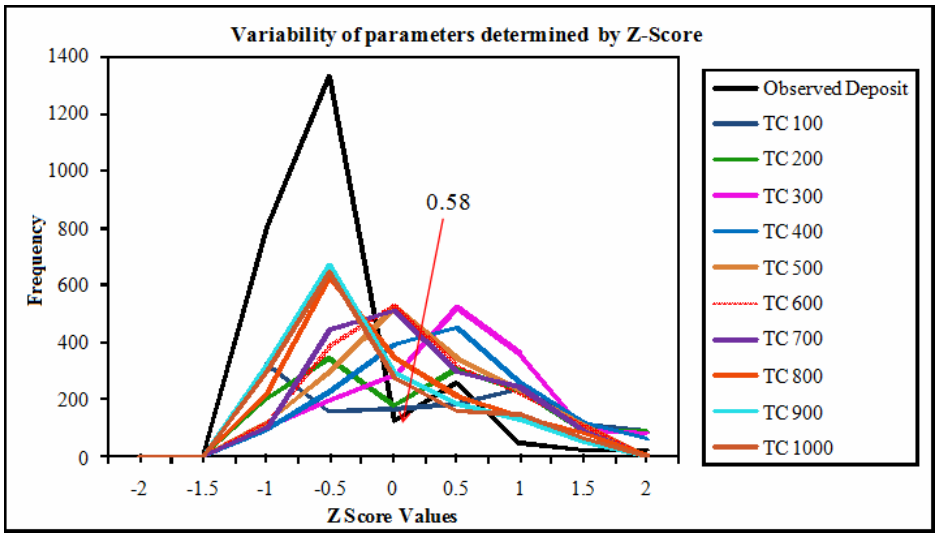

Figure 5.1: Sensitivity to Turbulence Coefficient (TC) values influencing deposit depth

Figure 5.1 depicts the variability with respect to the observed Z- Score values. The observed Z Score for observed depth values show a peak away from the mean (0.58) this is because of the fact that landslide are natural phenomena with characteristic variations. Moreover the observed deposit map consisted of a high range of values which led to convergence of information at and around a single point. Owing to the large range of values, the Z Score values for each pixel in the deposit area was but into frequency bins of Z Score values ranging from -2 to +2 with an interval of 0.5 and the graphs were thereby generated. The observed graph is for reference and helps determine the variability of the depth due to the affects of changing calibration values. Hence with respect to this observed map the output varied considerably. The Table 5.1 depicts the mean and the standard deviation values that help to depict the above graph. The coefficient of variation helps to quantify this variability with respect to varying turbulent coefficient values. It was observed that the coefficient of variation when the turbulence coefficient value was 100 $m.sec^{-2}$ the coefficient of variation was found to be 0.96 which indicates that the mean was more than the mean of the observed deposit but the results for deposit depth were more

consistent with this value. Similar trends of 0.92 were found for turbulence values of 200 m.sec^{-2}. Though the mean and standard deviations were found to be higher the prediction showed more consistency with respect to these values. The turbulence coefficient values of 800-900 m.sec^{-2} reveal values of mean nearer to the optimum observed value of 0.58 with a consistency in the prediction of depths of 0.80-0.91 but calibration values for maximum deposit depth (Table 5.1) reveals that the depths were largely under predicted as also the volume and the area. The lower values of mean may have resulted due to the range of values of depth for the deposit area being comparatively higher scaling down the mean to a small denomination.

Table 5.1: Quantifying the variability of the Z Score graphs

Turbulence Coefficient Values (m.sec-^{2})	Mean	Standard Deviation	Coefficient of Variation
100	1.78	1.72	0.97
200	1.74	1.60	0.92
300	1.44	0.90	0.62
400	1.22	0.72	0.59
500	0.97	0.56	0.57
600	0.93	0.56	0.60
700	0.92	0.55	0.60
800	0.74	0.59	0.80
900	0.62	0.56	0.90
1000	0.65	0.59	0.91

Z Score graphs for basal frictional angle were also generated to show the variability of the simulation results to the range of simulated values with respect to observed depth.

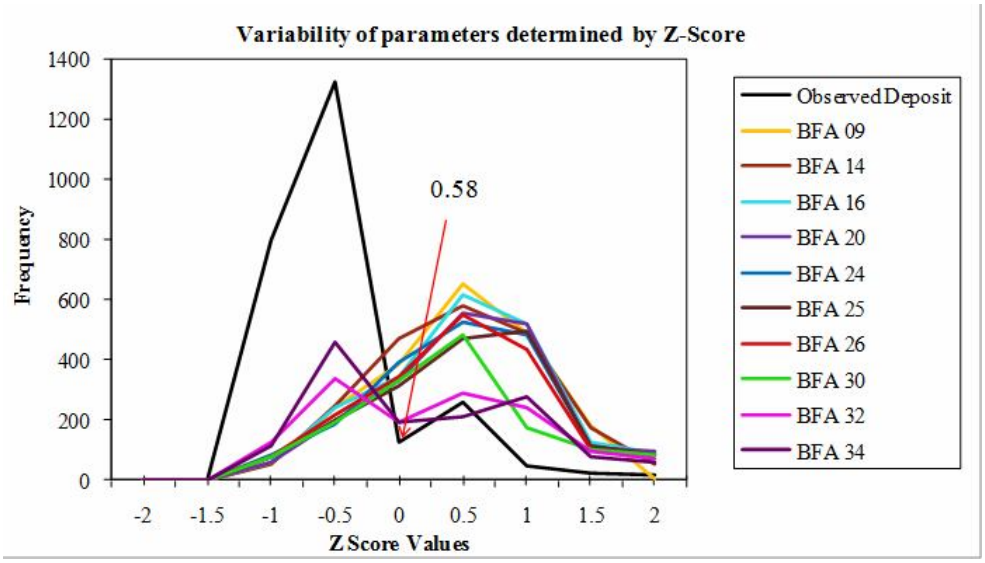

Figure 5.2: Sensitivity to Basal Frictional Angle (BFA) values influencing deposit depth

Similar variations were shown with varying basal frictional angle values. But it must be noted here that with the increasing values for Basal frictional angle in the range of $26^0 – 34^0$ less variation in depth is observed. This can be justified by the coefficient of variation values that show increasing consistency in the prediction of deposit depth from 0.58 - 0.98 m.sec, though Table 5.3 reveals that area was under predicted and volumes were over predicted.

Table 5.2: Quantifying the variability of the Z Score Graph

Basal Frictional Angle (^{0})	Mean	Standard Deviation	Coefficient of Variation
9	1.22	0.53	0.44
14	1.22	0.57	0.46
16	1.29	0.61	0.48
20	1.39	0.71	0.51
24	1.36	0.74	0.55
25	1.47	0.85	0.58
26	1.38	0.80	0.58
30	1.72	1.28	0.74
32	1.83	1.63	0.89
34	1.70	1.66	0.98

Sensitivity with changing scour rates values was also conducted to observe the variation. It was found that the depth values are most sensitive to higher values of scour rate and show values of depth and volume (c.f. Table 5.3) owing to the fact that there lies considerable uncertainty in the determination of the scouring rate values and synthetic ranges of value chosen can be liable for accurate predictions of the maximum deposit depth. Moreover volume changes have been observed in the calibration results as well.

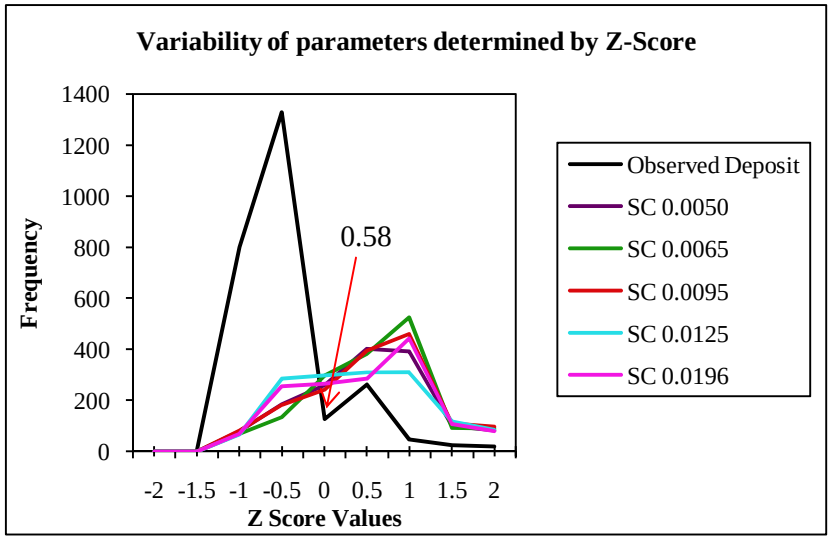

Figure 5.3: Sensitivity to Scouring rate (SC) values

The amount of variability observed in case of the scouring rate values was highest in case of 0.0196 m.sec but rather consistent. Least consistent values were observed for scouring rate of 0.0065 m.sec the mean value of which is much higher than the observed mean of 0.58 but the standard deviation values are closer to the observed standard deviation of 0.89. This shows that though the mean fort he maximum observed depth is greater the deviation is comparatively less.

Table 5.3: Quantifying the variability in the Z Score

Scouring Rate (m.sec)	Mean	Standard Deviation	Coefficient of Variation
0.005	1.74	1.23	0.71
0.0065	1.61	0.98	0.61
0.0095	1.70	1.15	0.67
0.0125	1.92	1.58	0.82
0.0196	1.94	1.58	0.81

But results for the observed depth for this value between 0.0050 m.sec to 0.0095 m.sec showed under prediction for depth. Hence what needs to be emphasised here is that though any synthetic range of value may provide deposit depths closer to the observed values there is no certainty that the same values in combination with other parameter will produce the same results. As has been observed in the present study a scouring rate of 0.0196 m.sec has lead to considerable over prediction of volume making it certain that scouring rates directly influence the volume of the material. Further analyses sensitivity to varying combination values the range of parameter values was conducted.

Inter and intra parameter calibration led to sensitivity of inter and intra parameter values as well results for which have been appended in the appendix. It is vivid that with value ranges of turbulence coefficient between100-300 $m.sec^{-2}$ the graphs did not produce wide ranges of values and hence compared to the observed graph were lower. But the prediction of depth varied greatly with higher values of turbulence coefficient. In the combinations with turbulence coefficients between 200 $m.sec^{-2}$ and 300 $m.sec^{-2}$, the basal frictional angle (26^0-34^0), the outputs for depth were predicted well between 5.12-8.5m. It was observed that with turbulence coefficients of 200 $m.sec^2$ and basal frictional angles of 24^0 - 26^0 near observed depths were found. So variability with respect to these values was lower as compared to turbulence coefficient between 700-1000 $m.sec^{-2}$ and varying basal frictional angles values. The curve for this range is visibly comparable to the observed deposit depth values but the range of deposit values are very low and go down to as low as 1.7m, the reason for peak at a single point similar to the observed depth. Similarly scouring rates of 0.0050-0.0095m.sec with basal frictional angles of 24^0-26^0 and turbulence coefficients 200-300 $m.sec^{-2}$ have shown visibly less variability and the calibration results depict deposit depth with slight over prediction and under prediction in some combinations with varying combinations.

Thus in a nutshell it can be summarised that the determination of the parameter ranges is very important in the prediction of the debris flow. Each of the parameter values and their resultant combination outputs also has uncertainty. Now emphasizing the main objective of the study it can be stated that the determination of this inherent uncertainty in the outputs of the model that is deposit extent, deposit depth and volume (scouring rate has not been dealt here) must be dealt with. This has been done in greater detail in the next chapter.

6. Uncertainty Analyses

The nature of all geomorphic studies implies a degree of Uncertainty (Jakob and Weatherly 2008). With the progress in the field of environmental modelling, dynamic models, that refer to simulations run forward in time, wherein the state of the model at time t is defined as a function of its state in a period or timestep preceding t, have been widely applied to the landslide prediction. The aim of this study is to quantify the inherent uncertainty in the model output, that is the deposit depth, deposit extent and the volume because it not possible to quantify the rheological parameters even after appropriate data collection or laboratory experiments. In case of numerical models there is an option of backward analysis by deriving calibrating the model and compare results with the observed event trying to fit the model parameter to the result. Hence any forward prediction involves knowledge of the range of parameter values that can best simulate results for an event. This uncertainty in the estimation of the parameter range is important in order to make quantitative risk assessments. Moreover determination of this uncertainty will lead to determination of the robustness of the model to various input parameters. Understanding the limitations of the environmental data is significant in responsible use of the uncertain data (Heuvelink et al. 2006). Research on uncertainty has focussed mainly on the identification and management of different types of uncertainties and their representation in simple overlay procedures (Davis and Keller 1996).

An attempt was made to determine the range of input parameters applicable for the case study under consideration with the help of an intensive model calibration using a wide range of parameter values. This was followed by sensitivity analyses using the Z Score method to determine the variability in the parameters for extent of the deposit, its maximum deposit depth, volume and the maximum velocity, the results for which have been discussed in the previous chapters.

6.1. Determination of the Random Values

In order to determine the uncertainty in the range of parameter input a Monte Carlo simulation was used to create 100 scenarios. The Monte Carlo method is based on the generation of innumerable trials to determine the expected value for random variables. Keeping in mind the time (approximately 15 minutes for each model simulation with a processor speed of 2Ghz and a 2Gb RAM) required for each model run the random values were kept at a limited 100 scenarios. The output generated from these random value simulations were then compared for area, deposit depth, volume and velocity. The variations with the random values for Turbulence Coefficient, Basal Frictional Angle and Scouring rates have been tabulated in Appendix III for each of the 100 realizations. Observing the generated outputs for deposit area, depth, volume and velocity it was found that the following range of random combinations could best predict the landslide. It is vivid that in all the random combinations the volumes and velocities were over predicted. But in some of the random combinations with turbulence coefficients of 674-690 $m.sec^2$, basal frictional angles between 9^0-14^0 and scouring rates of 0.0053-0.0063 m.sec, the volumes were closer to the observed but velocities were found to be very high.

Table 6.1: Parameter values providing near optimum results for deposit depth and velocity

Parameters	Area (m^2)	Deviation from observed area (2686)m^2	Maximum Depth (m)	Deviation from observed depth (6.4m)	Final volume (m^3)	Deviation from observed volume (1533 m^3)
0108_012_164	1945	348	6.99	-2.37	3795	-2242
0114_011_192	1915	378	6.30	-1.68	3740	-2187
0135_034_053	1596	697	8.79	-4.17	3107	-1554
0142_034_165	1509	436	8.68	-1.69	3046	-1493
0163_017_129	2052	241	4.99	-36	3625	-2072
0177_013_157	2293	393	4.62	1.78	3493	-1940
0234_026_162	1920	373	6.55	-1.93	3721	-2168
0250_030_109	1882	411	5.52	-0.90	3292	-1739
0315_026_158	2209	84	8.17	-3.55	3402	-1849
0451_013_082	2207	-262	2.51	4.48	2298	-745
0470_028_080	1980	313	7.00	-2.37	2584	-1031
0674_014_056	1861	84	2.26	4.73	1542	11
0678_018_063	1917	28	2.46	4.53	1555	-2
0690_009_053	2058	-113	2.32	4.67	1528	25

Again emphasizing the influence of the scouring rate on the volume of the material deposited a random combination with turbulence coefficient of 135 $m.sec^2$, basal frictional angle of 34^0 and scouring rate 0.0053 m.sec predicts significantly higher volumes with higher value of deposit depth. It is hence inferred that with that derivation of the best combination keeping all the predicted parameters is difficult and justifies that the concept of equifinality does not imply here because each of the random combinations would provide values different from the other for individual scenarios.. Moreover any change in the values of a particular parameter in the random combinations would lead to varying results. What is of more concern is to find the range of parameter value that can best determine all the parameters. The uncertainty in the determination of the most appropriate combination of parameter is vividly displayed in the Table (6.1) above. Hence quantification of this uncertainty in the accuracy of the prediction has been approached by a probabilistic method.

6.2. Probabilistic Method of quantifying uncertainty

Various methods have been discussed in order to determine the uncertainty in models as well as the error propagation (Heuvelink 1998; Crossetto and Tarantola 2001, Karssenberg 2005, etc). In this study a simple probabilistic approach has been taken to derive the uncertainty in the occurrence of runout in a particular pixel by using the above random combinations for parameter values. The most frequently used method is the determination of uncertainty using the probability density function (Heuvelink et al. 2006).

The observed deposit depth for the debris flow for the present scenario was 6.4 m. Considering it to be the highest depth at the deposit zone and assuming that each of the 100 realization would provide results of maximum depth of 6.4 at the deposit zone the probability of the pixels with a maximum deposit depth of more than 6.4m and less than 6.4 m was determined. Based on the Monte Carlo simulation for 100 scenarios with thickness of deposits it can be inferred for each pixel how many of the 100 scenarios

gives the probability of reaching a deposit depth of 6.4 m. Similarly probability of the deposit depth of 0-2 m, 2-4 m, 4-6 m and above 6 m was determined. This would quantify the probability of the pixels falling in distinct depth ranges. This approach will further help to determine the probability of the parameters to fall within a certain acceptable range as has been determined by the calibration of the parameters. Moreover it also determines the probability of exceeding the range of values. The probability of each of the random simulations has been illustrated in the Appendix III.

6.3. Quantifying overall uncertainty of runout in the deposit zone

To determine the uncertainty in the prediction of the deposit depth by the model the probability of each pixel being affected by 100 random simulations has been determined. This ascertains the probability of the pixels being affected by the debris flow of a given magnitude since the initial volume of the debris flow is known (437 m3). Now when the magnitude of landslide is known the probability of runout for each

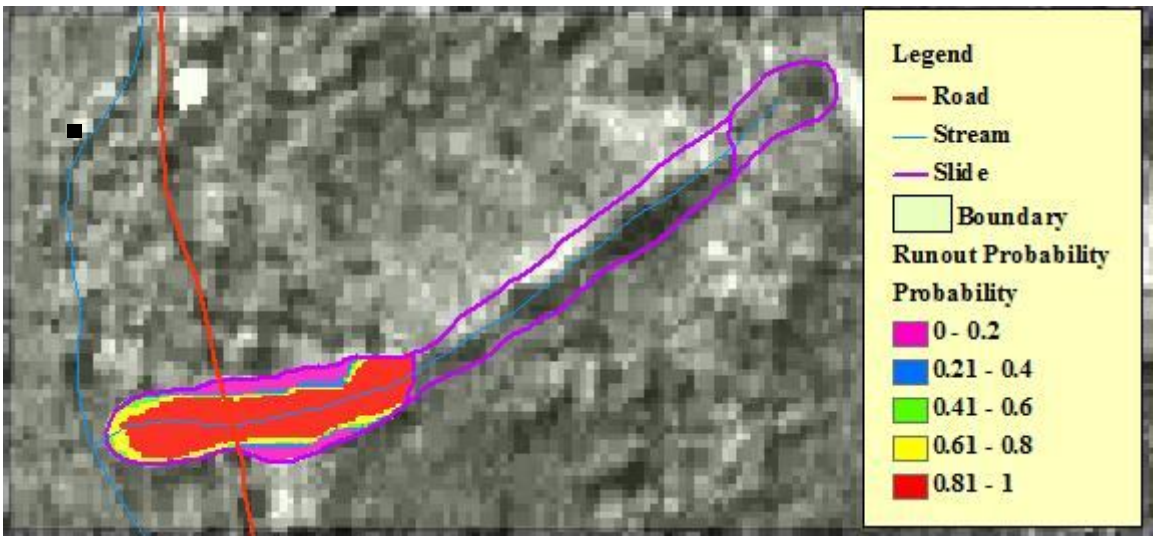

Figure 6.1: Prediction of the probability of runout in the deposit area

pixel was calculated by the number of pixels for which there were runouts divided by the number of occurrences (100) in this case. Thereby for each pixel the probability that landslide with a certain magnitude would reach or not was determined for the entire deposit area. The above map is the result of the probability of runout in each pixel. It was observed that the model predicted highest runout probability in the central part of the deposit area. Away from here towards the periphery the runout probability decreased considerably to as low as 0-0.2.

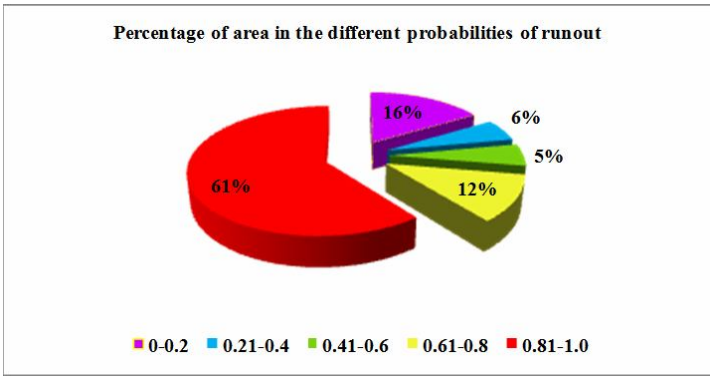

Figure 6.2: Percentage of area with probability of runout

This helps in the determination of the percentage of area in which the pixels reached a certain probability of runout. The Figure 6.3 below determines that 61% of the area has the probability of runout of 0.81-1 which is the central part of the deposit area in the map (Figure 6.2) whereas at the frontal part of the deposit zone the probability of runout encompasses 12% of the total area. The lowest occurrence of runout in a pixel is found in the periphery of the channel and covers an area of 16%.

6.3.1. Quantifying uncertainty of predicting deposit depth in the deposit zone

Similar probabilities for probability of the depth of the material reaching a particular pixel in the 100 random scenarios was determined by calculating the probabilities of deposit depths of varying heights affecting the runout area. This was done by calculating the probability in each of the depth classes. Assuming that the lowest depth is 0 and that of the highest is 6m since 6.4 m of debris depth in the deposit area has been observed the probability was calculated. The resulting map shows that the probability of deposit depth between 0-2m. It is clearly displayed that in the the central part of the deposit zone and towards the front probability of deposit lying between 0-2m is more than that along the road. Only a small section of the road consists of probability of reaching a runout of deposit depth 0-2m on the upper part of the road segment lying in the centre of the deposit area.

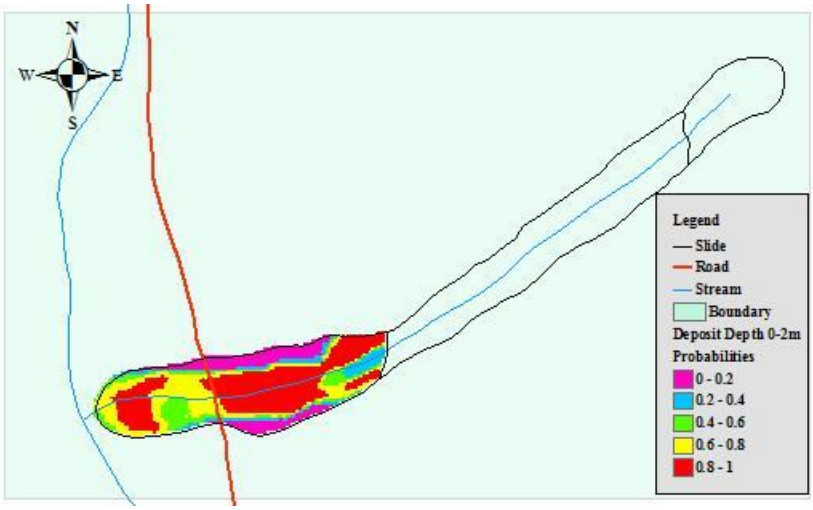

Figure 6.3: The probability of deposit depth between 0-2m

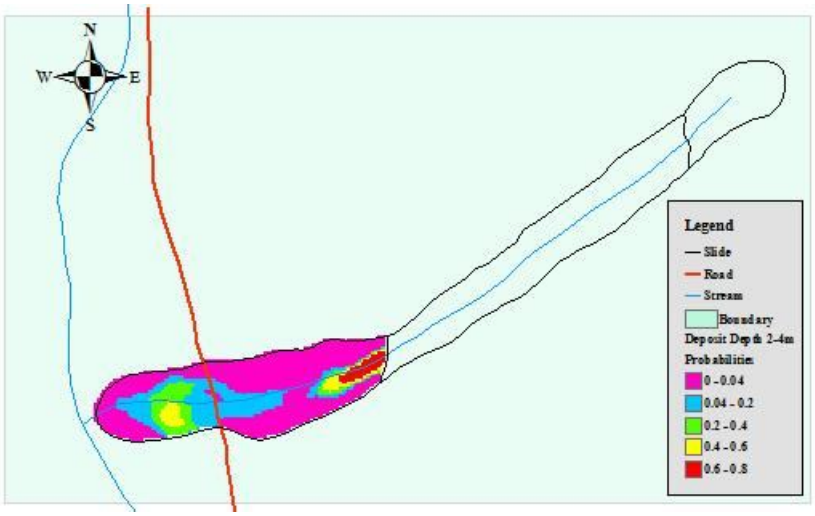

Figure 6.4: Probability of runout with deposit depth 2-4m

The area under the deposit depth with highest probabilities is (Figure 6.4) 38% of the total area which means only a small percentage of the total runout zone has the deposit depths of less than 2m most of the area is covered with depths greater than two meter. The Probabilities of depth values of 2m reduce towards the periphery of the deposit zone similar to Figure 6.2.

The probability for various deposit depths were conducted and the area covered by each of them reveal the amount of deposit area directly under the impact of deposit depths of 0-2m, 2-4m, 4-6m, and more than 6m. In case of depths between 2-4m the highest values probability of occurrence was found in the area just at the mouth of the fan indicating that

the deposit depth is highest at the location normal to the bed of the channel (Figure 6.5). The area around the periphery again falls in the zone lowest probability of runout. This indicates that the model is able to predict deposit depths at the bed normal position along the channel. It was found that in most of the cases the probability of occurrence of deposit of varying depths was lowest along the either periphery of the deposit area. In the central part of the deposit area the model is able to predict depth with utmost certainty but it is the periphery area and the part of the front for which the probabilities of occurrence of runout is found to be the lowest.

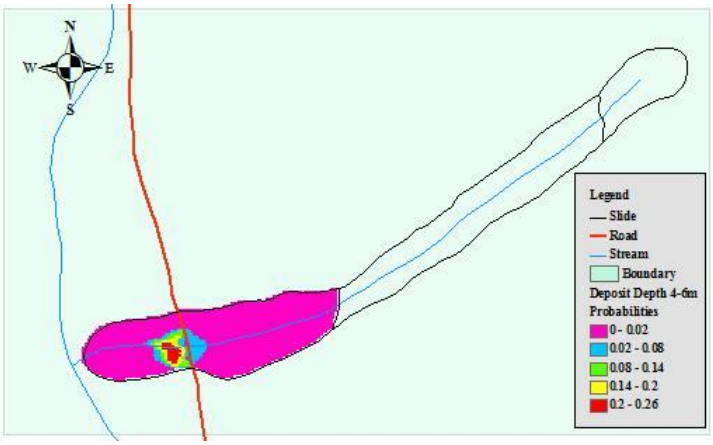

Figure 6.5: Probability of runout of deposit depth 4-6m

Probabilities for occurrence of runout for deposit depths of 4-6 m and >6 m portray that the impact of the debris surge reaching the road was found to be the highest in the middle section of the road running across the deposit area. Thus the probability of runout reaching the road with a depth of > 6m is found to be at the intersection of the road and the stream where the debris flow deposits all the load. Out of the 100 random simulations the probability of the pixels reaching the road is 96% of the total area. The probability of the area falling with deposit depth of 4-6 m is 89% of the 100 scenarios.

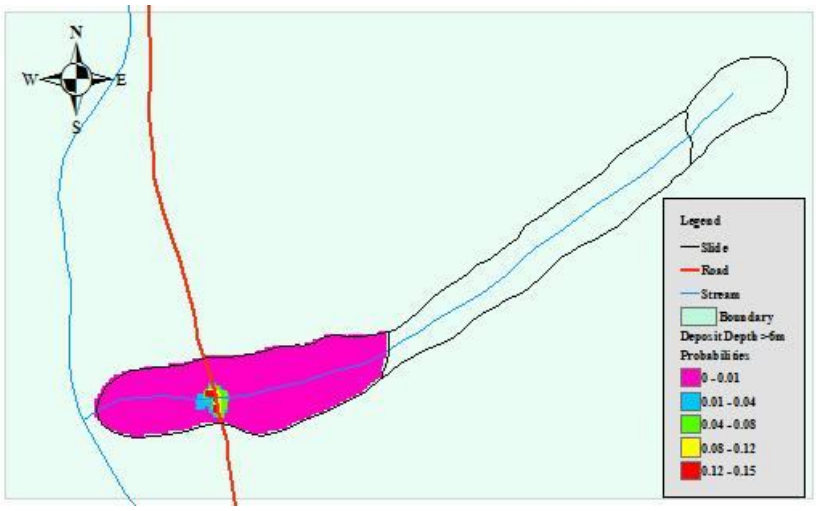

Figure 6.6: Probability of runout of deposit depth >6m

The following Figure (6.7) reveals the percentage of area falling in each of the probability classes for deposits with varying heights. It was found that the most of the simulations did not predict around the periphery of the deposit depth. This area covers mostly the lowest probability and the lowest extent in all the probabilistic analyses. As seen in figure (6.7) the lowest probability area cover a large area in the probability of deposit depths of 0-2 m and has the lowest area in the probability of deposit depths with 4-6 m and > 6 m.

All the above maps are useful for planners and policy makers as they provide the probability of occurrence of debris runout of varying depths in the deposit area. This will help demarcate areas where the debris flow surge will have the strongest impact. Moreover the delineation of the percentage of areas falling in different probability class helps to distinguish vulnerable areas from those of less vulnerable

for immediate action. Apart from this the demarcation of the area for which the model predicts deposit depths with utmost certainty can be done too.

More over it helps in the determination of the appropriate random values that can best predict the deposit depth and area.

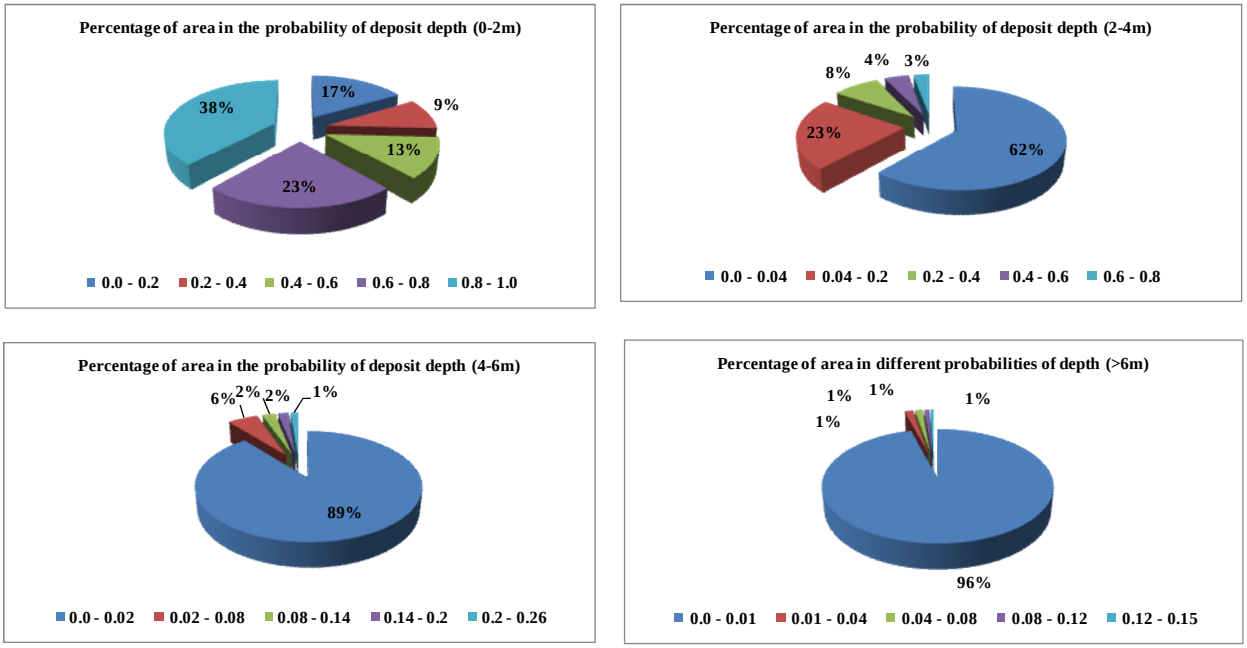

Figure 6.7: Percentage of area in each of the probability classes for varying deposit depths

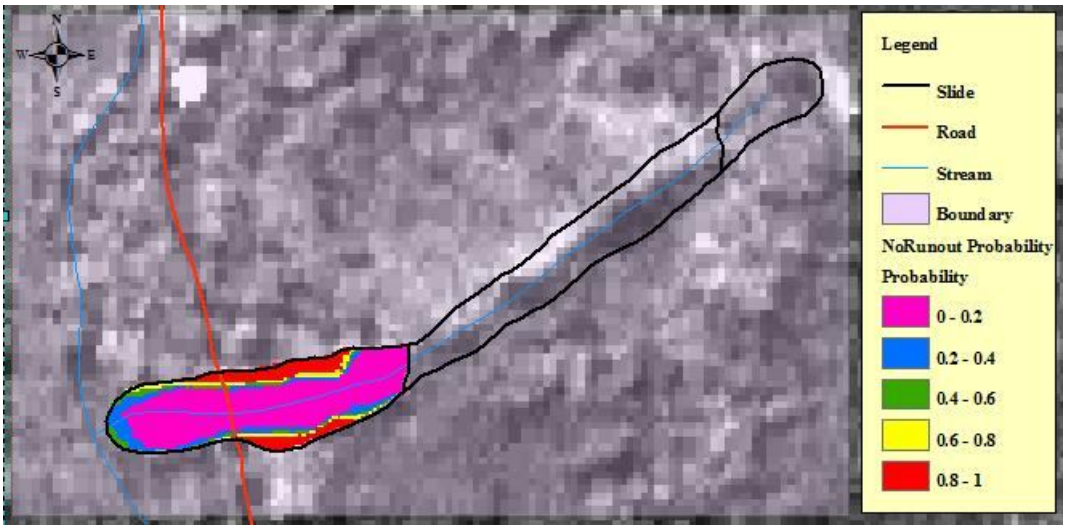

Figure 6.8: Uncertainty in the prediction of runout

Speaking about uncertainty it is important to demarcate zones or areas where no runout occurrences were found. The map below will relate to the overall uncertainty in the prediction of runout in the deposit area. The deposit area estimated as 2686 m^2 was able to predict the runout only in the central part of the bed as depicted by the zone in red with the highest probability of runout (0.81-1) in each pixel of the 100 random simulations conducted. The magnitude of occurrence of runout decreases away from the part of the channel normal to the bed. The part with probabilities between 0-0.2 are the areas most uncertain. Thus it is vivid that the highest uncertainty is found in the regions with probabilities of 0.8-1 lying along the channel slopes where the probability of the pixels reaching runout

was not found. The model is able to accurately predict runout in the bed normal part of the channel. It is here that the highest depth has been observed. Uncertainty ranges between 0.2-0.4 in areas lying at the frontal edge of the deposit zone and towards the periphery of the channel bed. The table below accounts for the percentage of area that is uncertain.

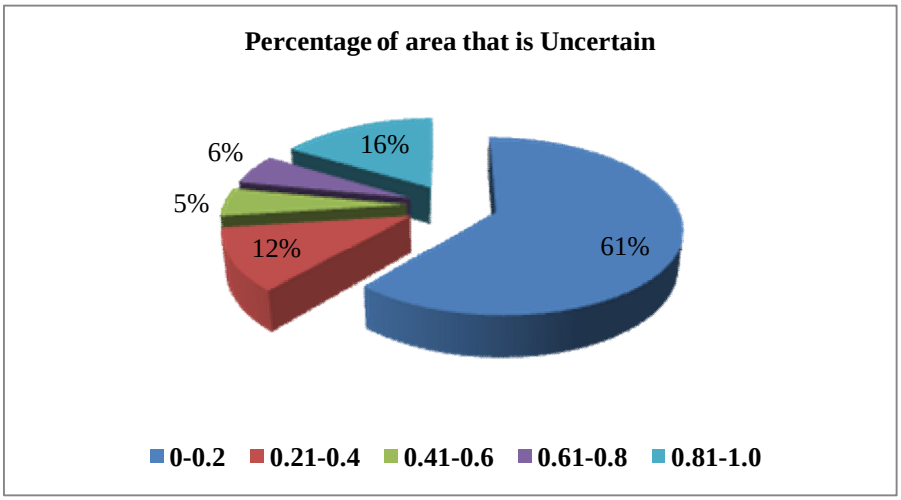

Figure 6.9: Percentage of area that is uncertain

It can be inferred from the above table that the model is able to predict runout in 61% of the deposit area accurately whereas there remains an uncertainty in the remaining 16% of the area. The rest of the areas with probabilities between 0.2-0.4, 0.4-0.6 and 0.6-0.8 are the ones which are moderately uncertain because they cover 12 %, 5% and 6% of the area respectively where varying probabilities of deposit depth were found to occur. This is the area that lies at the periphery of the bed normal deposit zone. This also reveals the ability of the model to predict the core of the deposit at the foot of the slope confined in the channel rather than on the opposite valley sides. This was verified by deriving the probability of the pixels with no runout in all the 100 random simulations with varying ranges of parameters. It hence determines in a way the probability of occurrence of and no occurrences of runout for each of the random simulations so as to determine the probability of predicting runout for the particular pixels for each of the parameter combinations. Moreover 16.31% area is uncertain of not having runout in the deposit zone which is almost similar to the uncertain area influenced by runout occurrences. But determination of the uncertainty of runout affecting an individual pixel alone will not be significant enough unless an overview of the amount and the velocity with which the runout is affecting each pixel in the deposit zone is known.

If such an output map (Figure 6.9) is generated for prediction of the areas where the debris flow have occurred and will occur in future then planning for relocation of the people affected as also measures for protection of the area can be done by policy makers.

Thus determination of the possible range of parameters suitable for the prediction of debris flow cab be derived if it is possible to derive the probability of the debris affecting the road running along the channel in the and lying in the landslide hazard zone and being most vulnerable to the aftermath of debris deposit. This determines the intensity of the debris flow affecting the road (c.f Appendix III, Table1). Thus for each random simulation the probability of the pixels affected by runout varies greatly form that of the observed probability of 0.96. In the deposit zone the magnitude of debris flow affecting the road along a channel and crossing a stream is 96% whereas that for each of the random simulations varies from 43% to 86%. It should be noted here that the lowest probability of a simulation in which the road was affected is 0.43 for the combination of parameters where the turbulence coefficient is 999 $m.sec^2$,

basal frictional angle of 11^0 and scouring rate of 0.0131 m.sec. But the parameter combination is not acceptable because the rate of scouring is too high for such an area which would result in exceeding final volumes. Similar combination (TC 998 m.sec-$^{-2}$, BFA 26^0 and SC 0.0190 m.sec) with higher rates of basal frictional angle has the probability for affecting the road of 0.76 which is comparatively higher. Thus it can be pointed out here that each of the combinations also has an inherent uncertainty while determining the prediction for occurrences of debris flow along the road. The most appropriate range of values for basal frictional angle predicting the deposit depth was found between 24^0-26^0 which maybe the case why the simulation combination provided such a result. The range of turbulence coefficient values between 200-300 m.sec^{-2} with combinations of basal frictional angle 22^0-34^0 and scouring rates of 0.0050-0.0125 m.sec has affected the road along the path of the flow with consistent probabilities of 0.71 to 0.72 whereas any variation away from this has led to under prediction or over prediction. Thus the uncertainty in the random simulations can hence be quantitatively verified. Thus predictions made with these parameter combinations will provide accurate predictions of 70-72% while the remaining 28-30% of the prediction is in apt uncertainty.

7. Conclusion

After analysis of all the results of calibration and determination of the amount of uncertainty in the prediction of the depth and error in the prediction of area and volume of the model it can be stated that mitigation and prevention of landslide hazard requires not only forecasting of the slope stability conditions but also the hazard area affected by the flow. It is inferred that the initial moving mass can determine the extent of the hazard zone and the rheological parameters are significant as they govern the movement of the material.

Thus the range of parameters available (Table 6.1) by random simulation will provide best results for deposit thickness or depth. The range of values and there calibrations provided under prediction of Results of calibration reveal that the basal frictional angle has a retarding influence on the velocity of the flow whereas the turbulence coefficient and the scouring rates initiate the velocity of the material thereby making the flow move ahead due to convective acceleration. What the model is near accurately able to predict is the deposit depth with the random parameter values (Turbulence coefficient of 114 m.sec-^{2}, Basal frictional angle of 11^{0} and a Scouring rate of 0.0192m.sec) with over prediction of volume and under prediction of deposit extent. Similar results have been provide by the random parameter (Turbulence coefficient of 234and 250 m.sec-^{2}, Basal frictional angle of 26^{0} and 30^{0} and Scouring rate of 0.0162 m.sec and 0.0109 m.sec) have been able to predict depth with slight variations. What is of concern is the determination of velocity which is over predicted. But tweaking with the range of parameters able to predict deposit depth values well may in course help determination of the velocity with more accuracy.

Thus the uncertainty in the range of parameter values is vivid by the determination of the probability of runout affecting the road in each of the random simulations. The overall uncertainty in the depiction of deposit depths is clearly portrayed in the maps with high uncertainty in 16% of the area of the deposit zone. Accurate predictions were found for 62% of the area whereas an area of 23% was considered to be moderately uncertain because there were occurrences of runout observed in this area though they were very low falling in the probability interval of 0.2-0.8.

Maps generated with prediction of this uncertainty can serve as base maps for relocation and management of hazard. It will serve as an important source of information for the planners and policy makers as well.

8. Recommendations

- Determination of the uncertainty for the particular range of input parameters for the rheological model for a single area will help prediction of landslide runout in an area where no landslide has occurred. This can be done if the applicability of using values of one landslide to a similar event is determined.
- Moreover possibility of using values of one landslide to another in the same environmental conditions is another topic of future research.
- Comparison of various events with the same range of parameters would help derive the possible ranges of parameter estimation for different landslide types. This would help a comparative evaluation of the uncertainty.
- Utilising the model at a regional scale to predict the occurrence of landslide with the same set of parameter values would determine the capability of the model and robustness for macro scale studies, though a difficult task.
- As far as the influence of topography on the model output is concerned a detailed information of the DEM and determination of the inherent uncertainty by changing the grid sizes of the DEM using different methods and conducting a sensitivity analysis with different grid sizes could be thought of as another topic of immense potential.
- Keeping in mind the various types of uncertainty prevalent in any model one aspect that can be emphasized for future research is the uncertainty in data interoperability from different GIS platforms and the loss of data in this respect.

References

Aleotti, P., 2004.Warning system for rainfall-induced shallow failures.Journal of Engineering Geology, 73(3-4): 247-265

Arattano, M., Marchi, L., 1999.Video-derived velocity distribution along debris flow surge. Physical Chemical Earth, Vol. 25, No. 9, pp 781-784

Arattano, M., Franzi,L. and Marchi, L., 2006.Influence of rheology on debris-flow simulation. Natural Hazards and Earth System Sciences, Vol. 6, 519-528

Armento, M.C., Genevois, R., Tecca, P.R., 2008.Comparison of two debris flows in the Cortina d' Ampezzo area, Dolomites, Italy.Landslides, 5:143-150

Ayotte, D., Hungr, O., 2000.Calibration of runout prediction model for debris flows avalanches, Proceedings of the Second International Congress on Debris Flows Hazard Mitigation: mechanics, prediction and assessment, A.A. Balkema, Rotterdam, 505–514

Barbolini, M., Natale, L., Savi, F., 2002.Effects of release condition uncertainty on avalanche hazard mapping.Natural Hazards, 25, 225-244

Begeuria, S., Van Asch, Th.W.J., Malet, J.P., Grondahl, S., 2009.A GIS based numerical model for simulating the kinematics of mud and debris flows over complex terrain.Natural Hazards and earth System Sciences, Vol. 9, Number 6, 1897-1909

Begueria, S., van Hees, M.J., Geertsema, M. 2009.Comparison of three landslide runout models on the Turnoff Creek rock avalanche, British Columbia. Landslide Processes: From geomorphologic mapping to dynamic modelling, CERG, UU& US- Strasbourg

Bertolo, P., Botini, G., 2008.Debris-flow event in the Frangerello Stream-Susa Valley (Italy)- calibration of numerical models for the back analysis of the 16th October, 2000 rainstorm. Landslides, 5:19-30

Bertolo, P., Wieckzorek, G.F., 2005.Calibration of numerical models for small debris flow in Yosemite Valley, California, USA.Natural hazards and earth System Sciences, 5, 993-1001

Brunsden, D., 1999.Some geomorphological considerations for the future development of landslide models.Geomorphology, 30, 13-24

Carrara, A., 1993. Uncertainty in evaluating landslide hazard and risk, Prediction and perception of Natural hazards.101-109

Carrara, A., Crosta, G., Frattini, P., 2008.Comparing models of debris flow susceptibility in the alpine environment.Gomorphology, 94, 353-378

Cepeda, J.,2007.The 2005 Tate's Cairn debris flow: back analysis, forward predictions and a sensitivity analysis.In: Ho and Li (eds) Interanational Forum on Landslide Disaster Management, Vol. I, Geotechnical division the HongKong Institute of Engineers

Choubey, V.D. and Litoria, P.K., 1990.Landslide hazard zonation in the Garhwal Himalaya. A terrain evaluation approach, 6th International Congress International Association of Engineering Geology, 6th -10th August.Balkema, Rotterdam, Amsterdam, The Netherlands, pp. 65-72

Chen, H. and Lee, C.F., 2003.A dynamic model for rainfall-induced landslides on natural slopes. Geomorphology, 51, 269-288

Chen, H. and Lee, C.F., 2004.Geohazards of slope mass movement and its prevention in Hong Kong.Engineering Geology, 76: 3 – 25

Crossetto, M., Tarantola, S., 2001.Uncertainty and sensitivity analysis: tools for GIS based model implementation.International Journal of Geographical Information Science, Vol. 15, No. 5, 415-437

Cruden, D.M. and Varnes, D.J., 1996.In: Turner A.K; Shuster, R.L., (eds) Landslides: Investigation and Mitigation. Transport Restoration Board, Special Report 247, pp 36-75

Corominas, J., 1996.The angle of reach as a mobility index for small and large landslides. Canadian Geotechnical Journal 33, 260–271

Coussot, P., Proust, S., Ancey, C., 1995.Rheological interpretation of deposits of yield stress fluids.Journal of Non-Newtonian Fluid Mechanics, 66, 55-70

Dai,F.C., Lee,C.F. and Ngai, Y.Y., 2002.Landslide risk assessment and management: an overview

Davis, T.J., Keller, C.P., 1996.Modelling uncertainty in natural resource analysis using fuzzy sets and monte Carlo simulation: slope stability prediction.International Journal of Geographical Science, Vol. 11, No.5, 409-434

Donatelli, M., Stöckle, C.O., Nelson, R.L., Francaviglia, R., 1999a. Evaluating cropping systems in lowland areas of Italy using the cropping system simulation model CropSyst and the GIS software . Proceedings Seventh ICCTA Conference, Firenze, Italy, 16–17 November 1998, pp. 114–121

Elkins Tanton, 2008.Rheological Models. Introduction to Geology, Spring 2008, MIT OpenCourseWare

Fannin, J. and Bowman, E.T. 2008.Debris flows - Entrainment, Deposition and Travel Distance. Geotechnical News, 25(4): 3-6

Fracollo, L., Papa, M., 2000. Numerical simulationof real debris flow events.Physical Chemical Earth (B), Vol. 25, No. 9, pp 757-763

Fortheringham, A. S. and Wegener, M.,2000. Spatial models and GIS – New potential and new models, Taylor & Francis

Geertsema, M., Hungr, O., Schwab, J.W., Evans, S.G., 2006.A large rockslide-debris avalanche in cohesive soil at Pink Mountain, northeastern British Columbia, Canada.Engineering Geology, 83, 64-75

Geertsema, M., Clague, J.J., Schwab, J.W., Evans, S.G., 2006. A recent large catastrophic landslides in northern British Columbia, Canada, Engineering Geology, 83, 120-143

Guzetti, F., Carrara, A., cardinali, M., Reichenbach, P.,1999. Landslide hazard evaluation : a review of current techniques and their application in the multiscale study, Central Italy. Geomorphology, 31, 181-216

Hammonds, J.S., Hoffman, F..O., Bartell, S.M., 1994.An introductory guide to uncertainty analysis in environmental and Health Risk Assessment. Oak Ridge National Library, Us DepartMent of Energy

Himesh, S., Rao, CVC., Mahajan, AU., 2000., Calibration And Validation Of Water Quality Model. CSIR Centre for Mathematical Modelling and Computer Simulation

Henrion and Small, 1992. Uncertainty: a guide to dealing with uncertainty in quantitative risk and policy analysis, Cambridge University press, pp 39

Heuvelink, G.B.M., 1998. Error Propagation in Environmental Modelling with GIS.London:Taylor & Francis

Heuvelink, G.B.M., Brown, J.D., van Loon, E.E., 2006. A probabilistic framework for representing and simulating uncertain environmental variables. International journal of Geographical Information Science, Vol. 21, No. 5, 497-513

Ho, K., Li, V., 2007.The 2007 International Forum on Landslide Disaster Management. Vol. I, Geotechnical Division, The HongKong Institution of Engineers.

Hungr, O., 1995. A model for the runout analysis of rapid flow slides, debris flows, and avalanches. Canadian Geotechnical Journal, 32, 610-623

Hunger,O., 1997. Some methods of landslide hazard intensity mapping. In Proceedings of the Landslide Risk Workshop. Edited by R.Fell and D.M.Cruden. A.A.Balkema, Rotterdam, The Netherlands, 215-226

Hungr, O., Evans, S.G., 1996.Rock avalanche runout prediction using a dynamic model. Landslides, Senneset (ed), Balkema, Rotterdam

Hungr, O., Evans, S.G., Bovis, M., Hutchinson, J.N., 2001.Review of the classification of the flow type.Environmental and Engineering Geoscience, VII, 221-238

Hungr, O., Evans, S.G., Bovis, M. and Hutchinson, J.N., 2001, Review of the classification of landslides of the flow type. Environmental and Engineering Geoscience, VII, pp 221-238

Hungr, O., Corominas, J.,Eberhardt, E., 2005.Estimating landslide motion mechanism, travel distance and velocity.In: Hungr, O., Fell, R., Couture, R., Eberhardt, E. (eds), Landslide Risk Management. Taylor and Francis, London, pp 99-128

Hungr, O., McDougall, S., Wise, M., Cullen, M., 2007.Magnitude –frequency relationships of debris flows and debris avalanches in relation to slsope relief. Geomorphology, 96, 355-365

Hurlimann, M., Copons, R., Altimir, J., 2006.Detailed debris flow hazard assessment in Andorra: A multidisciplinary approach. Geomorphology, 78, 359-372

Hurlimann, M., Rickenmann, D., Medina, V.,Bateman, A., 2008.Evaluation of approaches to calculate debris-flow parameters for hazard assessment. Engineering Geoloogy, doi:10.1016/j.enggeo.2008.03.012

Hussin, Y., 2009.Standardized to normal distribution and probability, NRM-Module 5, Statistics, ITC, The Netherlands

Hutchinson, J.N., 1986. A sliding-consolidation model for flow slides. Canadian Geotechnical Journal 23, 115– 126

Hutchinson, J.N. 1988. Mass Movement. In: Encyclopedia of Geomorphology. Fairbridge, R.W. (ed). Reinhold Book Corp., New York, pp 688-696, 1968

Hwang, D., Karimi, A. H. and Byun, D.W., 1998. Uncertainty analysis of environmental models within GIS environments. Computers and Geosciences, Vol. 24, No. 2, pp119- 130

IPCC, Conceptual basis for uncertainty analyses. Annex 1, 2006

Jakob, M. and Hungr, O., 2005. Debris-flow hazards and related phenomena, Published by Springer and Praxis, Ch 2, pg 9-20.

Jakob, M., Weatherley, H., 2008. Integrating uncertainty: Canyon Creek hyperconcentrated flows of November 1989and 1990. Landslides, 5:83-95

Karam, S.K., 2005. Landslide Hazards Assessment and Uncertainties, Phd Thesis, Deptt. Of Civil and Environmental Engineering, Massachusetts Institute of Technology

Karssenberg, D., Jong, K.De., 2005. Dynamic environmental modelling in GIS:2 Modelling error propagation. InternationalJournal of Geographical Information Science, Vol. 19, No. 6, 623-637

Karssenberg, D., Jong, K, De., 2005.Dynamic environmental modelling in GIS:2Modelling error Propagation.International Journal Of Geographical Information Science, Vol. 19, No. 6. 623-637

Kocyigit, O., Gurer, I., 2006.Effects of Voellmy coefficients on determining runout distance: A case study of Uzungol, Turkey. G.U.Journal of Science, 20(3): 79-85

Kundu, P.K., Cohen, I.M., 2002.Fluid Mechanics, Second Edition, Academic Press

Kuriakose, S.L., Sankar, G., Muraleedharan, C., 2008. History of Landslide susceptibility and chorology of landslide-prone areas in the Western Ghats of Kerala, India. Environmental Geology, DOI 10.1007/s00254-008-1431-9

Kuriakose, S.L., 2009a. History of landslide susceptibility and chorology of landslide-prone areas in the Western Ghats of Kerala, India, Environmental Geology, 57(7), 1153-1568.

Kuriakose, S.L., van Beek, L.P.H. and van Westen, C.J., 2009 (In Press b). Parameterizing a physically based shallow landslide model in a data poor region. Earth Surface Processes and Landforms, 34(6), 867-881.DOI: 10.1002/esp.1794.

Kuriakose, S.L, Quan Luna, B, Begueria Portugues, S, van Westen, C.J, 2009c. Modelling the runout of a debris flow of the Western Ghats, Kerala, India; Geophysical Research Abstracts, Vol 11(EGU2009-4276). European Geosciences Union Annual General Assembly 2009, 19-24 April, Vienna, Austria.

Legros, F., 2002.The mobility of long runout landslides.Engineering Geology, 63, 301-331

Laigle, D.,Coussot,P.,1997.Numerical modelling of mudflows.Journal of Hydraulic Engineering 123,617–623

Lilburne and Tarantola, 2009. Sensitivity analysis of spatial models, International Journal of Geographical Information Science, Vol. 23, No. 2, 151-168

Lodwick, W.A., Monson, W., Svoboda, L., 1990.Attributable error and sensiticity analysis of map operations in geographic information systems:suitability analysis.International Journal of Geographical Information Systems, 4,413-428

Lowry, J.H., Miller, H.J.,Hepner, G.F., 1995.A GIS based sensitivity analysis of community vulnerability to hazardous contaminants on Mexico/Us border. Photogrammetric Engineering and Remote Sensing, 61, 1347-1359

McDougall, S., Hungr, O., 2004.A model for the analysis of rapid landslide motion across three dimensional terrain. Canadian Geotechnical Journal, 41: 1084-1097

McDougall, S., Hungr, O., 2005.Dynamic modelling of entrainment in rapid landslides. Canadian Geotechnical Journal, 42: 1437-1448

McKinney, M.D., Mackey, B.G., Zavitz, B.L., 1999. Calibration and sensitivity analyses of a spatially distributed solar radiation model.International Journal of Geographical Information Science, 13, 49-65

Mc Kinnon, M., Hungr, O., McDougall, S., 2008. Dynamic analyses of Canadian landslides. Geohazards

Merz, B. and Thieken, A. H.: Separating natural and epistemic un-certainty in flood frequency analysis, Journal Of Hydrology, 309, 114–132,2005

Naef, D., Rickenmann, D., Rutschmann, P., McArdell, B.W., 2006. Comparison of flow resistance relations for debris flows using a one-demensional finite element simulation model. Natural Hazards and Earth System Sciences, 6, 155-165

Oberkampf, W.L., 2005. Uncertainty Quantification using evidence Theory.Advanced Simulation and Computing Workshop, Error estimation, Uncertainty Quantification nad Reliability in Numerical Simulations,Sandia National Laboratories

Price, J., 2006.Lagrangian and Eulerian Representations of Fluid Flow: Kinematics and the Equations of motion. Woods Hole Oceanographic Institution, MIT Open course ware

Prochaska, A.B., Santi, P.M., Higgins, J.D., Cannon, S.H., 2008 et al 2004 Debris- flow runout predictions based on the average channel slope (ACS). Engineering Geology, 98, 29-40

Revellino, P., Hungr, O., Guadagno, F.M., Evans, S.G., 2008.Velocity and runout simulation of destructive debris flows and debris avalanches in pyroclastic deposits, Campania region, Italy. Environmental Geology, 45:295-311

Revellino, P., Guadagno, F.M., Hungr, O., 2008.Morphological methods and dynamic modelling inlandslide hazard assessment of the Campania Apennine carbonate slope. Landslides, 5:59-70

Rickenmann, D., 1999. Empirical relationships for debris flow. Natural Hazards, 19:47-77

Rifai,R., 2008. Spatial modelling and risk assessment of Sidoarjo Mud Volcanic flow. MSc Thesis , ITC, The Netherlands

Santolo, A.S.di., Evangelista, A., 2008.some observations on the prediction of the dynamic parameters of debris flows in pyroclastic deposits in the Campania region of Italy.Natural Hazards, DOI 10.1007/s11069-008-9334-3

Saltelli, A., Tarantola, S., Campolongo, F., Ratto, M., 2004. Sensitivity Analysis in Practice, A Guide to Assessing Scientific Models. Wiley, New York, 232pp

Sassa, K.,Fukuoka, H.,Wang, F.,Wang, G., 2007.Progress in Landslide Science.Springer Berlin Heidelberg New York.

Savage, S.B., Hutter, K., 1989.The motion of a finite mass of granular material down a rough incline. Journal of fluid mechanics, Vol. 199, 177-215

Scheidegger, 1994 A.E. Scheidegger, Hazards: singularities in geomorphic systems, Geomorphology 10, pp. 19–25

Scott, M., 2004. Uncertain models and modelling uncertainty.Dept of Statistics, University of Glasgow EMS workshop, Nottingham

Soeters, R., van Westen, C.J., 1996.Slope instability recognition, analysis, and zonation.In: Turner A.K., Schuster R.L., (eds) Landslide investigation and mitigation. Transportation Research Board, National Research Council Special Report, 247, National Academy

Sosio, R., Crosta, G.B., Hungr, O., 2008.Complete dynamic modeling calibration for the Thurweiser rock avalanche (Italian Central Alps). Engineering Geology, 100, 11-26

Swiler, L.P., Guinta, A.A., 2007. Aleatory and Epistemic Uncertaintyquantification for Engineering Applications.Sandia Technical Report, SAND2001-2670C

Thampi, P.K., Mathai, J., Sankar, G. and Sidharthan, S., 1997. Evaluation study in terms oflandslide mitigation in parts of Western Ghats, Kerala. 2005, 11, April

Thomas, M. F., 2001.Landscape sensitivity in time and space - An introduction. Catena, 42: 83-98

van Asch, Th.W.J., Malet, J.P., van Beek, L.P.H., Amitrano, D., Techniques, advances, problems and issues in numerical modelling of landslide hazard, Unpublished

van Beek, L.P.H., 2002. Assessment of the influence of changes in Landuse and Climate on Landslide Activity in a Mediterranean Environment. PhD Thesis, University of Utrecht, Utrecht, The Netherlands, 363 pp

van Loon, A.J., 2004.From speculation to model: the challenge of launching new ideas in the earth sciences. Earth-Science Reviews, 65, 305-313

van Westen, C.J., Rengers, N., Terlien, MTJ., and Soeters, R., 1997. Prediction of the occurence of slope instability phenomena through GIS-based hazard zonation. Geol Rundsch, 86: 404-414

van Westen, C.J., van Asch, Th.W.J., Soeters, R., 2005.Landslide hazard and risk zonation-why is it so difficult?Bulletin in Engineering geology and Environment, DOI 10.1007/s10064-005-0023-0

van Westen, C.J., Castellanos Abella, E.A. and Kuriakose, S.L., 2008.Spatial data for landslide susceptibility, hazard and vulnerability assessment: An overview. Engineering Geology, 102(3-4): 112-131

Vijith, H., Madhu, G., 2007.Estimating potential landslide sites of an upland sub watershed in Western Ghats of Kerala (India) through frequency ratio and GIS.Environmental Geology, DOI 10.1007/s00254-007-1090-2

Willenberg, H., Eberhardt, E., Leow, S., McDougall, S., Hungr, O., 2009.Hazard assessment and runout analysis for an unstable rock slope above an industrial site in the Riviera valley, Switzerland

Wong, H.N., Ho, K.K.S., 1997. Travel distance of landslide debris. Proceedings of the 7th International Symposium on Landslides, pp. 417– 422

Zhang, J. and Goodchild, M.F., 2002.Uncertainty in Geographical Information, Taylor & Francis, London

Zhang, X., Hormann, G., Fohrer, N., 2008.An investigation of the effects of model structure on model performance to reduce discharge simulation uncertainty in two catchments. Advances in Geosciences, 18, 31-35

Appendix I

Progress Chart

Month	1	2	3	4	5	6	7	8	9	10	11	12	13	14	15	16	17	18	19	20	21	22	23	24	25	26	27	28	29	30	31
July	Proposal Updating and Submission												Organization of Dataset Understanding of the Model and Initial Simulation					Model Run							Literature review for calibration values Model run with Turbulence Coefficient Parameter						
	Literature review																	Chapter Writing													
August	Literature review			Model Runs with Angle of Internal Friction							Progress Report		Rectification of conceptual errors					Model Runs with Basal Frictional Angle													
													Chapter Writing																		
September	Rectification of Mean and SD Values					Progress Report				Deriving Z score Values for depth							Creation of Z score Graphs							Data analysis						
October	Chapter Writing				Pre Mid Term preparation								Mid Term Preparation						Chapter Writing					Sensitivity analyses with scouring rate						
													Model Runs for Scouring Rate																		
November	Random Number Generation (Monte Carlo) & Model Simulation												Uncertainty analyses					Assimilation of Result				Chapter Writing								
December	Chapter Writing												Correction implemented					Preparation of the Thesis												

Appendix II

Table I: Randomly simulated parameters and variability with respect to observed values

Parameters* Randomly Simulated	Area (m^2)	Deviation from area (m^2)	Maximum Depths(m)	Deviation from depth	Maximum Velocity (m.sec)	Deviation from velocity	Volume (m^3)	Deviation from volume
0108_012_0.0164	1945	741	6.99	-0.59	19.24	-8.04	3795	-2242
0114_011_0.0192	1915	771	6.30	0.10	19.47	-8.27	3740	-2186
0129_020_0.0168	1989	697	7.74	-1.34	19.08	-7.88	3938	-2384
0135_029_0.0145	1728	958	8.31	-1.91	18.72	-7.52	3352	-1799
0135_034_0.0053	1596	1090	8.79	-2.39	18.40	-7.20	3107	-1554
0142_034_0.0165	1509	1177	8.68	-2.28	18.45	-7.25	3046	-1493
0146_027_0.0156	1858	828	8.11	-1.71	18.75	-7.55	3650	-2096
0152_030_0.0077	1790	896	8.61	-2.21	19.32	-8.12	3545	-1992
0163_017_0.0129	2052	634	4.99	1.41	22.99	-11.79	3625	-2071
0170_016_0.0052	1982	704	4.40	2.00	22.73	-11.53	3301	-1748
0176_027_0.0152	1825	861	8.05	-1.65	19.56	-8.36	3677	-2124
0177_013_0.0157	2293	393	4.62	1.78	22.77	-11.57	3493	-1939
0183_027_0.0110	1965	721	7.86	-1.46	21.23	-10.03	3889	-2336
0197_033_0.0180	1561	1125	8.38	-1.98	19.10	-7.90	3097	-1544
0198_010_0.0081	2039	647	2.90	3.50	26.25	-15.05	2831	-1278
0207_022_0.0119	2009	677	4.60	1.80	23.71	-12.51	3406	-1852
0214_024_0.0064	2022	664	4.53	1.87	22.72	-11.52	3281	-1727
0234_026_0.0162	1920	766	6.55	-0.15	21.43	-10.23	3721	-2168
0247_032_0.0170	1846	840	7.76	-1.36	23.32	-12.12	3580	-2027
0250_030_0.0109	1882	804	5.52	0.88	24.72	-13.52	3292	-1739
0253_026_0.0119	1975	711	4.22	2.18	24.26	-13.06	3128	-1575
0266_026_0.0180	1933	753	4.09	2.31	25.02	-13.82	3065	-1512
0270_026_0.0115	1948	738	3.91	2.49	24.99	-13.79	2936	-1382
0283_029_0.0162	1929	757	4.79	1.61	24.47	-13.27	3243	-1690
0298_034_0.0083	1804	882	7.56	-1.16	21.85	-10.65	3280	-1727
0303_015_0.0183	1993	693	2.47	3.93	26.94	-15.74	2588	-1034
0315_026_0.0158	2209	477	8.17	-1.77	21.75	-10.55	3402	-1849
0352_026_0.0124	1845	841	3.19	3.21	26.46	-15.26	2510	-957
0353_019_0.0182	2055	631	2.51	3.89	26.82	-15.62	2505	-952
0355_019_0.0061	2084	602	2.66	3.74	29.19	-17.99	2361	-807
0356_014_0.0142	1987	699	2.35	4.05	28.55	-17.35	2359	-806

0380_016_0.0119	2050	636	2.44	3.96	29.13	-17.93	2339	-785
0399_033_0.0114	1759	927	4.09	2.31	25.98	-14.78	2618	-1065
0399_033_0.0188	1761	925	4.17	2.23	25.93	-14.73	2618	-1065
0405_024_0.0153	1956	730	2.73	3.67	27.24	-16.04	2449	-895
0409_010_0.0093	2203	483	2.56	3.84	30.60	-19.40	2271	-718
0416_030_0.0182	1729	957	3.42	2.98	27.39	-16.19	2338	-785
0423_024_0.0155	1953	733	2.58	3.82	27.56	-16.36	2401	-848
0436_014_0.0123	2057	629	2.42	3.98	29.68	-18.48	2249	-695
0451_013_0.0082	2207	479	2.51	3.89	29.97	-18.77	2298	-744
0470_028_0.0080	1980	706	7.00	-0.60	24.62	-13.42	2584	-1031
0470_028_0.0171	1828	858	2.89	3.51	27.83	-16.63	2386	-833
0497_013_0.0194	2095	591	2.32	4.08	31.59	-20.39	2288	-735
0497_033_0.0057	1727	959	3.15	3.25	28.24	-17.04	2061	-508
0503_016_0.0137	2129	557	2.47	3.93	31.81	-20.61	2411	-857
0509_019_0.0127	2130	556	2.48	3.92	29.60	-18.40	2427	-873
0532_013_156	2006	680	2.35	4.05	33.81	-22.61	2171	-617
0542_015_0.0103	2156	530	2.44	3.96	31.89	-20.69	2259	-705
0550_021_0.0114	2043	643	2.32	4.08	29.39	-18.19	2351	-797
0566_013_0.0081	1994	692	2.40	4.00	32.93	-21.73	2027	-474
0571_013_0.0169	2091	595	2.40	4.00	36.20	-25.00	2224	-671
0575_028_0.0191	1853	833	2.69	3.71	28.89	-17.69	2217	-664
0583_027_0.0149	1843	843	2.54	3.86	28.25	-17.05	2266	-713
0586_022_0.0123	2089	597	2.35	4.05	29.93	-18.73	2308	-754
0590_024_0.0108	2075	611	2.38	4.02	29.77	-18.57	2312	-759
0597_030_0.0131	1876	810	2.62	3.78	29.28	-18.08	2191	-637
0601_025_0.0113	2018	668	2.40	4.00	29.91	-18.71	2281	-727
0619_011_0.0176	1976	710	2.46	3.94	40.41	-29.21	1761	-208
0632_011_0.0160	2126	560	2.61	3.79	39.79	-28.59	1782	-229
0639_027_0.0137	1893	793	2.36	4.04	28.51	-17.31	2221	-668
0648_024_0.0099	2151	535	2.44	3.96	30.14	-18.94	2187	-634
0659_019_0.0154	2097	589	2.27	4.13	33.58	-22.38	2232	-679
0664_025_0.0101	2161	525	2.30	4.10	30.17	-18.97	2227	-674
0667_030_0.0067	1777	909	2.30	4.10	29.86	-18.66	1709	-155
0674_014_0.0056	1861	825	2.26	4.14	32.57	-21.37	1542	12
0676_028_0.0119	1874	812	2.38	4.02	28.66	-17.46	2152	-598
0678_018_0.0063	1917	769	2.46	3.94	37.87	-26.67	1555	-2
0682_009_0.0061	1834	852	2.25	4.15	39.95	-28.75	1418	135
0686_018_0.0050	1869	817	2.49	3.91	32.46	-21.26	1320	233
0687_016_0.0058	1986	700	2.35	4.05	36.35	-25.15	1571	-17
0688_019_0.0178	2065	621	2.39	4.01	38.84	-27.64	2103	-550
0690_009_0.0053	2058	628	2.32	4.08	39.69	-28.49	1528	26
0712_028_0.0095	1941	745	2.19	4.21	29.27	-18.07	2098	-544
0717_032_0.0099	1869	817	2.51	3.89	28.95	-17.75	1989	-435
0738_011_0.0141	1956	730	2.54	3.86	46.47	-35.27	1302	251
0751_032_0.0133	1877	809	2.56	3.84	30.00	-18.80	2022	-469

0770_017_0.0081	2012	674	2.56	3.84	37.27	-26.07	1838	-285
0772_024_0.0079	1984	702	2.40	4.00	31.53	-20.33	1869	-316
0782_033_0.0191	1906	780	2.55	3.85	28.84	-17.64	2186	-633
0812_030_0.0169	1852	834	2.32	4.08	29.42	-18.22	2064	-511
0826_031_0.0136	1892	794	2.36	4.04	29.37	-18.17	2056	-503
0829_028_0.0145	2166	520	2.46	3.94	30.39	-19.19	2386	-833
0834_029_0.0095	2029	657	2.42	3.98	30.16	-18.96	2054	-501
0844_032_0.0135	1863	823	2.44	3.96	30.82	-19.62	1959	-406
0847_022_0.0181	2031	655	2.34	4.06	43.44	-32.24	2031	-477
0855_018_0.0134	1968	718	2.39	4.01	46.52	-35.32	1762	-209
0874_022_0.0151	1939	747	2.32	4.08	40.98	-29.78	1990	-437
0875_016_0.0124	1909	777	2.41	3.99	49.32	-38.12	1328	226
0884_028_0.0074	1873	813	2.44	3.96	38.59	-27.39	1246	308
0918_024_0.0157	2084	602	2.42	3.98	36.83	-25.63	1974	-421
0922_021_0.0162	2023	663	2.34	4.06	48.26	-37.06	1679	-126
0922_023_0.0120	1949	737	2.60	3.80	36.97	-25.77	1958	-404
0951_023_0.0107	1943	743	2.63	3.77	34.83	-23.63	1885	-331
0953_024_0.0088	1884	802	2.64	3.76	33.00	-21.80	1732	-178
0955_028_0.0091	2115	571	2.44	3.96	39.13	-27.93	1600	-47
0958_022_0.0158	2141	545	2.34	4.06	50.38	-39.18	1812	-259
0968_009_0.0129	1498	1188	2.49	3.91	35.31	-24.11	906	647
0972_013_0.0160	1860	826	2.46	3.94	39.77	-28.57	1128	425
0983_028_0.0190	2199	487	2.48	3.92	34.68	-23.48	2281	-728
0999_011_0.0131	1505	1181	2.59	3.81	36.50	-25.30	942	611

Table II: Randomly simulated parameters and variability with respect to observed values

Random parameter* combinations	Probability	Random paramater combinations	Probability	Random paramater combinations	Probability
0108 _012_0.0164	0.64	0253_026_0.0119	0.71	0470_028_0.0080	0.75
0114_011_0.0192	0.65	0266_026_0.0180	0.68	0470_028_0.0171	0.67
0129_020_0.0168	0.71	0270_026_0.0115	0.70	0497_013_0.0194	0.72
0135_029_0.0145	0.64	0283_029_0.0162	0.67	0497_033_0.0057	0.72
0135_034_0.0053	0.70	0298_034_0.0083	0.71	0503_016_0.0137	0.77
0142_034_0.0165	0.65	0303_015_0.0183	0.67	0509_019_0.0127	0.74
0146_027_0.0156	0.70	0315_026_0.0158	0.78	0532_013_0.0156	0.65
0152_030_0.0077	0.70	0352_026_0.0124	0.62	0542_015_0.0103	0.77
0163_017_0.0129	0.74	0353_019_0.0182	0.74	0550_021_0.0114	0.70
0170_016_0.0052	0.71	0355_019_0.0061	0.67	0566_013_0.0081	0.68
0176_027_0.0152	0.67	0356_014_0.0142	0.67	0571_013_0.0169	0.72
0177_013_0.0157	0.78	0380_016_0.0119	0.71	0575_028_0.0191	0.74
0183_027_0.0110	0.71	0399_033_0.0114	0.70	0583_027_0.0149	0.65
0197_033_0.0180	0.61	0399_033_0.0188	0.72	0586_022_0.0123	0.70
0198_010_0.0081	0.70	0405_024_0.0153	0.71	0590_024_0.0108	0.74
0207_022_0.0119	0.71	0409_010_0.0093	0.77	0597_030_0.0131	0.74

0214_024_0.0064	0.72	0416_030_0.0182	0.71	0601_025_0.0113	0.72
0234_026_0.0162	0.64	0423_024_0.0155	0.71	0619_011_0.0176	0.64
0247_032_0.0170	0.65	0436_014_0.0123	0.70	0632_011_0.0160	0.77
0250_030_0.0109	0.70	0451_013_0.0082	0.80	0639_027_0.0137	0.70

Table III: Randomly simulated parameters and variability with respect to observed values

Random parameter* combinations	Probability	Random parameter combinations	Probability
0648_024_0.0099	0.78	0826_031_0.0136	0.74
0659_019_0.0154	0.75	0829_028_0.0145	0.81
0664_025_0.0101	0.78	0834_029_0.0095	0.74
0667_030_0.0067	0.64	0844_032_0.0135	0.75
0674_014_0.0056	0.65	0847_022_0.0181	0.70
0676_028_0.0119	0.70	0855_018_0.0134	0.72
0678_018_0.0063	0.65	0874_022_0.0151	0.62
0682_009_0.0061	0.65	0875_016_0.0124	0.65
0686_018_0.0050	0.59	0884_028_0.0074	0.62
0687_016_0.0058	0.70	0918_024_0.0157	0.75
0688_019_0.0178	0.72	0922_021_0.0162	0.72
0690_009_0.0053	0.75	0922_023_0.0120	0.68
0712_028_0.0095	0.77	0951_023_0.0107	0.68
0717_032_0.0099	0.75	0953_024_0.0088	0.65
0738_011_0.0141	0.68	0955_028_0.0091	0.75
0751_032_0.0133	0.75	0958_022_0.0158	0.80
0770_017_0.0081	0.72	0968_009_0.0129	0.43
0772_024_0.0079	0.68	0972_013_0.0160	0.65
0782_033_0.0191	0.78	0983_028_0.0190	0.86
0812_030_0.0169	0.74	0999_011_0.0131	0.43

*Note: The random simulation values have three parameters in a single combination (eg. 0999_011_131) in which the first values is for turbulence coefficient, the second for basal frictional angle and the third for scouring rate.

Table IV: Calibration with the turbulence coefficient and basal frictional angle

Turbulence Coefficient ($m.sec^2$)	Basal Frictional Angle (^{0})	Area (m^2)	Deviation observed area (2686 m^2)	Max. Depth (m)	Deviation depth (6.4m)	Final volume (m^3)	Deviation volume (1533m^3)
100	9	1825	861	5.58	0.82	3199	-1666
100	14	1916	770	7.18	-0.78	3319	-1786
100	16	1855	831	7.13	-0.73	3355	-1822
100	20	1750	936	7.73	-1.33	3312	-1779
100	24	1867	819	7.78	-1.38	3236	-1703
100	25	1834	852	8.00	-1.60	3228	-1695
100	26	1792	894	8.06	-1.66	3146	-1613

100	30	1634	1052	8.25	-1.85	2904	-1371
100	32	1551	1135	8.47	-2.07	2791	-1258
100	34	1489	1197	8.29	-1.89	2627	-2615.80
200	9	2006	680	2.86	3.54	2653	-2641.80
200	14	2027	659	3.26	3.14	2796	-1263
200	16	2027	659	3.55	2.85	2885	-1352
200	20	1936	750	4.33	2.07	3118	-1585
200	24	1919	767	4.60	1.80	3118	-1585
200	25	1942	744	5.00	1.40	3197	-1664
200	26	1973	713	6.56	-0.16	3513	-1980
200	30	1836	850	7.40	-1.00	3188	-1655
200	32	1745	941	7.85	-1.45	3055	-1522
200	34	1653	1033	8.26	-1.86	2999	-1466
300	9	1977	709	2.52	3.88	2103	-570
300	14	1992	694	2.33	4.07	2253	-720
300	16	1930	756	2.37	4.03	2290	-757
300	20	2029	657	2.85	3.55	2486	-953
300	24	1993	693	3.38	3.02	2650	-1117
300	25	1947	739	3.50	2.90	2648	-1115
300	26	1914	772	3.60	2.80	2623	-1090
300	30	1833	853	4.23	2.17	2634	-1101
300	32	1722	964	4.55	1.85	2596	-1063
300	34	1798	888	7.31	-0.91	3213	-1680

Table V: Calibration with the turbulence coefficient, basal frictional angle and scouring rate

Turbulence Coefficient ($m.sec^2$)	Basal Frictional Angle (^{0})	Scouring Rate (m.sec)	Area (m^2)	Deviation observed area (2686 m^2)	Max. Depth (m)	Deviation depth (6.4m)	Final volume (m^3)	Deviation volume (1533m^3)
100	9	0.0065	1882	804	5.68	0.72	3487	-1934
100	9	0.0095	1904	782	6.47	-0.07	3611	-2058
100	9	0.0125	1871	815	6.35	0.05	3621	-2068
100	14	0.0065	1844	842	6.91	-0.51	3717	-2164
100	14	0.0196	1881	805	7.54	-1.14	3783	-2230
100	16	0.0095	1937	749	7.70	-1.30	3835	-2282
100	26	0.0065	1723	963	9.02	-2.62	3424	-1871
100	32	0.0095	1539	1147	9.05	-2.65	3128	-1575
100	34	0.0095	1498	1188	8.89	-2.49	3021	-1468
200	9	0.0065	2034	652	2.74	3.66	2802	-1249
200	9	0.0095	2044	642	2.71	3.69	2786	-1233
200	9	0.0125	2076	610	2.77	3.63	2799	-1246
200	14	0.0125	2091	595	3.21	3.19	3002	-1449
200	14	0.0196	2008	678	3.80	2.60	3250	-1697

200	24	0.005	1947	739	5.12	1.28	3287	-1734
200	24	0.0065	2018	668	5.01	1.39	3500	-1947
200	24	0.0095	2053	633	5.11	1.29	3478	-1925
200	24	0.0125	2047	639	5.62	0.78	3723	-2170
200	24	0.0196	2057	629	6.73	-0.33	3916	-2363
200	25	0.005	1939	747	5.91	0.49	3469	-1916
200	25	0.0065	1938	748	5.90	0.50	3546	-1993
200	25	0.0095	2033	653	5.55	0.85	3694	-2141
200	25	0.0125	2039	647	6.51	-0.11	3849	-2296
200	32	0.0196	1646	1040	8.10	-1.70	3166	-1613
200	34	0.0196	1613	1073	8.01	-1.61	3147	-1594
300	9	0.0125	2035	651	2.64	3.76	2243	-690
300	9	0.0196	2050	636	2.45	3.95	2575	-1022
300	14	0.0196	2047	639	2.40	4.00	2484	-931
300	16	0.0095	2112	574	2.49	3.91	2543	-990
300	26	0.0196	1933	753	3.77	2.63	2886	-1333
300	32	0.005	1757	929	4.68	1.72	2743	-1190
300	32	0.0125	1906	780	6.51	-0.11	3572	-2019
300	34	0.0065	1794	892	6.10	0.30	3122	-1569
300	34	0.0095	1795	891	6.73	-0.33	3250	-1697

Appendix III

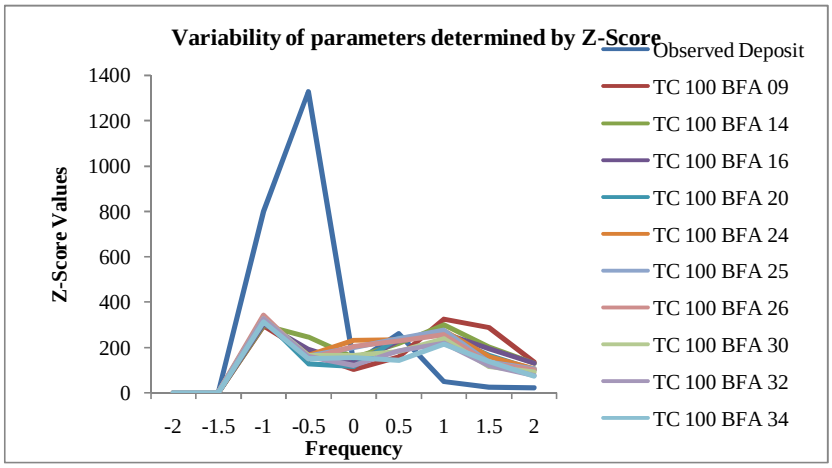

Sensitivity of Turbulence Coefficient (TC 100) and Basal frictional angle (BFA) to depth

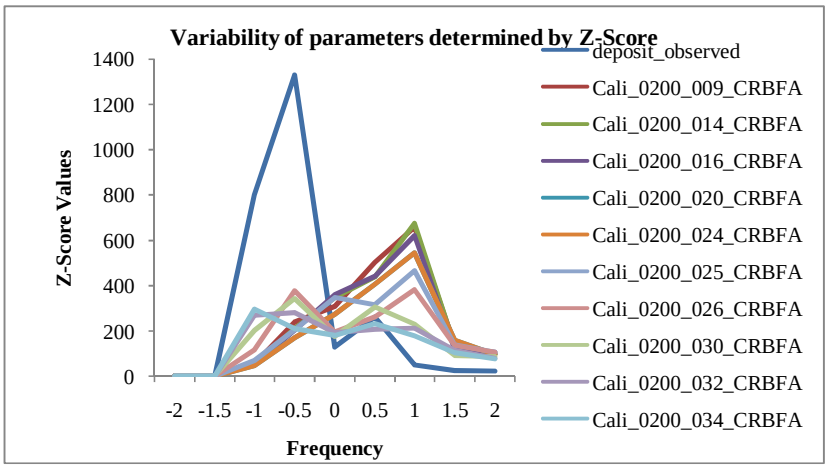

Sensitivity of Turbulence Coefficient (TC 200) and Basal frictional angle (BFA) to depth

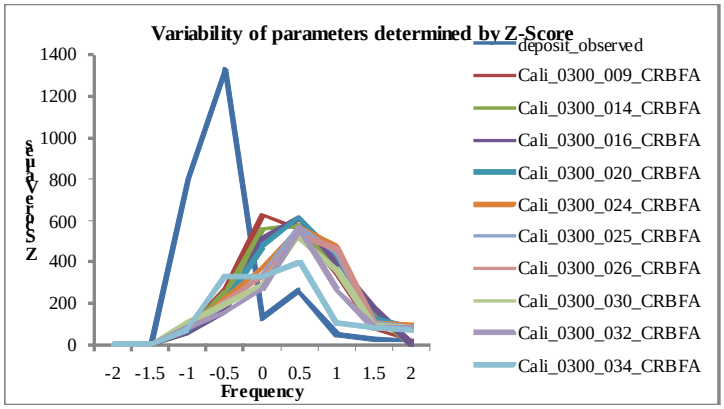

Sensitivity of Turbulence Coefficient (TC 300) and Basal frictional angle (BFA) to depth

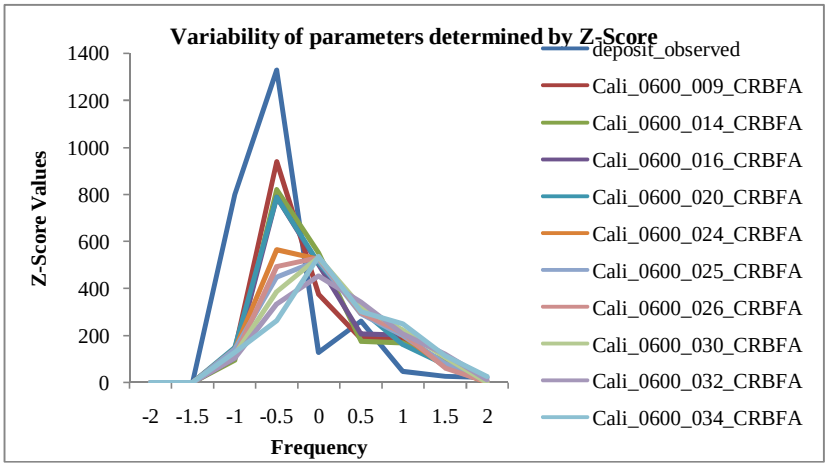

Sensitivity of Turbulence Coefficient (TC 600) and Basal frictional angle (BFA) to depth

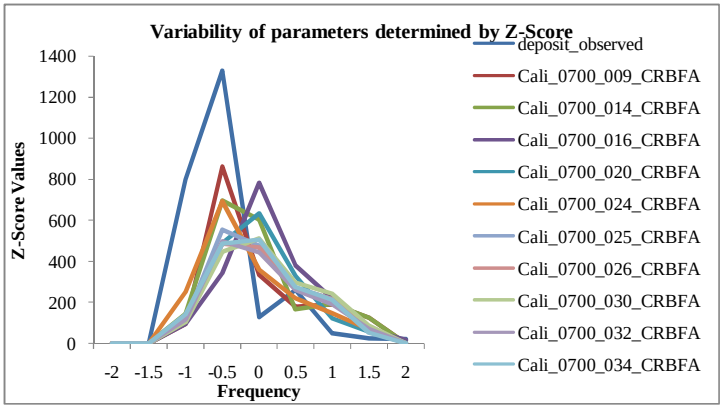

Sensitivity of Turbulence Coefficient (TC 800) and Basal frictional angle (BFA) to depth

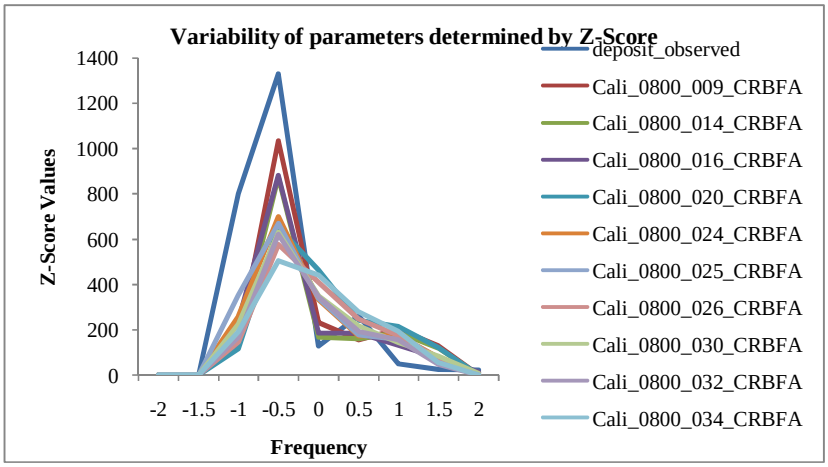

Sensitivity of Turbulence Coefficient (TC 800) and Basal frictional angle (BFA) to depth

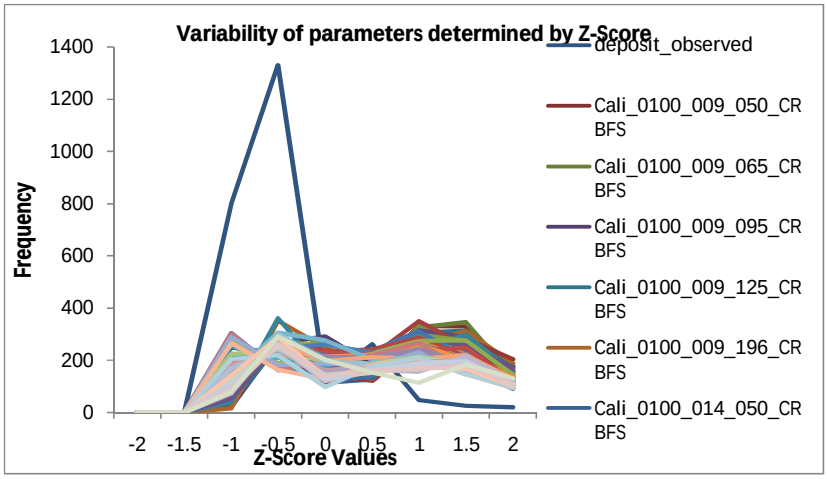

Sensitivity of Turbulence Coefficient (TC 100) and Basal frictional angle (BFA) and Scouring rate (SC) to depth

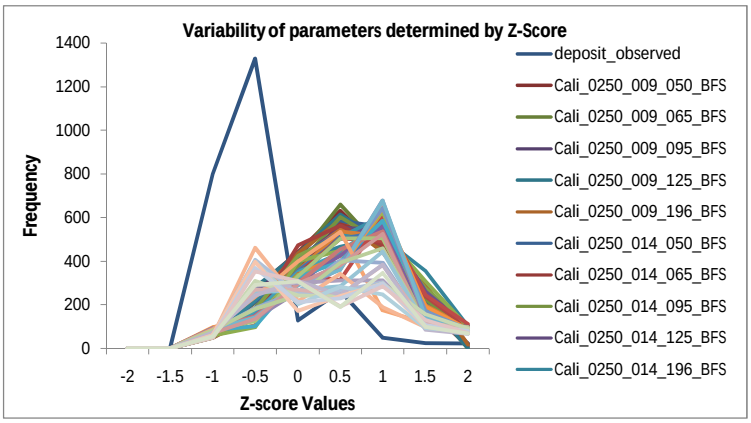

Sensitivity of Turbulence Coefficient (TC 250), Basal frictional angle (BFA) and Scouring rate (SC) to depth

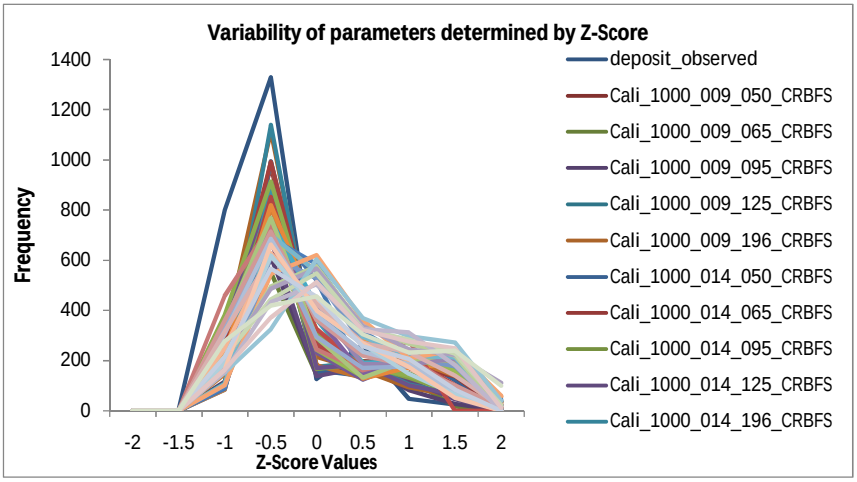

Sensitivity of Turbulence Coefficient (TC 1000) and Basal frictional angle (BFA) and Scouring rate (SC) to depth